

Lectures outline

- 1- remind of gaseous detectors part
- 2- trigger example with gaseous detector
- 3- **Calorimeter detectors** (*one word about neutron interaction*)
- 4- trigger with calorimeter det. (and MM gaseous detector)
- 5- magnets (briefly)

Thanks to Laurent Serin (LAL) for the calorimetry part.

Calorimeter detectors

Energy measurements



Outline

1- Calorimeter definition & history, illustration with some major physics results

2- Electromagnetic interaction and shower development

3- Electromagnetic calorimeters technologies

4- e/γ reconstruction, calibration and performance

4- Hadronic shower development

5- Hadronic calorimeters technologies

6- Jets reconstruction calibration and performance

7- Missing transverse energy measurement

8- Conclusion

Slides categories

- * For information*
- ** Useful to know*
- *** Needs to know*

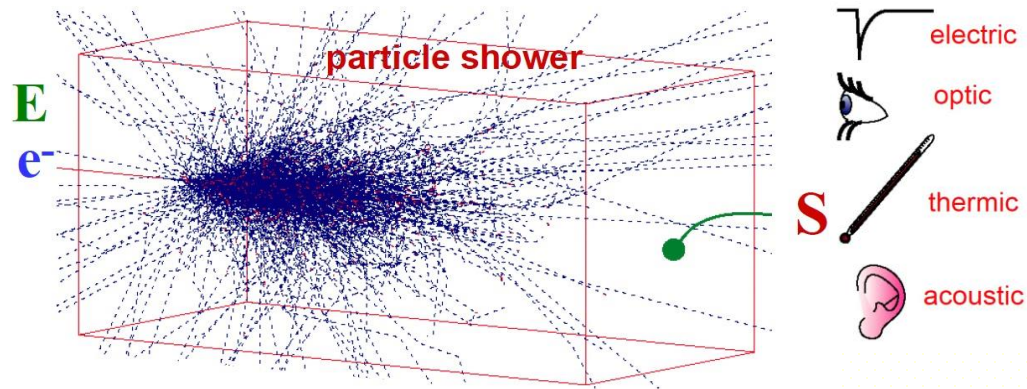
Calorimetry definition

History of calorimeters

**Illustration with some major
physics results**

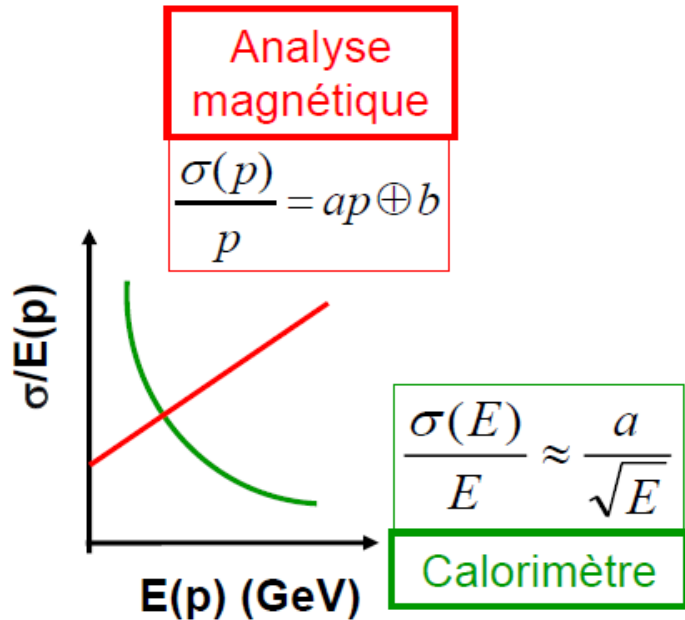
Calorimetry definition

- Experimental technique used in Nuclear Physics, Particle Physics and Astroparticle to detect a particle and measure some of its properties based on total or partial absorption of the particle in a fiducial volume
- Destructive process :
Particle is absorbed in the medium or exit it quite modified
- Particle energy is converted in a detectable signal.
- Key element of any High Energy Physics (HEP) experiment



Calorimeters needed for HEP

Sensitive to **all charged and neutrals** particles in final state
Good resolution at high energy, and “**sizeable**” detectors



Calorimeter shower depth $\sim \ln E/E_c$
 almost energy independent
 → Calorimeter can be compact detector

Magnetic spectrometer :

$$\sigma(p) / p \sim p / (BL^2)$$

→ Detector size has to grow quadratically to maintain resolution

Calorimeter can also provide:

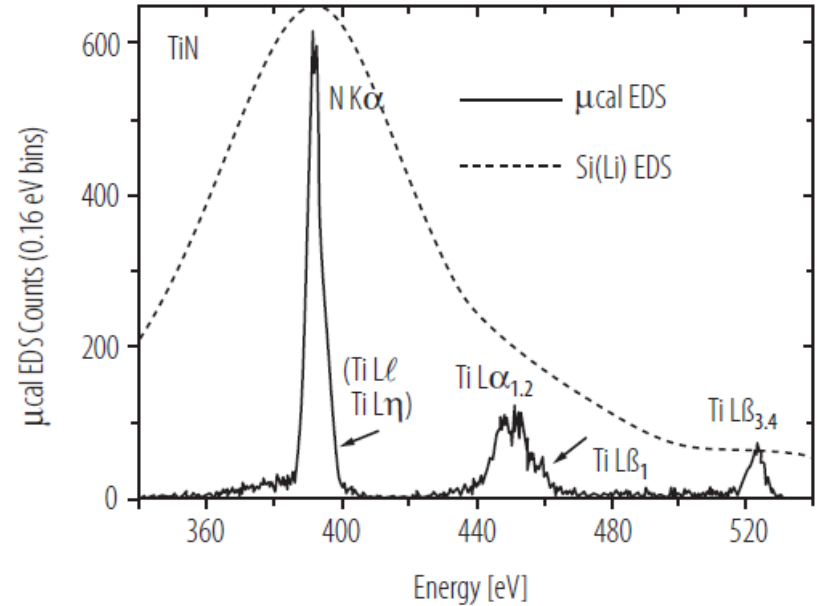
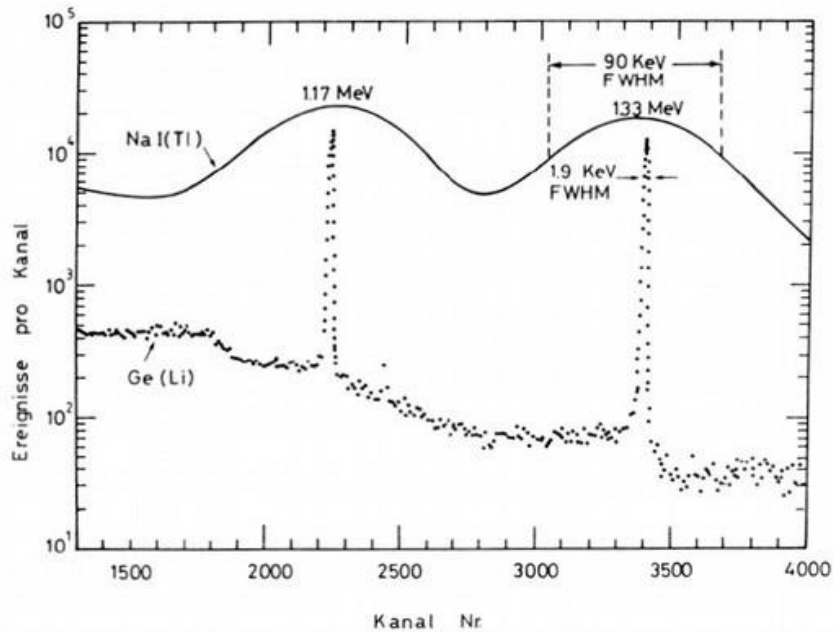
- Position/angular measurement
- Time measurement
- **Trigger**
- Particle identification (e, γ , π , μ , h...)

ATLAS : calo $\sigma(E)/E \sim \frac{10\%}{\sqrt{E}} \oplus 0.7\%$
 tracking $\sigma(p) / p \sim 5 \cdot 10^{-4} p \oplus 1\%$

At 40 GeV for electrons similar energy resolution

Interlude : cryogenic μ calorimeter

Definitely best energy resolution for very low energy but not the subject of this lesson



At **100 MeV**, solid state (Si, Ge) detectors have $\sim 25/30$ better resolution than scintillators

At few **hundred eV**, cryogenic bolometer can have 50 better resolution
Ok for event energy measurement but not individual particle energy measurement

Classification of calorimeters

Per particle type

Electromagnetic calorimeters :

$e^{+/-}$, γ and π^0

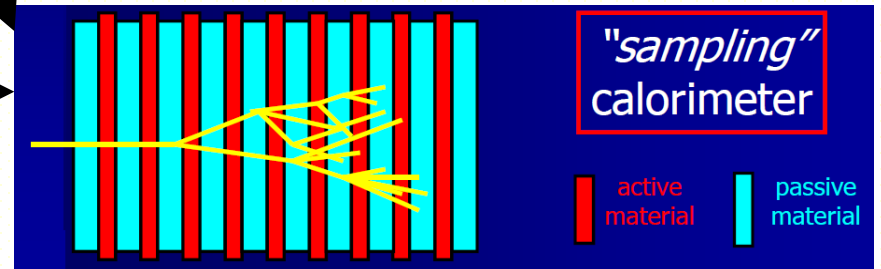
Per construction technique



Full absorption detector, active medium for energy degradation and signal generation

Hadron calorimeters :

Charged and neutral hadrons, jets



Alternate layers of absorbers to degrade particle energy and active medium to provide detectable signal

Classification of calorimeters

By signal detection technology

Homogeneous Calorimeters	Scintillation/ Crystal
	Semiconductor
	Cherenkov
	Ionization (Noble Liquids)
Sampling Calorimeters	Scintillation
	Gas
	Solid State
	Liquids
	<i>Common Absorbers: Pb, Fe, Cu, U, W</i>

Existing Electromagnetic Calorimeters

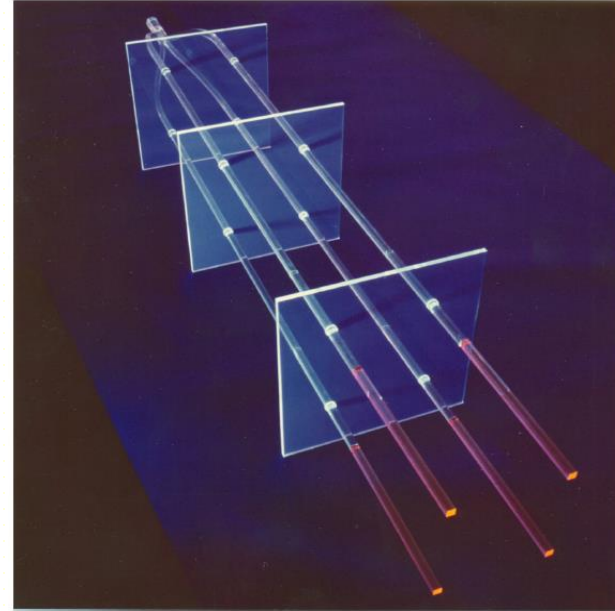
Technology/Experiment	Depth	Resolution	Year
NaI(Tl) (Crystal Ball)	$20X_0$	$2.7\%/E^{1/4}$	1983
$\text{Bi}_4\text{Ge}_3\text{O}_{12}$ (BGO) (L3)	$22X_0$	$2\%/\sqrt{E} \oplus 0.7\%$	1993
CsI (KTeV)	$27X_0$	$2\%/\sqrt{E} \oplus 0.45\%$	1996
CsI(Tl) (BaBar)	$16-18X_0$	$2.3\%/E^{1/4} \oplus 1.4\%$	1999
CsI(Tl) (BELLE)	$16X_0$	1.7% for $E_\gamma > 3.5$ GeV	1998
PbWO_4 (PWO) (CMS)	$25X_0$	$3\%/\sqrt{E} \oplus 0.5\% \oplus 0.2/E$	1997
Lead glass (OPAL)	$20.5X_0$	$5\%/\sqrt{E}$	1990
Liquid Kr (NA48)	$27X_0$	$3.2\%/\sqrt{E} \oplus 0.42\% \oplus 0.09/E$	1998
Scintillator/depleted U (ZEUS)	$20-30X_0$	$18\%/\sqrt{E}$	1988
Scintillator/Pb (CDF)	$18X_0$	$13.5\%/\sqrt{E}$	1988
Scintillator fiber/Pb spaghetti (KLOE)	$15X_0$	$5.7\%/\sqrt{E} \oplus 0.6\%$	1995
Liquid Ar/Pb (NA31)	$27X_0$	$7.5\%/\sqrt{E} \oplus 0.5\% \oplus 0.1/E$	1988
Liquid Ar/Pb (SLD)	$21X_0$	$8\%/\sqrt{E}$	1993
Liquid Ar/Pb (H1)	$20-30X_0$	$12\%/\sqrt{E} \oplus 1\%$	1998
Liquid Ar/depl. U (DØ)	$20.5X_0$	$16\%/\sqrt{E} \oplus 0.3\% \oplus 0.3/E$	1993
Liquid Ar/Pb accordion (ATLAS)	$25X_0$	$10\%/\sqrt{E} \oplus 0.4\% \oplus 0.3/E$	1996

Example of calorimeters

Fixed target calorimeters : NA5 at CERN (1978) QCD measurements
One of the first segmented calorimeter



24 (φ) x 10 (θ) cells
EM section : Scintillator/Pb
Had section : Scintillator/Fe
using two different Wave Length
Shifter (WLS)



Main idea : guide the light of both
section in single rod read by two
PM behind yellow (EM) and
green (Had) filters

Example of calorimeters

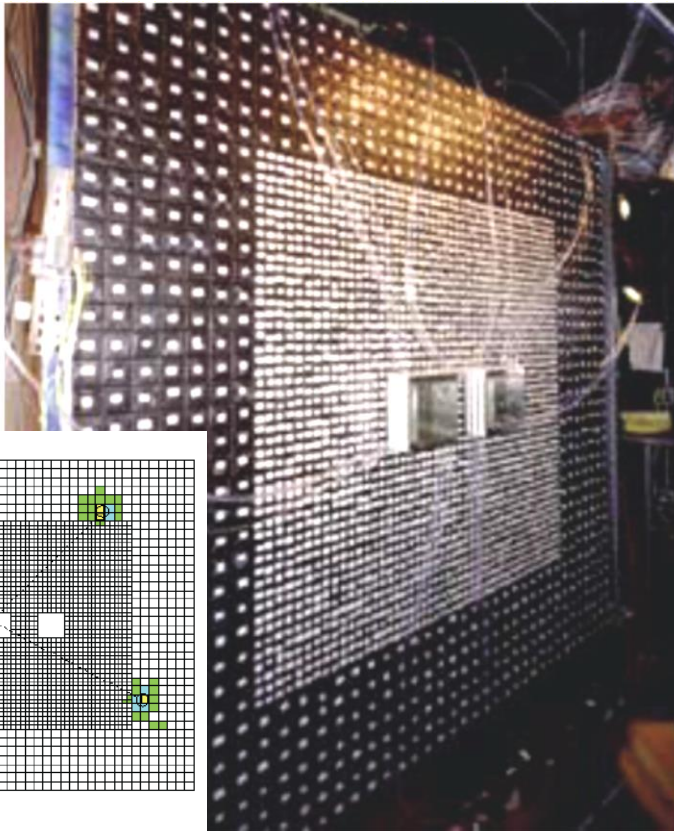
Fixed target calorimeters : CP violation in K decays experiment : NA31 / NA48 / KTeV

→ Need to measure accurately $K_L \rightarrow \pi^0 \pi^0 \rightarrow 4\gamma$ ($\text{Br}(K_L \rightarrow 3\pi^0)/(\text{Br}(K_L \rightarrow 2\pi^0)) \sim 300$)

→ Shower separation + invariant mass : fine granularity and energy resolution

→ Homogeneous calorimeters

KTeV 3100 pure CsI crystals



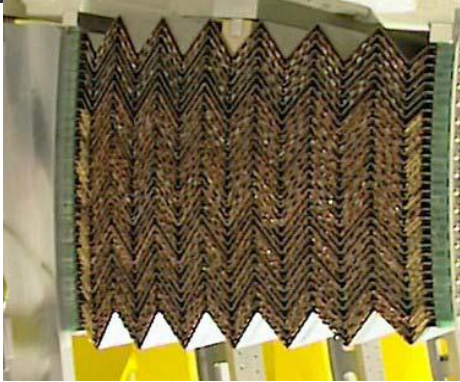
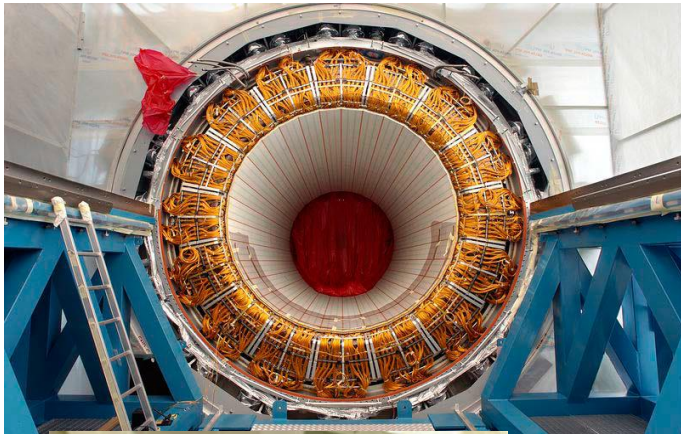
Liquid Krypton calorimeters,
still in used in K experiments at CERN



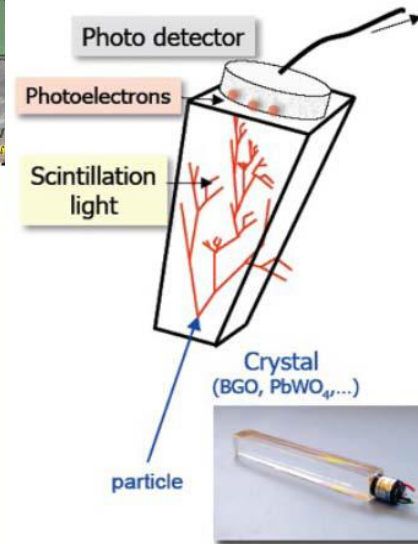
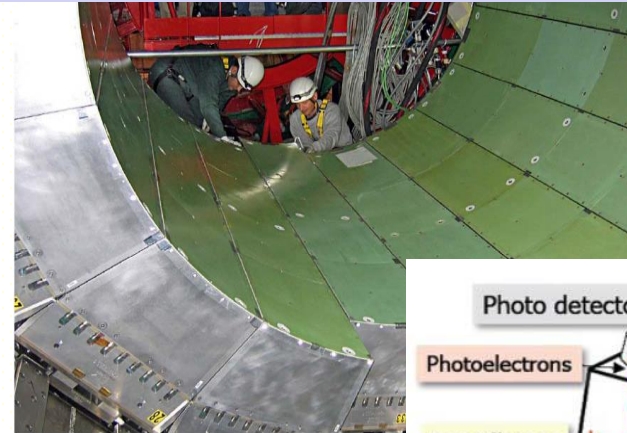
LHC calorimeters

LHC electromagnetic calorimeters, two different approaches

ATLAS : Liquid Argon / Lead sampling electromagnetic calorimeter



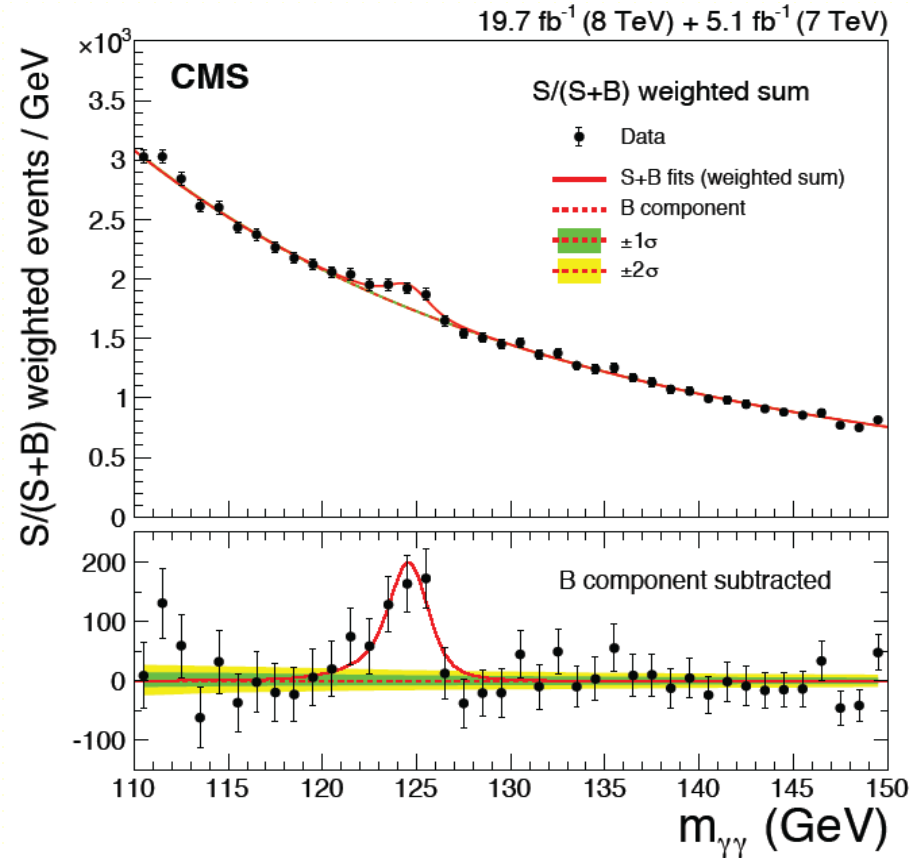
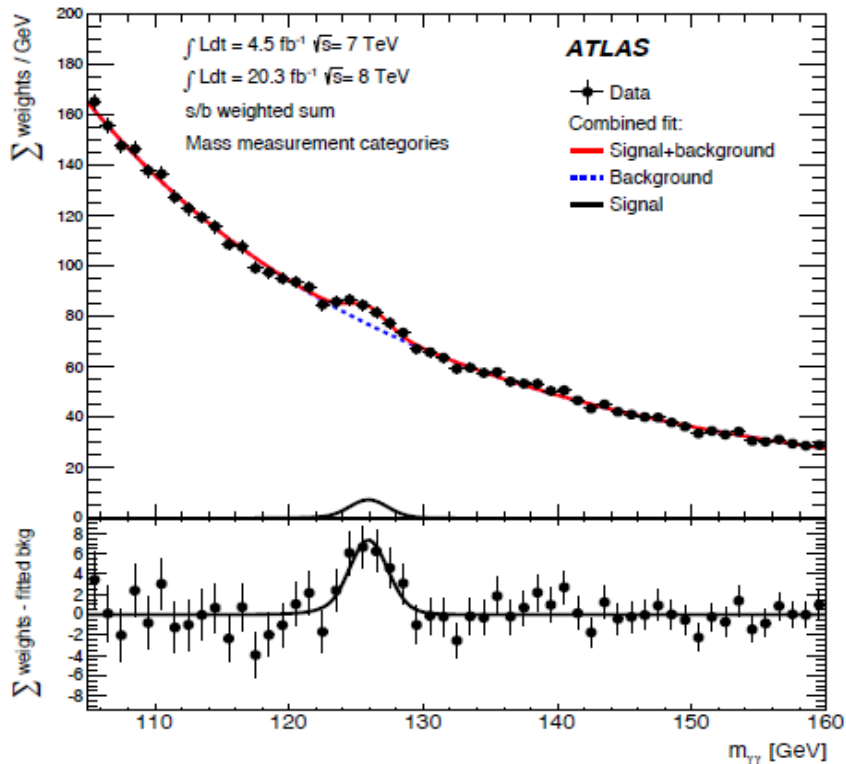
CMS : Homogeneous calorimeter PbWO_4 crystals



Key detector of Higgs discovery

ATLAS calorimeter better than CMS or CMS better than ATLAS ?

H → γγ in ATLAS and CMS



Quite a similar result with different detectors (similar S/\sqrt{B} , scales as $1/\sigma_{(\text{masse})}$)

CMS : Energy resolution

ATLAS : Granularity (jet rejection) and angular resolution

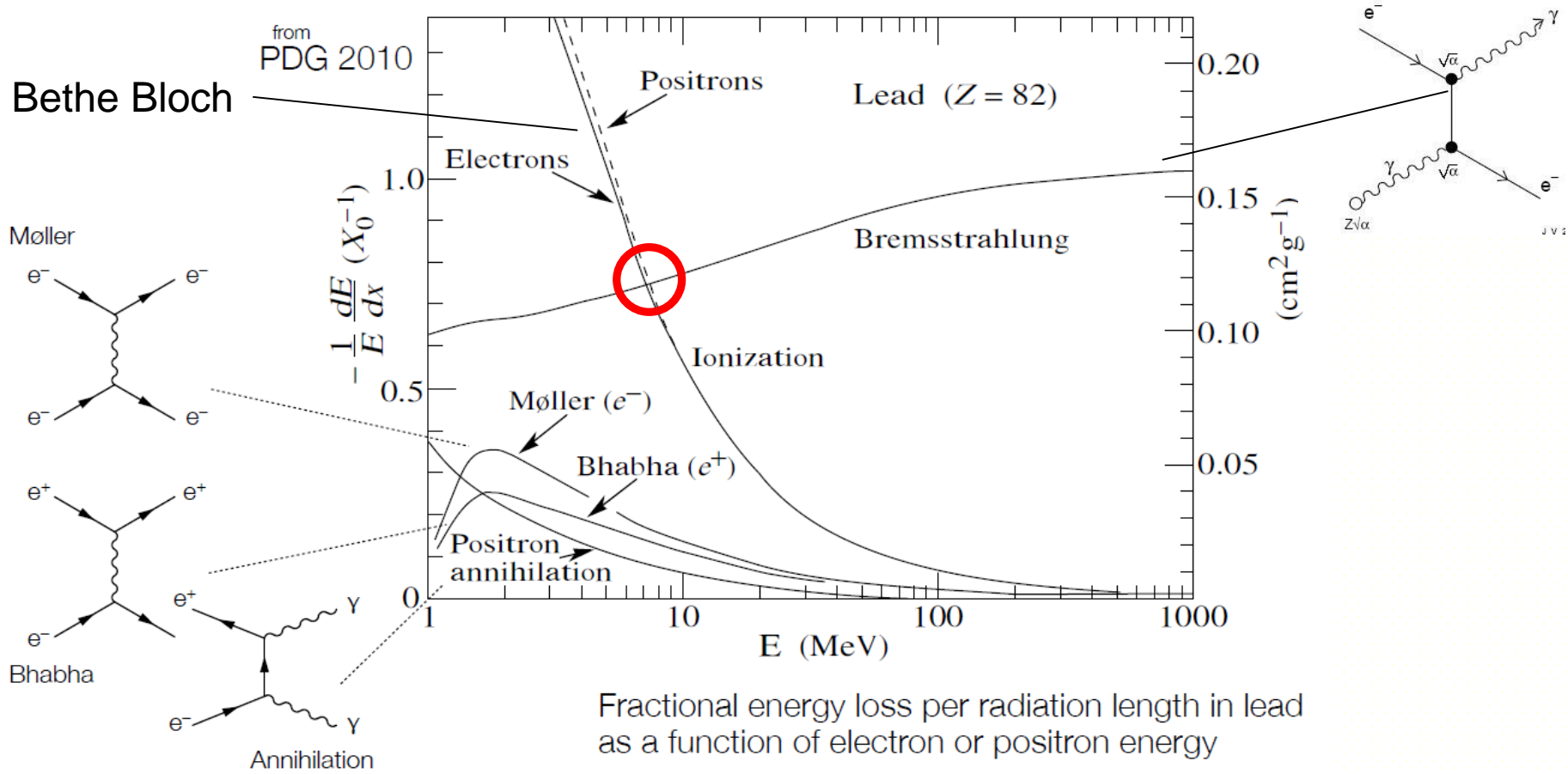
$$m_{\gamma\gamma} = 2 E_1 E_2 (1 - \cos(\theta))$$

$$\frac{\Delta m_{\gamma\gamma}}{m_{\gamma\gamma}} = \frac{1}{2} \left(\frac{\Delta E_1}{E_1} \oplus \frac{\Delta E_2}{E_2} \oplus \frac{\Delta \theta_{\gamma\gamma}}{\tan(\theta_{\gamma\gamma}/2)} \right)$$

**

Electromagnetic interaction and shower development

e⁺/e⁻ interaction in matter



Critical energy E_c : defined by $(dE/dX)_{\text{ion}} = (dE/dx)_{\text{brem}}$

Radiation length : mean distance after which an electron has lost by radiation all but a fraction 1/e of its initial energy X_0 ($E(\text{after } 1 X_0) = E(\text{initial})/e$)

Summary for e+/e-

1) Above critical energy E_c (~a few MeV) fractional energy loss dominated by bremsstrahlung, below dominated by ionization/excitation

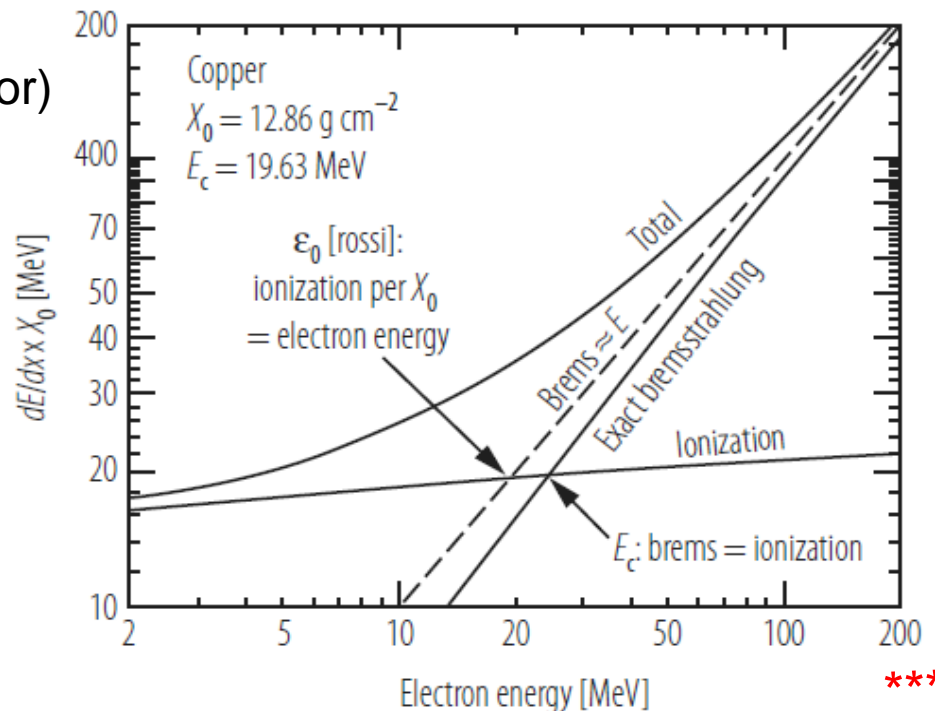
2) Energy loss by ionisation almost independent of incident energy, by radiation linear with energy

3) $\epsilon_0 = 610 \text{ MeV} / (Z + 1.24)$

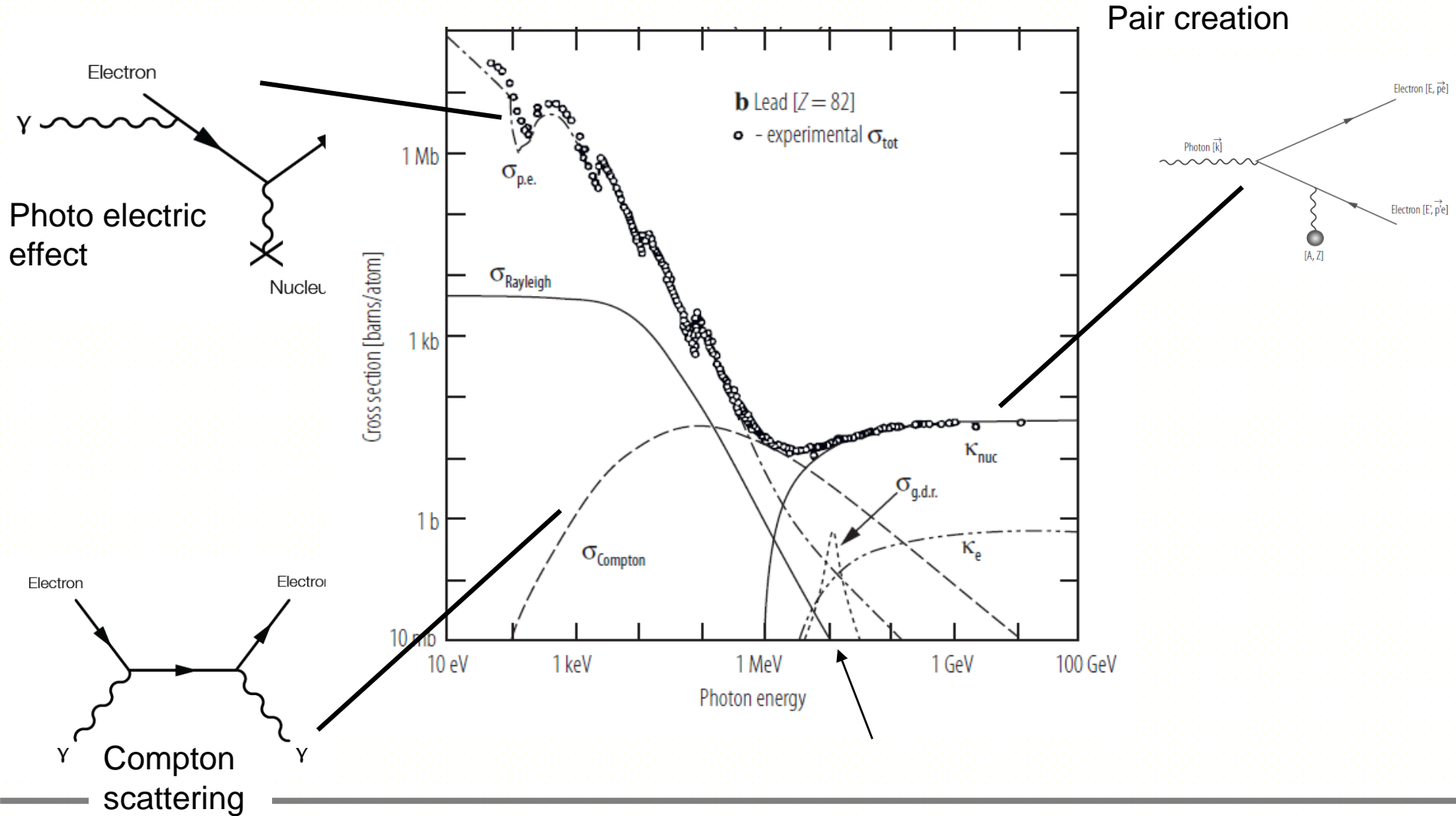
$$X_0 = \frac{716.4 \text{ g.cm}^{-2}}{Z(Z+1) \ln(187/\sqrt{Z})}$$

High Z material provide low critical energy and small radiation length (compact detector)

(You should divide by the density ρ to have X_0 in cm)



Photon interaction in matter



Photon interaction in matter

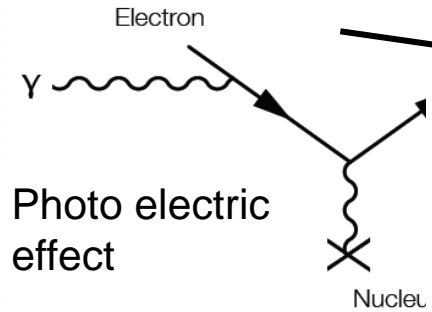
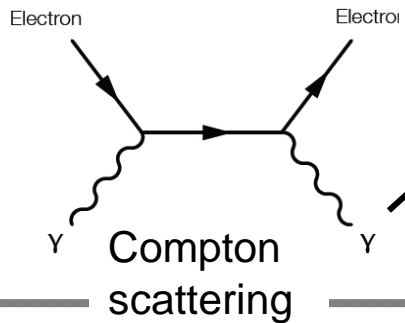
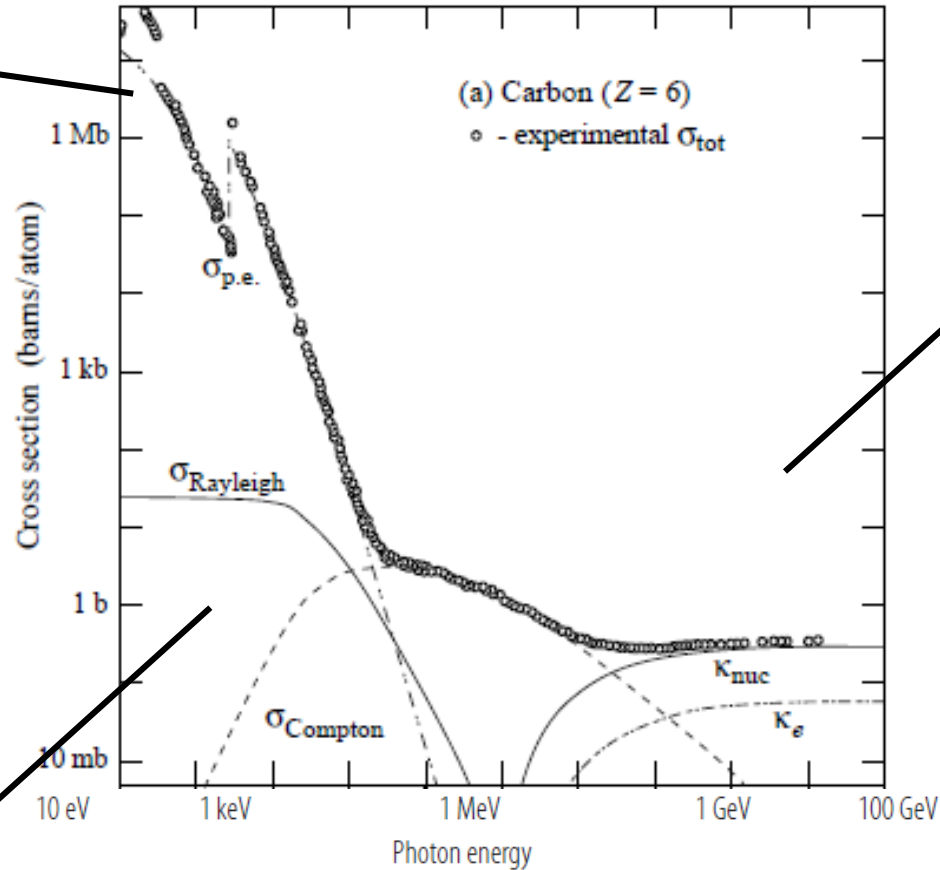


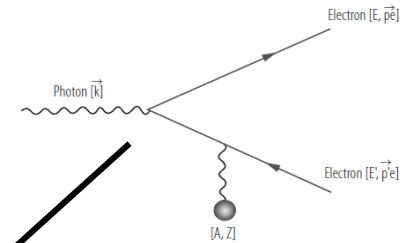
Photo electric effect



Compton scattering



Pair creation



Summary for γ

- 1) Above a few $m_e c^2$, photon interaction is dominated by pair production.
Cross section is constant with energy (similar fractional energy loss in brem)
Probability that a high energy photon is **not** converted into e+e- pair **after $9/7 X_0$ is $1/e$** (37 %) $\sigma = 7/9 A/(X_0 N_A)$.
- 2) At intermediate energy (keV \rightarrow GeV), Compton scattering contribution
For high Z, max of cross section \sim pair creation cross-section
For small Z, max of cross section $>$ pair creation cross-section
- 3) Low energy photon ($<$ MeV) is dominated by photo-electric effect
 Z^5 dependence of cross-section.
In low Z material, photon can show large mean free path length and escape detection.

A simplified EM shower model

EM shower model :

- After 1 X_0 , $e^{+/-} \rightarrow e^{+/-} \gamma$ and $\gamma \rightarrow e^+ e^-$ with proba 100 %
- Equal energy split
- Cascade stops when electron/positron reaches ε (~critical energy)

1) What is the number of particles after $n X_0$ $N(n) =$

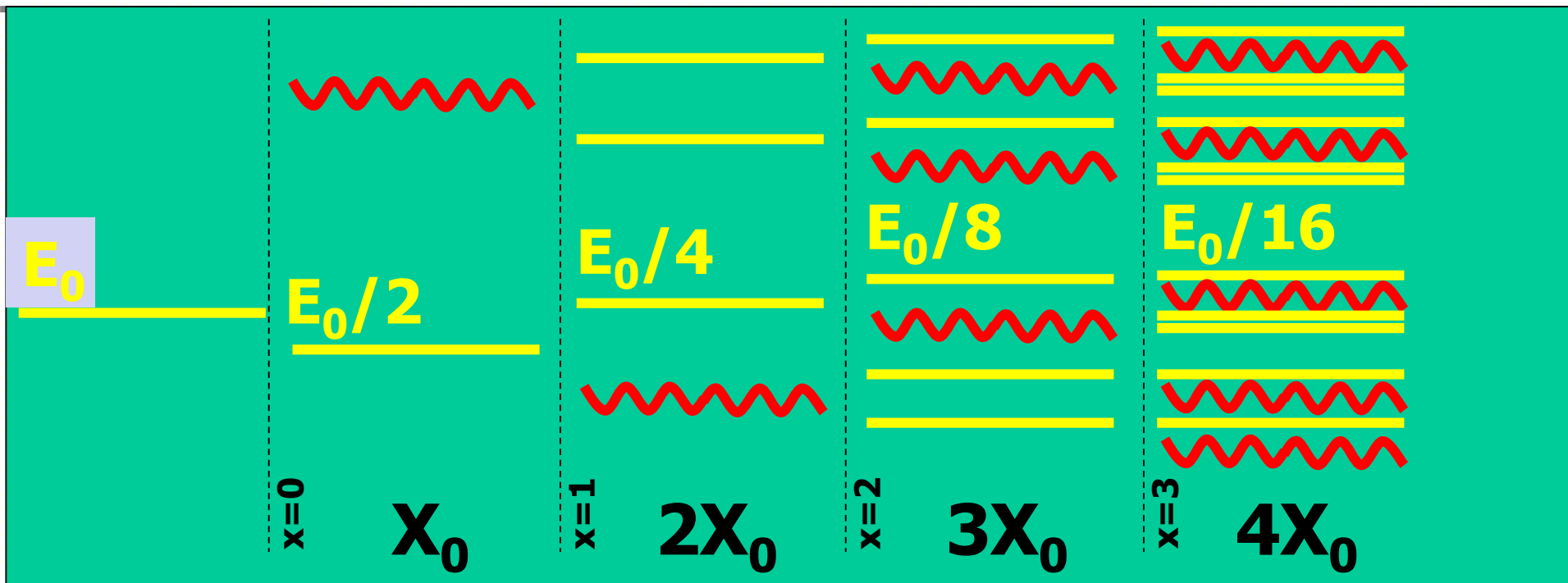
2) What is the charged particle energy after $n X_0$ $E(n) =$

3) The cascade process stops when $E = \varepsilon$ (E_c) at $n_{\max} =$
What is the total number of particles at n_{\max} $N_{\max} =$

4) By defining s_0 as the track length of electrons below the critical energy, compute the total track length T of all charged particles $T =$
(neglect 1 wrt $2^{n_{\max}}$)

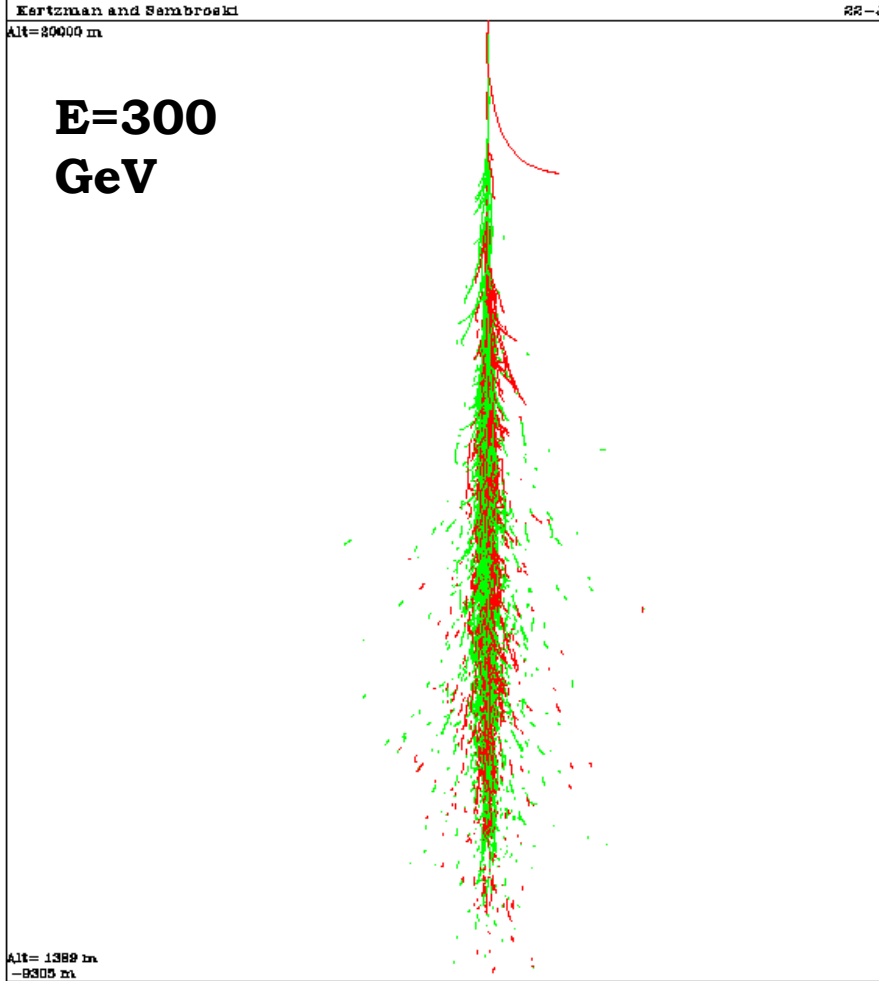
Conclude about the energy resolution if you measure T ?

Simplified EM shower model

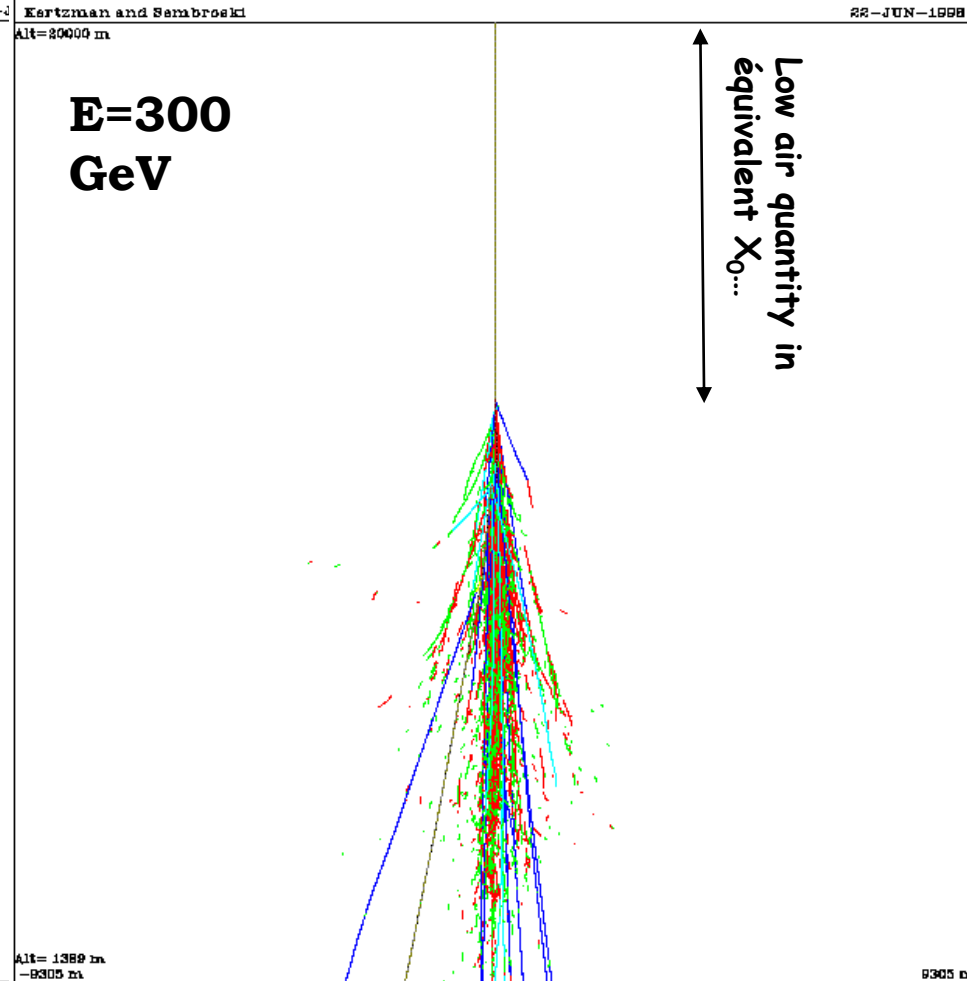


EM shower versus Had. shower in air

Electromagnetic shower



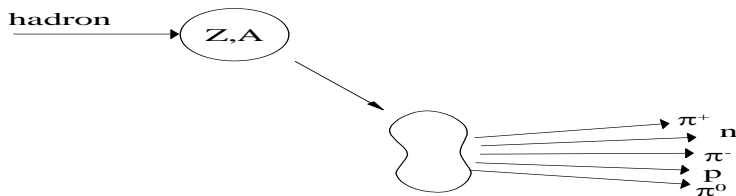
Hadronic shower



Total amount of air at sea level $\sim 23.X_0$

Implication : the hadronic showers

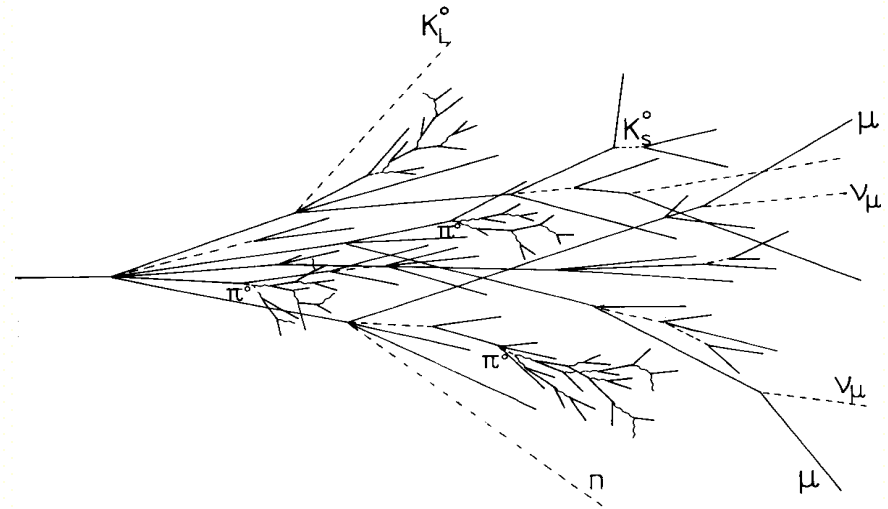
In an hadronic shower, there will be production of many π , K and neutrons. π^0 will give an EM component (from 15 to 20% of initial E), some of the π et K at low energies will give – by decay - μ , ν . Neutrons are difficult to detect (neutral, heavy part.) and will escape. This gives with neutrino the invisible energy of the shower.



Multiplicity varies with $E \propto \ln(E)$
 \Rightarrow Quick development of the shower

$$\sigma_{inel} \approx \sigma_0 A^{0.7} \quad \sigma_0 \approx 35 \text{ mb}$$

\sim independant of the energie
 above 1 GeV for p, π , K...



$$n(\pi^0) \approx \ln E(\text{GeV}) - 4.6$$

example 100 GeV: $n(\pi^0) \approx 18$

Remarq : energy profil deposition are different between EM and Had.
 showers : higher multiplicity for hadronic interaction at the beginning of the
 shower development.

secondaries : $p_t \approx 0.35 \text{ GeV}/c$

How the hadronic shower is produced ?

Secondary particles production in hadronic showers are coming from "spallation" :

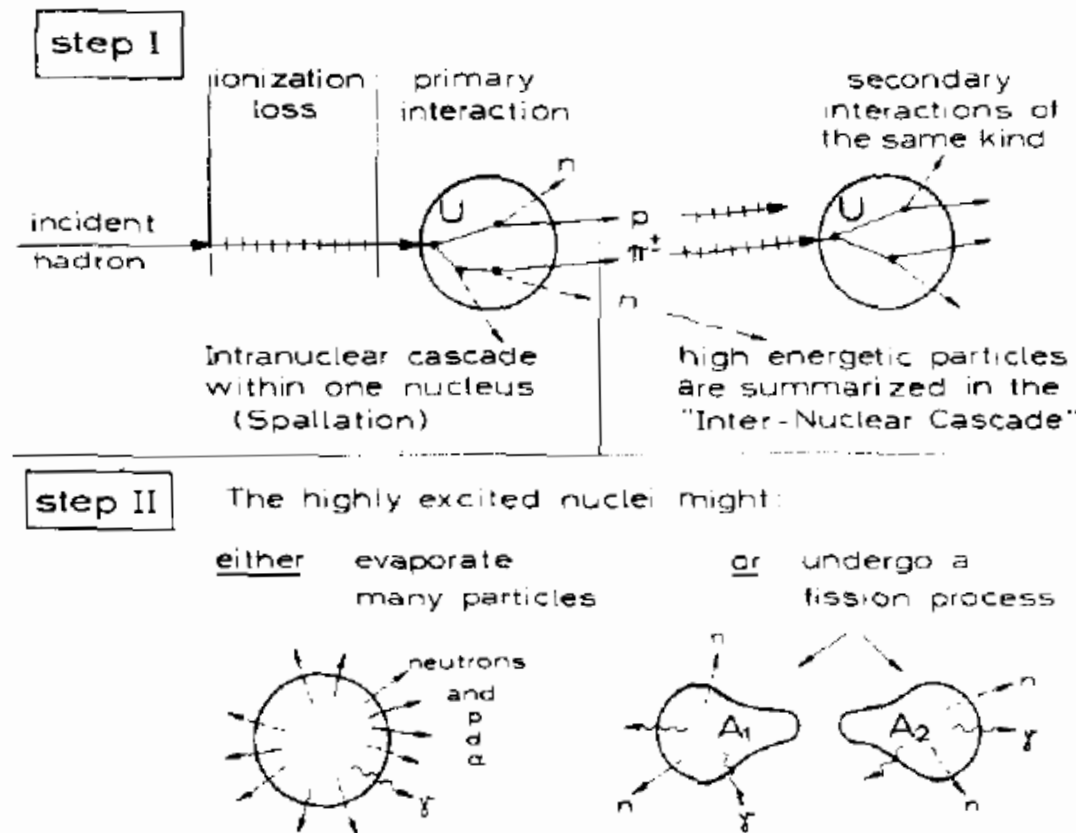
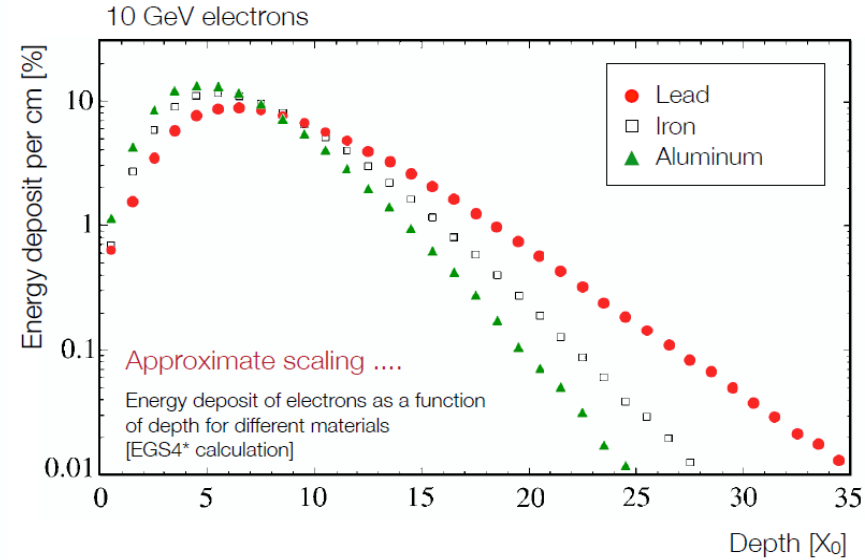
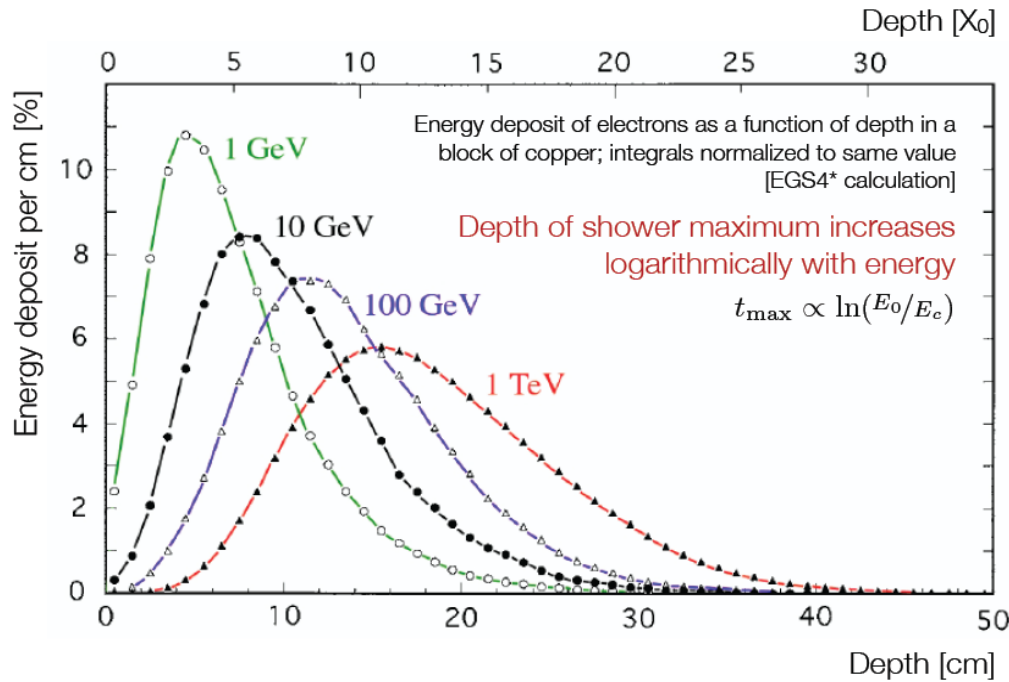


Fig. 6. Step I: Development of an "internuclear cascade". From one nucleus an intranuclear cascade releases a few high energetic spallation products, which are able to initiate further intranuclear cascade processes. Step II: The highly excited nuclei remaining from each intranuclear cascade deexcite.

Longitudinal shower development (1)



Longitudinal profile well described by

$$\frac{dE}{dt} = E_0 b \frac{(bt)^{a-1} e^{-bt}}{\Gamma(a)},$$

$$t_{\max} = \frac{a-1}{b} = \ln\left(\frac{E_0}{E_c}\right) + C_{\gamma e}$$

-0.5 for e+/-
+0.5 for γ

$$\varepsilon(\text{Pb}) = 7 \text{ MeV}, \quad \varepsilon(\text{Al}) = 39 \text{ MeV}$$

Shower starts early in low Z material
(t_{\max} dependence with E_c)

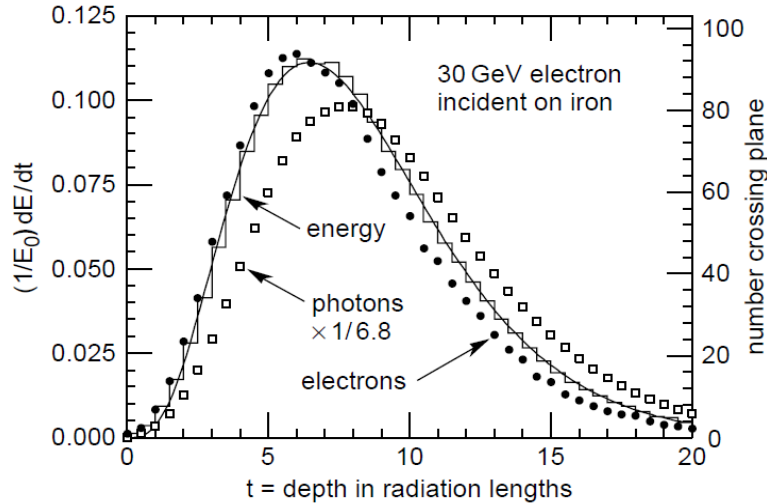
$$[dE/dx * X_0 \sim Z \times 1/Z^2 = 1/Z]$$

Not true when looking at depth in cm !

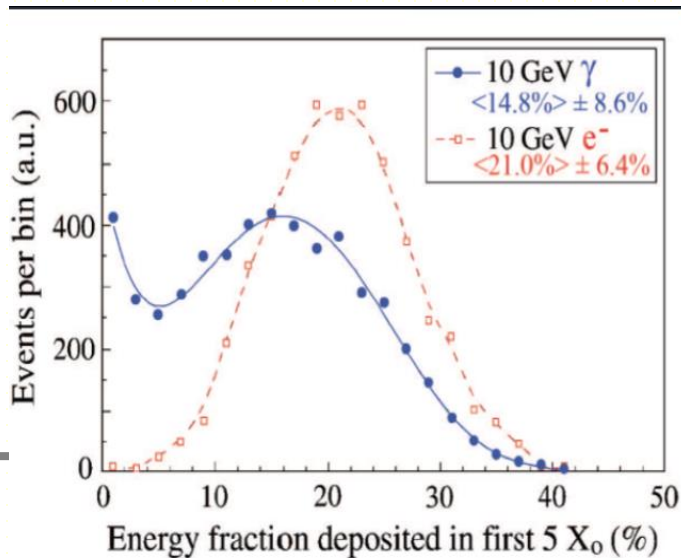
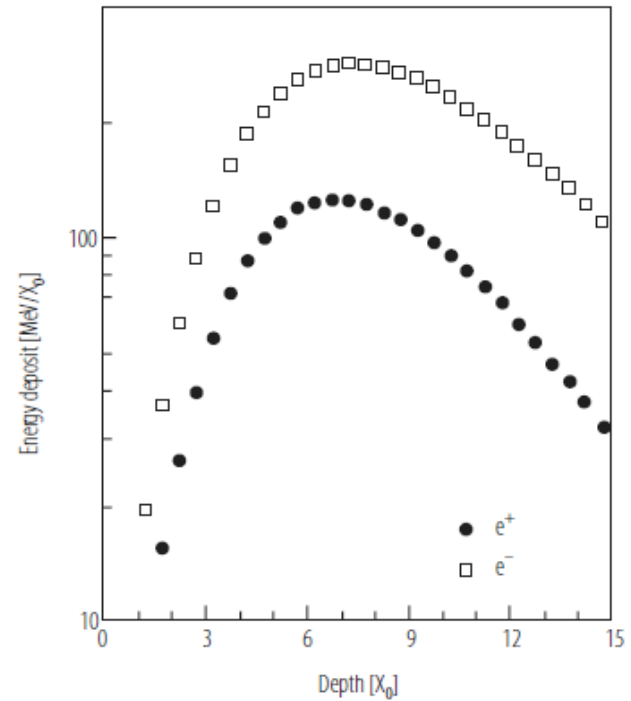
Radiation length Al : 89 mm, Pb 5.6 mm

Longitudinal shower development (2)

Higher penetration power of photons

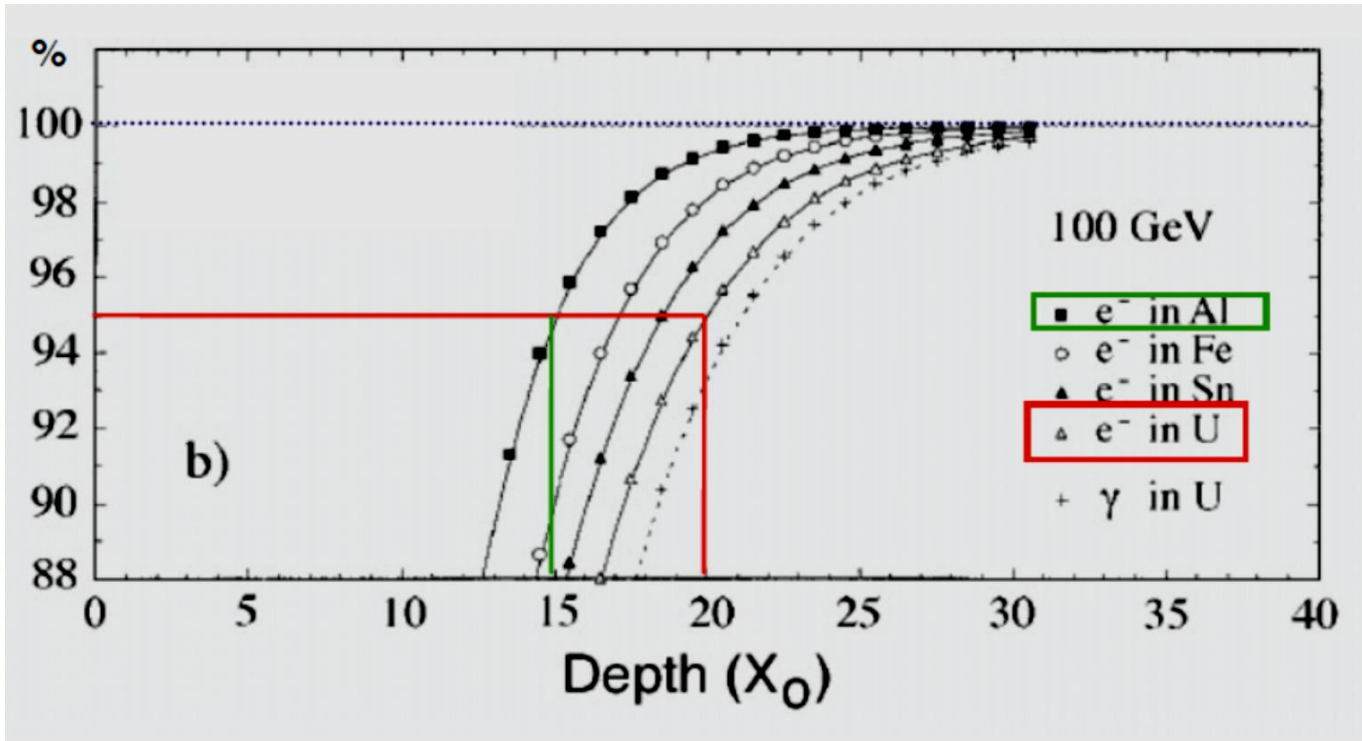


Fraction of energy deposited by e^- and e^+



75 % deposited by e^- , 25 % by e^+
 Why ?

Shower containment

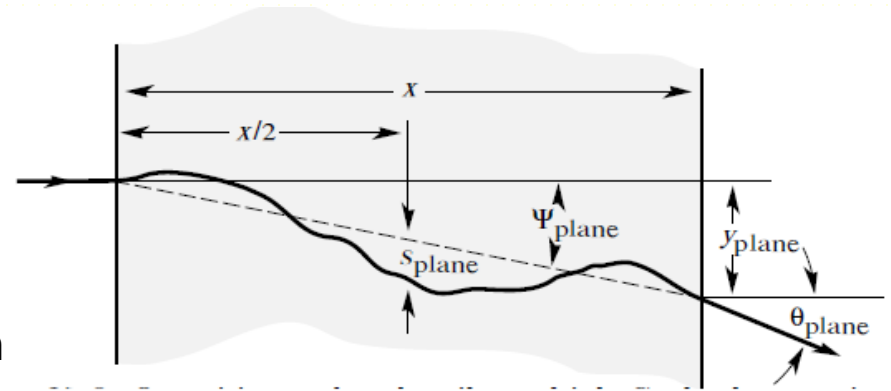


100 GeV electron contained in **15** X_0 of Al and **20** X_0 of U
but remind that $X_0(\text{Al}) = 89$ mm and $X_0(\text{U}) = 3.2$ mm, i.e. **130** vs **6** cm !

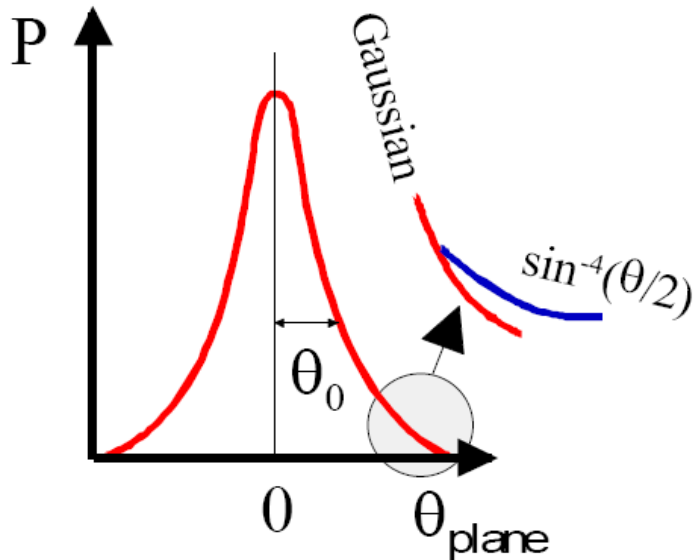
Useful parameterisation of containment $L(95\%) = t_{\max} + 0.08Z + 9.6 [X_0]$

Multiple scattering

Charge particle interaction with nuclei
 → Momentum transfer (p)
 → Particle deflexion (θ) (Rutherford scattering formula $1/\sin^4(\theta)$)
 → If thick material (absorber) multiple scattering. On average null effect on position but see as a fluctuation (θ_0) / r.m.s.



$$\theta_0 = \frac{13.6 \text{ MeV}}{\beta c p} z \sqrt{\frac{L}{X_0}} \left\{ 1 + 0.038 \ln \left(\frac{L}{X_0} \right) \right\}$$



θ_0
 -smaller for high energy (p)
 -smaller if small material thickness (L)
 - smaller if large radiation length

Lateral shower development (1)

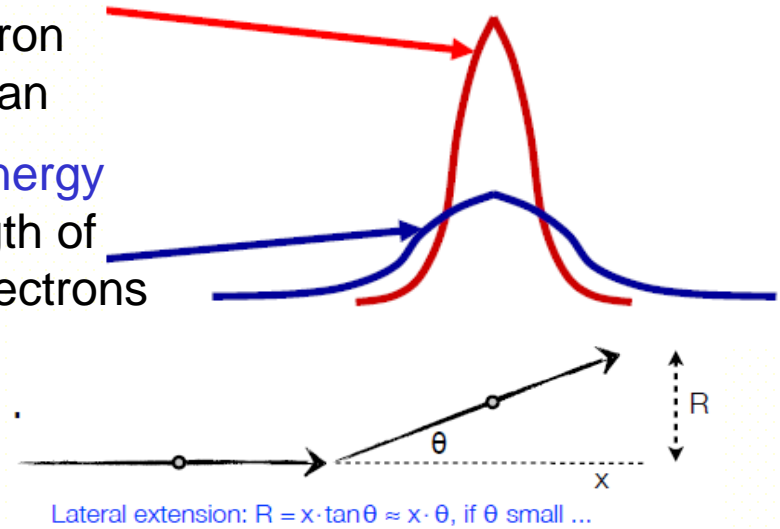
Pair creation and multiple scattering :

At shower start, dominated by electron/positron scattering along shower axis. Mostly Gaussian

Compton and photo-electric effect at small energy

Process are isotropic. Large penetration length of low energy photon Compton and by photo-electrons

$$\langle \theta \rangle = \frac{21.2 \text{ MeV}}{E_e} \sqrt{\frac{x}{X_0}}$$



Main contribution comes from low energy electron, E_c

If one assume that the approximate range of electrons is about $1 X_0$,

$\rightarrow \langle \theta \rangle = 21 \text{ MeV} / E_c$ and lateral extension $R = X_0 \langle \theta \rangle$

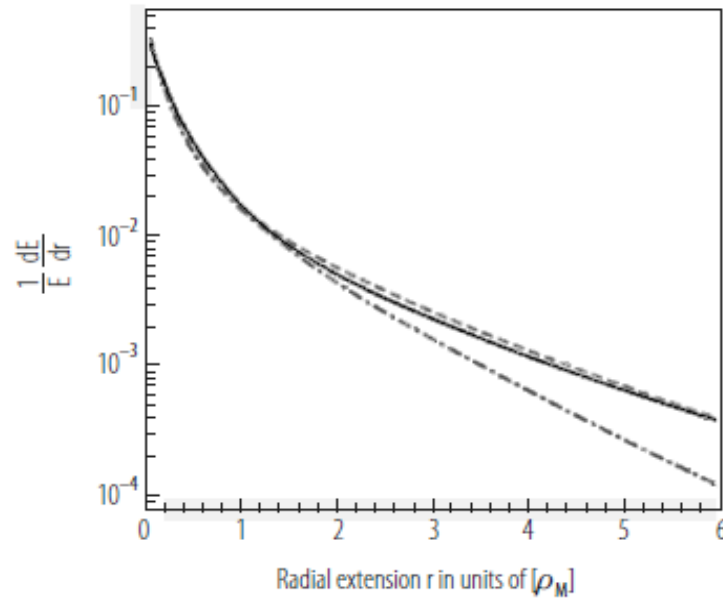
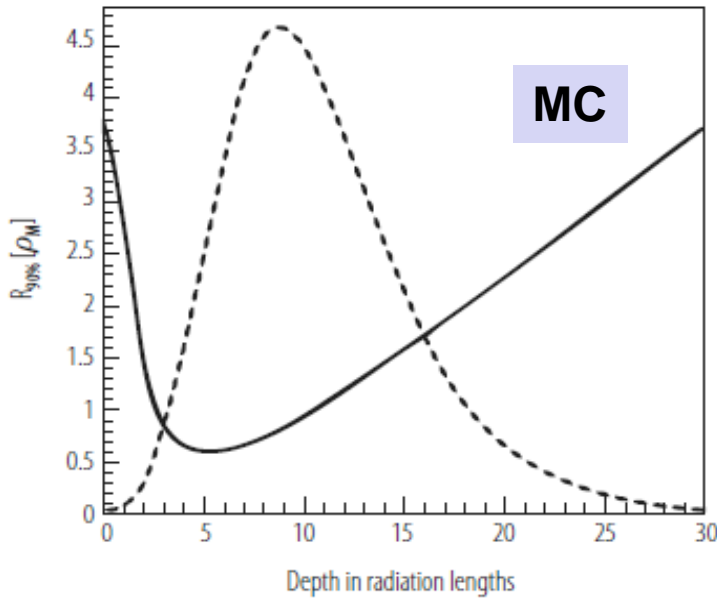
Molière Radius is defined as $R_m = 21 \text{ MeV} / E_c \cdot X_0$

Convenient parameter to estimate lateral shower containment

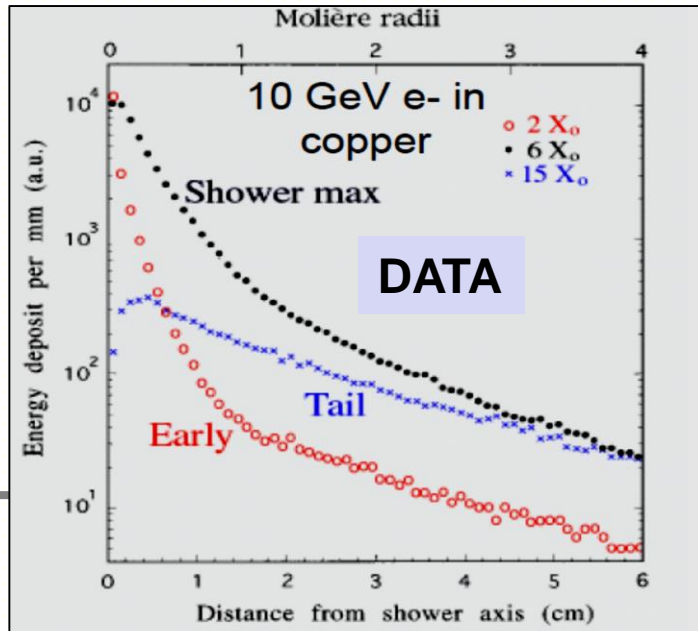
87 % (96%) of the energy of a electron shower are contained in 1 (2) R_m

Molière Radius governed by material density

Lateral shower development (2)



	R_m
Cu	15.2mm
Al	44 mm
Pb	16 mm



- Core of shower well described with R_m independently of the material (as X_0 in depth)
- Same lateral shower in Cu and Pb while longer depth by 2.5
- Tails at large distance. Z^5 dependence of photo electric cross section

Material properties

Material	Z	Density [g cm ⁻³]	ϵ_c [MeV]	X_0 [mm]	ρ_M [mm]	dE/dx mip [MeV cm ⁻¹]	λ_{int} [mm]
C	6	2.27	8.3	188	48	3.95	381
Al	13	2.70	43	89	44	4.36	390
Fe	26	7.87	22	17.6	16.9	11.4	168
Cu	29	8.96	20	14.3	15.2	12.6	151
Sn	50	7.31	12	12.1	21.6	9.24	223
W	74	19.30	8.0	3.5	9.3	22.1	96
Pb	82	11.30	7.4	5.6	16	12.7	170
U 238	92	18.95	6.8	3.2	10	20.5	105
Concrete		2.50	55	107	41	4.28	400
Glass		2.23	51	127	53	3.78	438
Marble		2.93	56	96	36	4.77	362
Si	14	2.33	41	93.6	48	3.88	455
Ar (liquid)	18	1.40	37	140	80	2.13	837
Kr (liquid)	36	2.41	18	47	55	3.23	607
Xe (liquid)	54	2.95	12	24	42	3.71	572
Polystyrene		1.032	94	424	96	2.00	795
Plexiglas		1.18	86	344	85	2.28	708
Quarz		2.32	51	117	49	3.94	428
Pb glass		4.06	15	25.1	35	5.45	330
Air (2C,1atm)		0.0012	87	304m	74m	0.0022	747m
H ₂ O		1.00	83	361	92	1.99	849
PbWO ₄		8.3		8.9	20	10.2	207
CeF ₃		6.16		16.8	26	7.9	259
LYSO		740		11.4	20.7	9.6	209

Formulae for compound material : $1/X_0 = \sum w_j / X_j$

Summary of useful definition

Energy loss by radiation :

$$\langle E(x) \rangle = E_0 e^{-\frac{x}{X_0}} \quad \gamma \text{ absorption (e+e-)} \quad \langle I(x) \rangle = I_0 e^{-\frac{7}{9} \frac{x}{X_0}}$$

Radiation length:

$$X_0 = \frac{180A}{Z^2} \frac{\text{g}}{\text{cm}^2}$$

Critical energy:

[Attention: Definition of Rossi used]

$$E_c = \frac{550 \text{ MeV}}{Z}$$

Shower maximum:

$$t_{\max} = \ln \frac{E}{E_c} - \begin{cases} 1.0 & e^- \text{ induced shower} \\ 0.5 & \gamma \text{ induced shower} \end{cases}$$

Longitudinal energy containment:

$$L(95\%) = t_{\max} + 0.08Z + 9.6 [X_0]$$

Transverse Energy containment:

$$R(90\%) = R_M$$

$$R(95\%) = 2R_M$$

$$R_M = (21 \text{ MeV} / E_c) \cdot X_0$$

$$\sim 1/Z * Z (Z/A)$$

Small dependence with Z

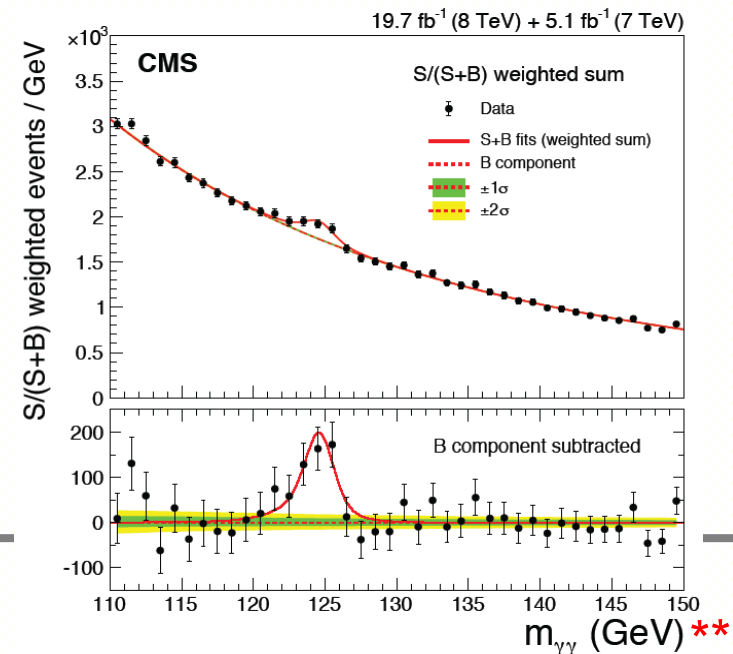
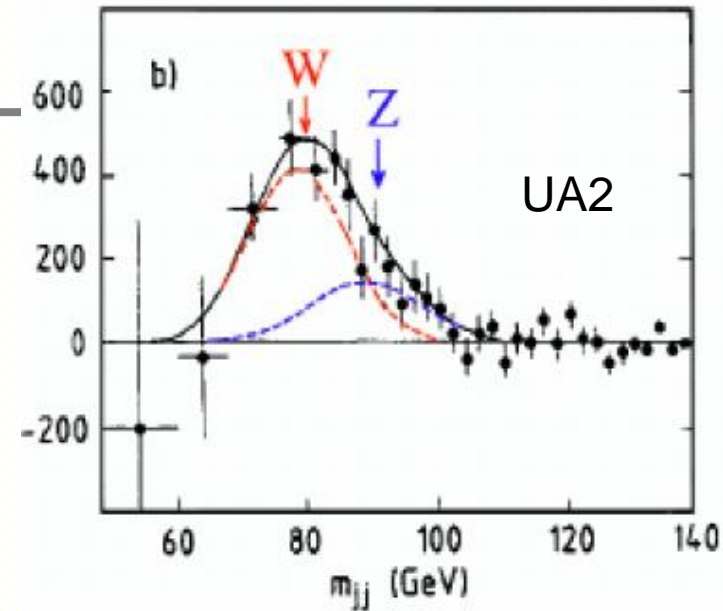
Energy resolution

Detectable visible energy subject to fluctuation
 → Finite energy resolution

$$\sigma(E) = \sqrt{\sigma_1^2 + \sigma_2^2 + \sigma_3^2} = \sigma_1 \oplus \sigma_2 \oplus \sigma_3$$

Most of the sources of fluctuation can be considered uncorrelated :

- Shower fluctuations
- Sampling fluctuations in sampling calorimeter
- Signal quantum fluctuations (photo detectors..)
- Leakage
- Noise in the readout
- Specific technology effects (recombination, light attenuation, gas saturation....)
- Specific to detector construction (mechanics tolerance, electronics response...)



Energy resolution

Usually parameterized as

$$\frac{\sigma}{E} = \frac{a}{\sqrt{E}} \oplus \frac{b}{E} \oplus c$$

▶ **a** stochastic term:

- ◆ intrinsic statistical shower fluctuations
- ◆ sampling fluctuations
- ◆ signal quantum fluctuations (e.g. photo-electron statistics)

▶ **b** is the noise term:

- ◆ electronic readout noise
- ◆ pileup noise in high luminosity environment: fluctuations of energy from sources other than the primary particle (e.g. particles from other collisions in the same or in previous bunch crossings)

▶ **c** is the constant term that incorporates all other systematics:

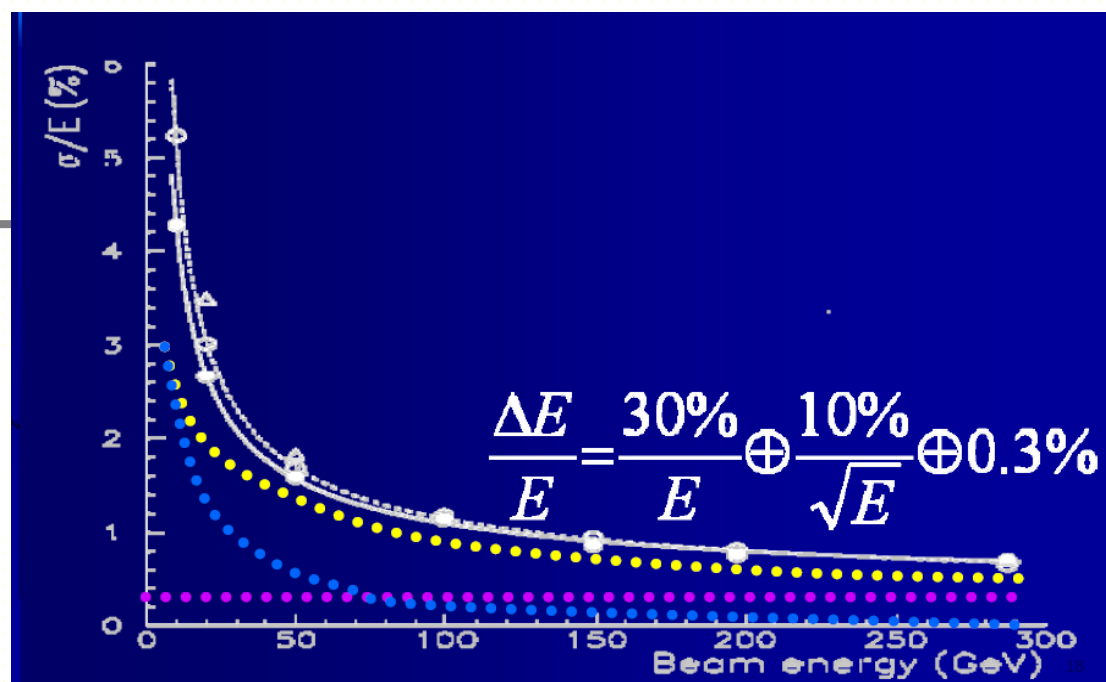
- ◆ detector response non-uniformity (hardware or calibration)
- ◆ imperfections in calorimeter construction and geometry (e.g. not fully hermetic, cracks...)
- ◆ longitudinal leakage
- ◆ energy lost in dead material upfront...
- ◆ dominant contribution at high energies

Energy resolution

Usually parameterized as

$$\frac{\sigma}{E} = \frac{a}{\sqrt{E}} \oplus \frac{b}{E} \oplus c$$

Quadratic sum !



Questions: which term is affected by:

- fluctuations in the # of particles in the shower? **$1/\sqrt{E}$ (a)**
- global scale (gain) shift? **1 (c)**
- electronics noise? **$1/E$ (b)**
- global offset (pedestal) shift? **$1/E$ (b)**
- shower particles escaping the calorimeter? **1^* also $1/\sqrt{E}$ if upstream**
- fluctuations in the # of photo-electrons detected ? **$1/\sqrt{E}$ (a)**
- pile-up (remnants of earlier events)? **$1/E$ (b)**
- radioactivity ? **$1/E$ (b)**
- presence of dead material? **1 (c)**
- statistical uncertainty of scale (gain) constants? **1 (c)**
- statistical uncertainty on offset (pedestal) constants? **$1/E$ (b)**

Electromagnetic calorimeter technologies :

Homogeneous calorimeters

Sampling calorimeters

Homogeneous calorimeters

- Combine both the role of absorber and signal generation.
- Total volume sensitive to the deposited energy. (Large fraction of visible energy)



Advantage

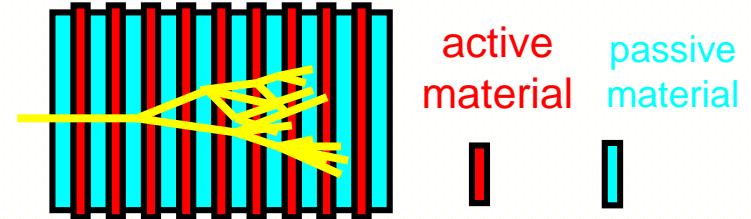
- Best energy resolution ($1/\sqrt{E}$ term) limited by physical factors as number of photo-electrons if ideal calo (no leakage)
- Intrinsically linear in principle
- Well suited for low energy application (nuclear spectroscopy, medical application...)

Disadvantage

- Limited segmentation (especially in depth)
- Can not be used for hadronic shower to keep "reasonable" detector size.
- Cost (Pb or Cu less expensive than crystals, Silicon or noble liquid)

Sampling calorimeters

- Shower is sampled in active layers interleaved with absorbers

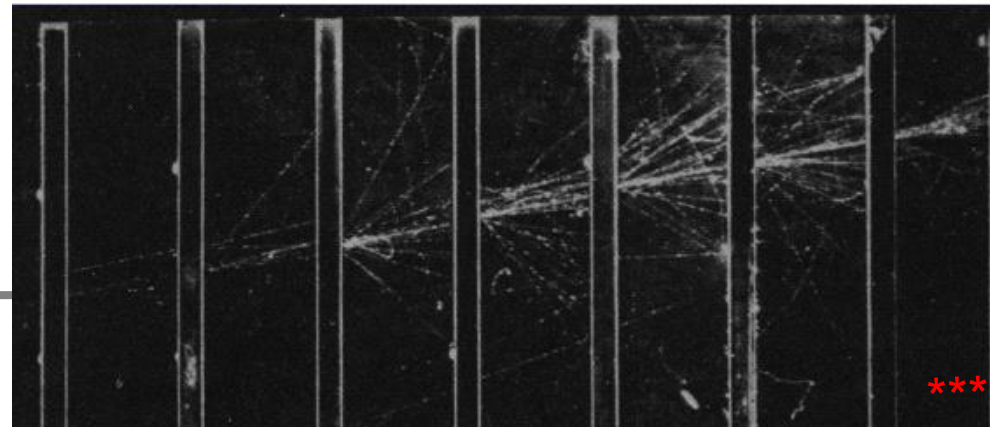


Advantage

- Can achieve easily lateral and longitudinal segmentation
- Angular measurement and particle Identification
- cheaper calorimeter (in principle !) as absorber not too expensive
- Only possibility for Hadron calorimeters

Disadvantage

- Small fraction of energy seen
- Stochastic term degraded

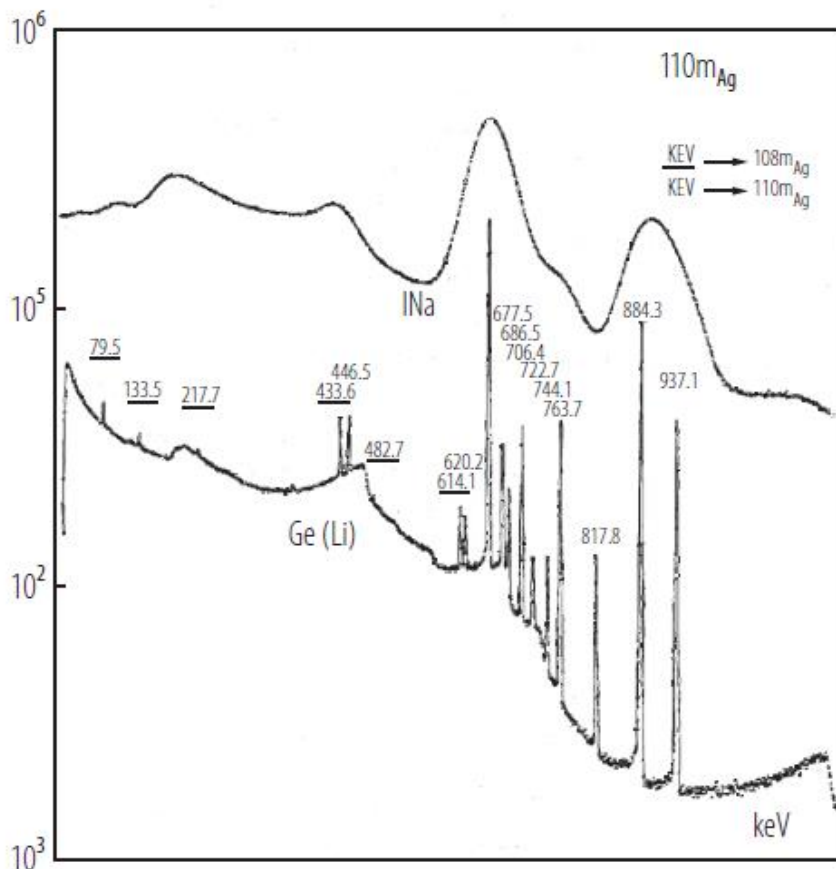


Homogeneous calorimeter technology

Should be dense enough to contain EM shower, give enough signal

- **Semiconductor Si, Ge** : very low threshold to create electron-hole pair (2.9 eV in Ge)
→ *Use in nuclear spectroscopy, medical application*
- **Cerenkov** : high refractive index induces cerenkov light with relativistic charged particle
→ *Lead glass, OPAL @LEP*
- **Scintillators** : ionisation tracks converted in light in crystals (fluorescence)
→ *NaI(Tl) (Crystal Ball), L3 (BGO), Babar, Belle, KTeV (CsI), PbWO₄ (CMS)*
- **Noble Liquids** : cryogenics detectors. Ionisation produces charge and light (scintillation)
→ *Kr (NA48, KEDR)*

Si/Ge low energy homogeneous calorimeters



Ge : energy to create an electron-hole pair at 77 K : 2.9 eV

1 MeV \rightarrow $N = 3.4 \cdot 10^5$ pairs

$\sigma_E/E \sim 1/\sqrt{N} = 0.17\%$

Even better due to Fano factor (pairs created not statistically independent, constrained by total energy of incident particle, similar to binomial variance) $F = 0.13$ in Ge

$\sigma_E/E \sim \sqrt{(F/N)} = 0.06 \%$

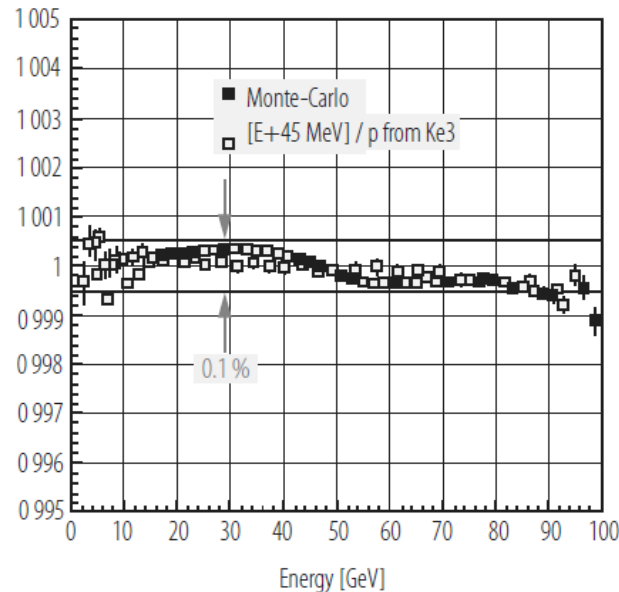
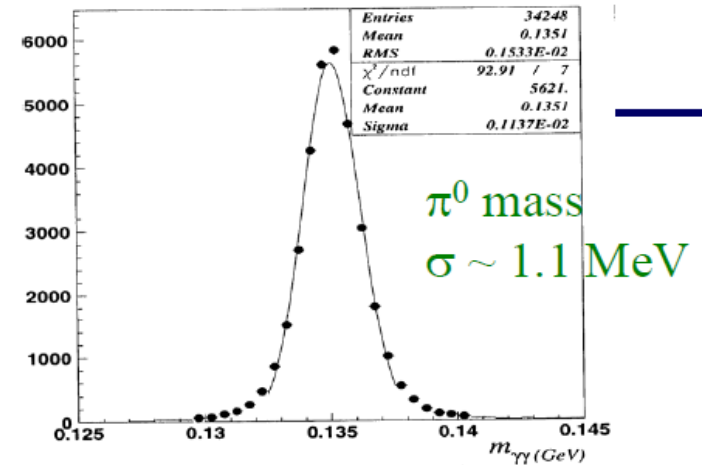
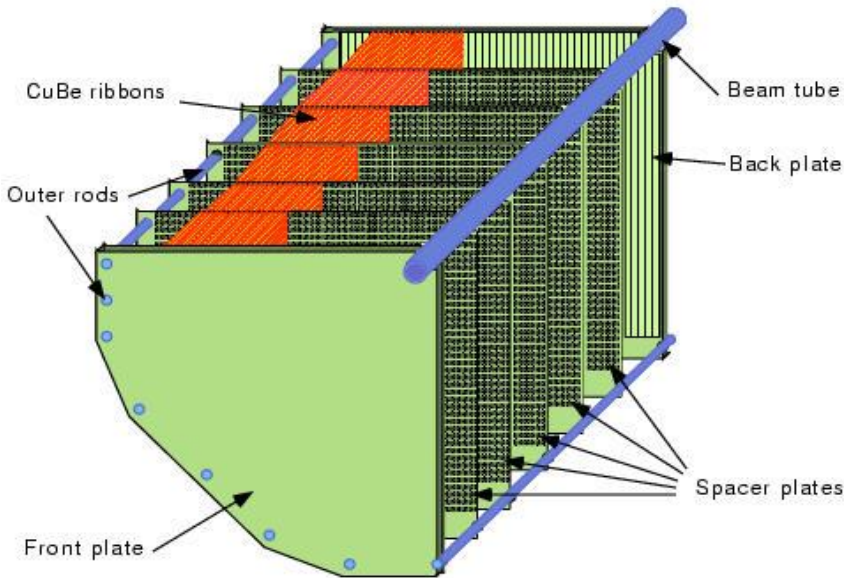
Popular detectors in Nuclear physics (AGATA for instance)

Noble liquid homogeneous calorimeters

NA48 : Fixed target experiment for CP violation, and now NA62 rare Kaon decays
 1 MeV resolution needed on π^0 mass

Liquid Krypton @ 120 K

LKr CALORIMETER ELECTRODE STRUCTURE



Linearity as important as resolution

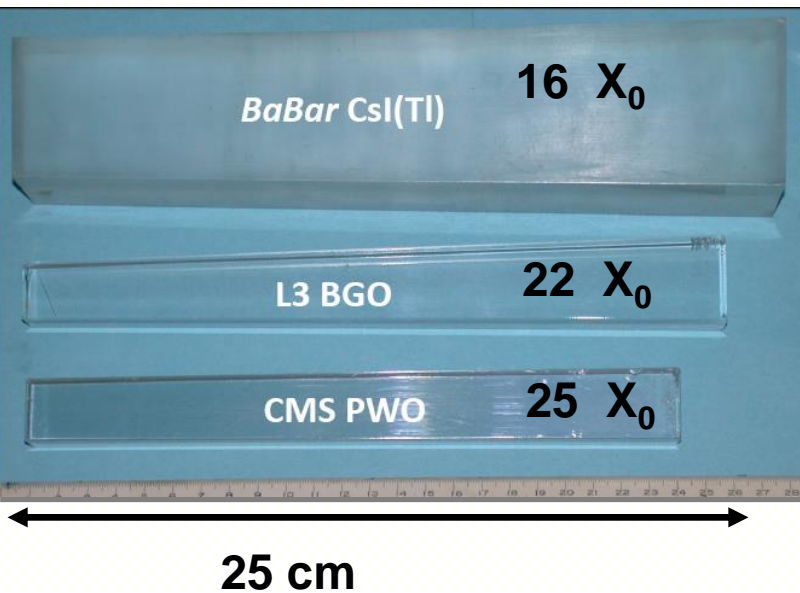
Need a careful control of upstream dead material

Homogeneous crystals calorimeters

Crystal	light	ρ [g/cm ³]	X_0 [cm]	τ [ns]	λ [nm]	Output	Damage (Gy)
NaI	Scint	3.67	2.59	250	410	1 (40000 ph/MeV)	10
BGO	Scint	7.13	1.12	300	410	0.15	10 *
BaF ₂	Scint	4.89	2.05	600	310	0.20	10 ⁵ *
CsI (TI)	Scint	4.53	1.85	35 (1000)	420	0.05 (0.45)	10 ³
PbWO ₄	Scint	8.28	0.89	5-15	430	0.01	10 ⁴ *
CeF ₃	Scint	6.16	1.68	10-30	325	0.10	
Pbglas5	Cer	4.08	2.54	fast	< 350	0.00015	
Pbglas6	Cer	5.20	1.69	fast	< 350	0.00023	

* Hygroscopy ~2%/°C *

Homogeneous crystals calorimeters



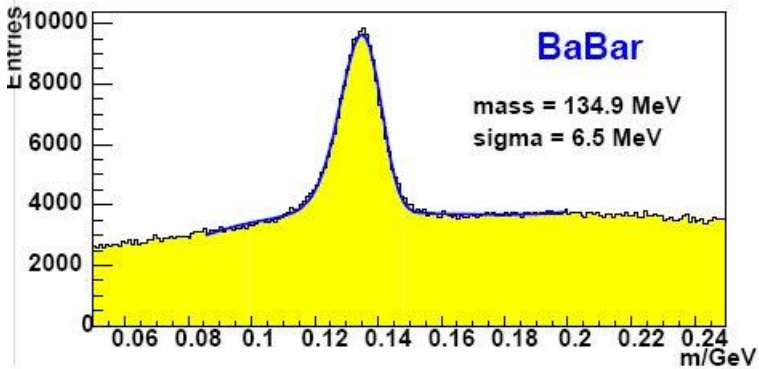
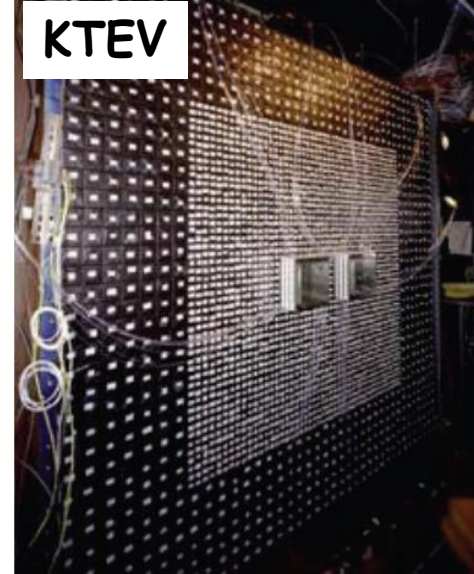
Growing crystals not always easy task
By construction non uniform response from one crystal to another (up to 10-20%), different transparency

Homogeneous crystals calorimeters

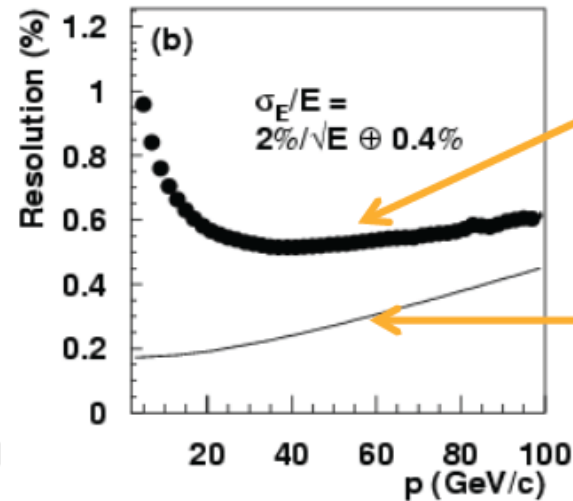
Babar



KTEV



$$\frac{\sigma_E}{E} = \sqrt{\left(\frac{0.066\%}{E_n}\right)^2 + \left(\frac{0.81\%}{\sqrt[3]{E_n}}\right)^2 + (1.34\%)^2}, \quad E_n = E/\text{GeV},$$



E/P resolution

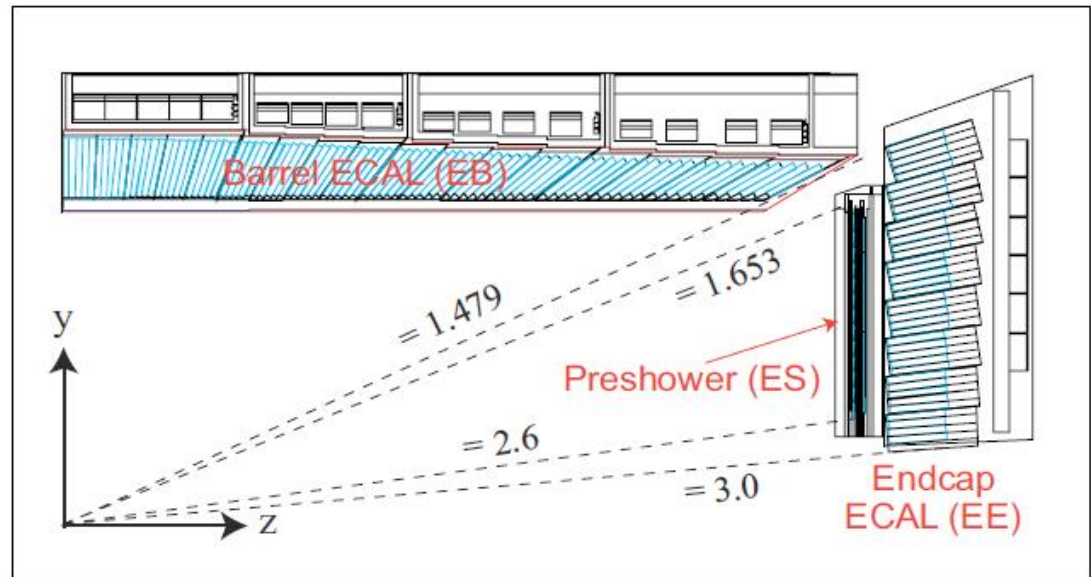
Estimated momentum resolution

CMS calorimeter

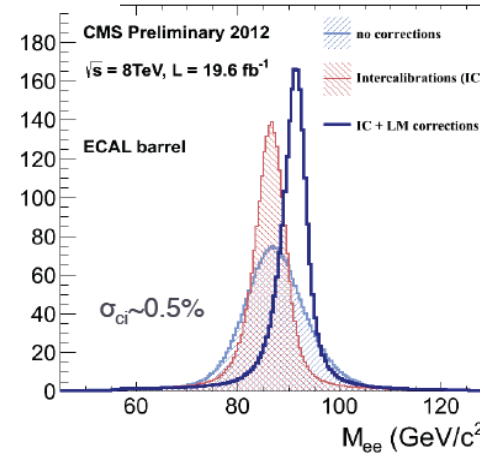
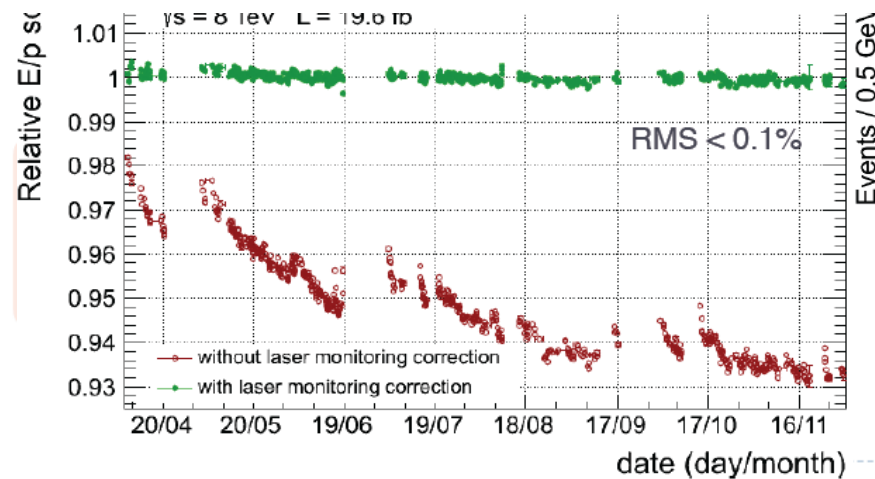
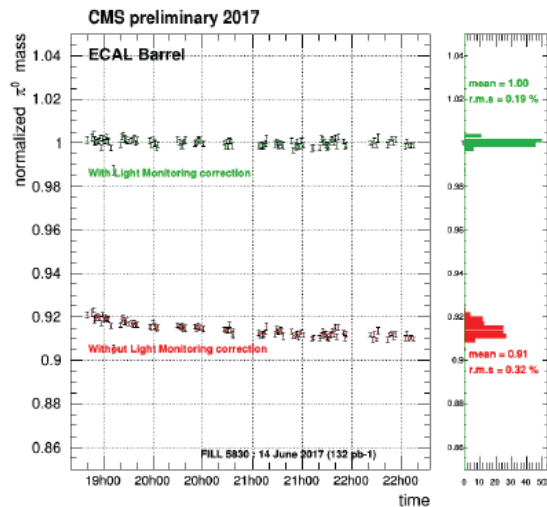
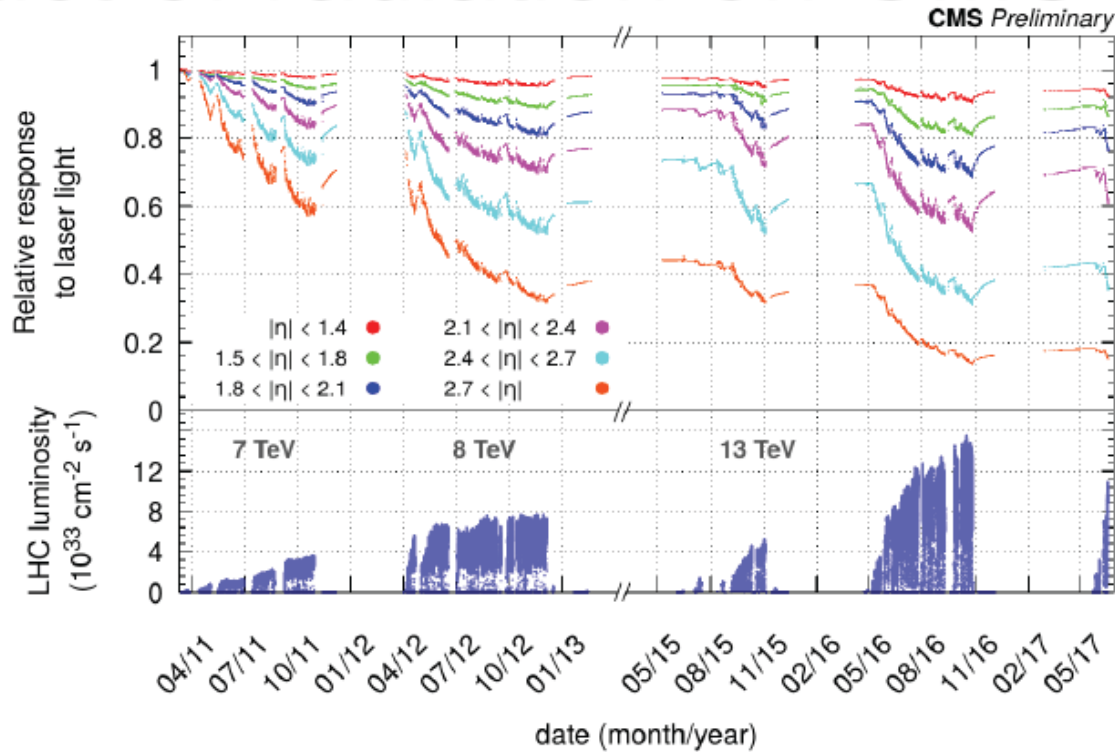


Scintillator : PbWO_4 [Lead Tungsten]
Photosensor : APDs [Avalanche Photodiodes]

Number of crystals: ~ 70000
Light output: 4.5 photons/MeV



Impact of radiation on CMS calo



Performance of homogeneous calorimeters

Technology (Experiment)	Depth	Energy resolution	Date
NaI(Tl) (Crystal Ball)	$20X_0$	$2.7\%/E^{1/4}$	1983
Bi ₄ Ge ₃ O ₁₂ (BGO) (L3)	$22X_0$	$2\%/\sqrt{E} \oplus 0.7\%$	1993
CsI (KTeV)	$27X_0$	$2\%/\sqrt{E} \oplus 0.45\%$	1996
CsI(Tl) (BaBar)	$16-18X_0$	$2.3\%/E^{1/4} \oplus 1.4\%$	1999
CsI(Tl) (BELLE)	$16X_0$	1.7% for $E_\gamma > 3.5$ GeV	1998
PbWO ₄ (PWO) (CMS)	$25X_0$	$3\%/\sqrt{E} \oplus 0.5\% \oplus 0.2/E$	1997
Lead glass (OPAL)	$20.5X_0$	$5\%/\sqrt{E}$	1990
Liquid Kr (NA48)	$27X_0$	$3.2\%/\sqrt{E} \oplus 0.42\% \oplus 0.09/E$	1998

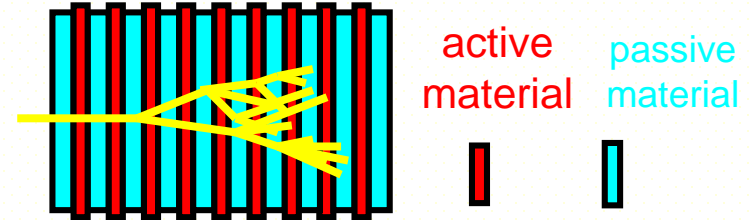
Homogeneous

For crystals/Cerenkov stochastic term contains both shower fluctuation and photo-electron statistics (converting photons in electrical signal).

Example : Lead Glass : Cerenkov only if e^\pm with $E > 0.7$ MeV and photon-detector provides 1000 photo-electrons/GeV
 Expected resolution for 1 GeV ? \rightarrow stochastic term ?

Sampling calorimeters

- Shower is sampled in active layers interleaved with absorbers

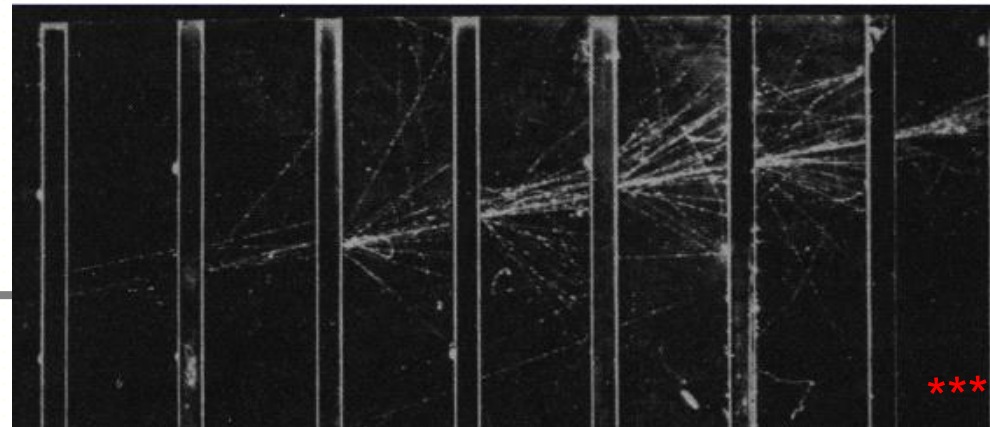


Advantage

- Can achieve easily lateral and longitudinal segmentation
- Angular measurement and particle Identification
- cheaper calorimeter (in principle !) as absorber not too expensive
- Only possibility for Hadron calorimeters

Disadvantage

- Small fraction of energy seen
- Stochastic term degraded



EM sampling calorimeter technology

Absorber with dense material with low critical energy (high Z) for shower development (U, Pb, W...). All technologies possible for active layers :

- **Scintillators**
→ U + scint (Zeus@Hera) , Pb + scint (CDF@Tevatron)
- **Gaseous detectors**
→ Pb + wire chambers (ALEPH@LEP)
- **Liquid Argon :**
→ LAr + Pb (Cello , NA31, SLD, H1@Hera, ATLAS@LHC)
→ LAr + U (D0@Tevatron)
Kr considered as option at SSC & LHC
- **Semiconductors**
→ Si+W (Pamela, Calice@ILC, CMS HGCal@HL-LHC)

Sampling calorimeter

Simplified model of previous :
Active medium : counts only charged particle produced in absorber shower development.
 $N_{max} = E/E_c$, 2/3 are charged particles

Pb : $E_c = 7.4$ MeV
For 1 GeV shower, $N_{ch} \sim 90$
 $\sigma(N_{ch})/N_{ch} = 1/\sqrt{N_{ch}} = 10\%$
Typical best stochastic term of sampling EM calorimeter

Key parameters :

Sampling frequency : Number of times a high energy electron/ γ is sampled. Linked to absorber thickness (t).

Thinner is t, higher is the sampling frequency, better is the resolution, but if too small correlated signals in two active layers

Sampling fraction : Fraction of energy deposited by a mip in active layer

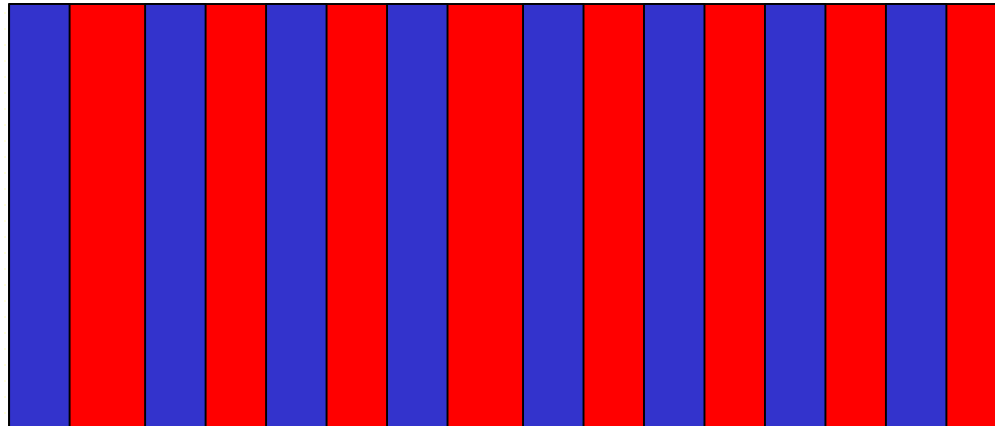
$$f_{smp} = \frac{E_{mip}(active)}{E_{mip}(active) + E_{mip}(absorbeur)}$$

$E_{mip} = (dE/dx) * distance$
t for passive material, s for active

Fractional energy response $f_R = (E_{active}) / (E_{active} + E_{passive})$ (includes showering process)

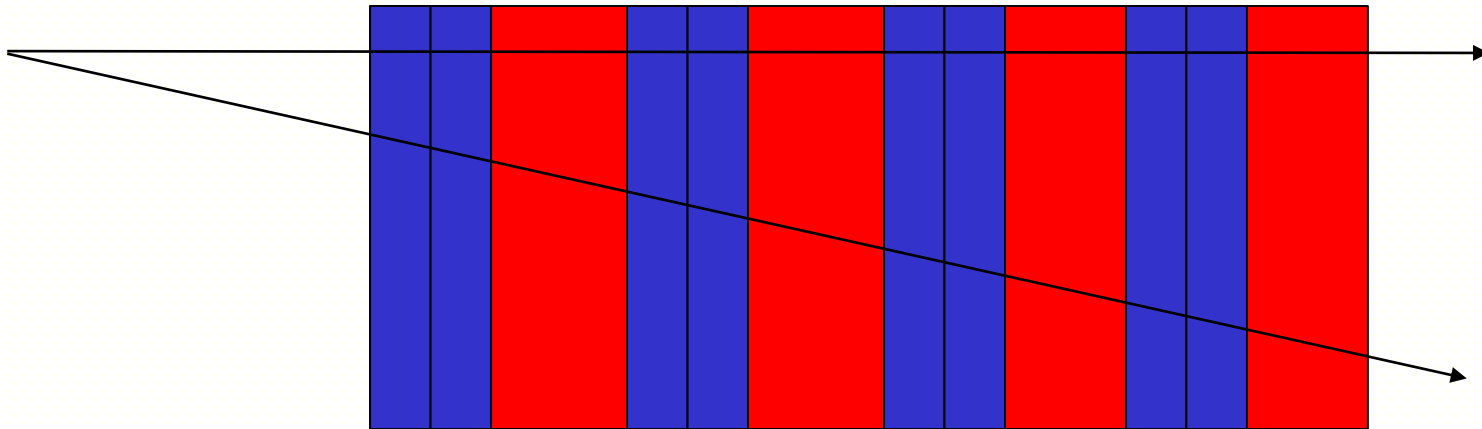
Sampling Calorimeter

Blue absorber (t) , red active medium (s)



Sampling Calorimeter

Blue absorber (t) , red active medium (s)



Same sampling fraction but smaller sampling frequency

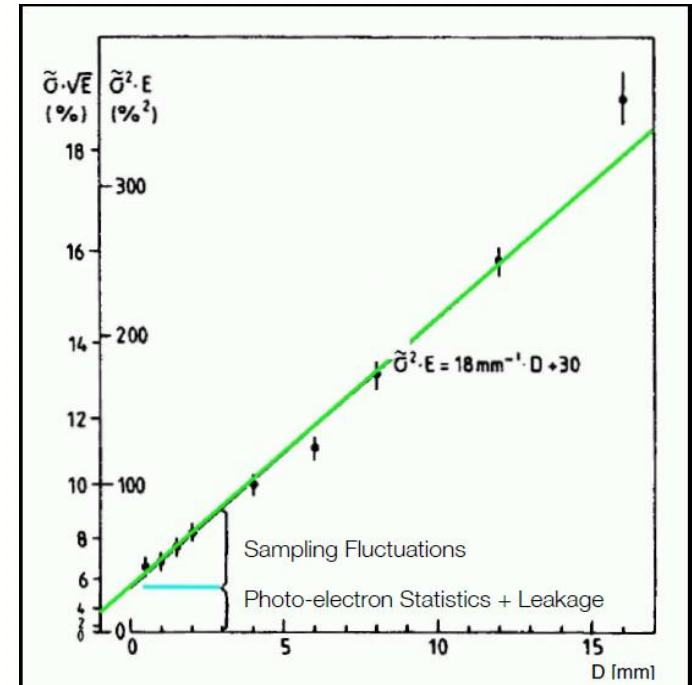
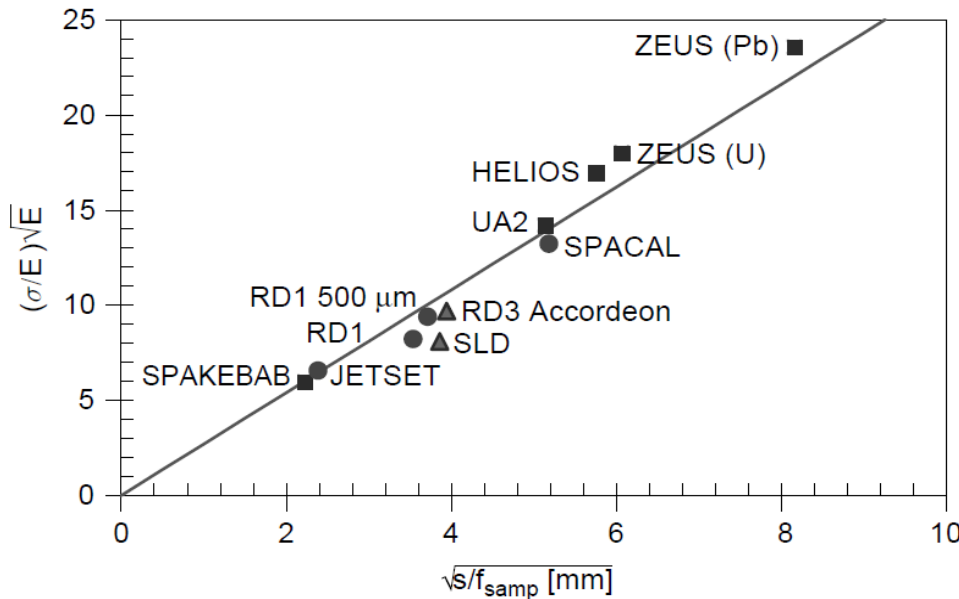
(4 / 8) \rightarrow worse stochastic term

Angular effect : constant sampling fraction but smaller frequency

EM sampling calorimeter E resolution

Total track length detectable $\rightarrow T_d = f_{\text{samp}} \cdot T$

\rightarrow expect energy resolution as $1/\sqrt{T_d} \sim 1/\sqrt{f_{\text{samp}}}$

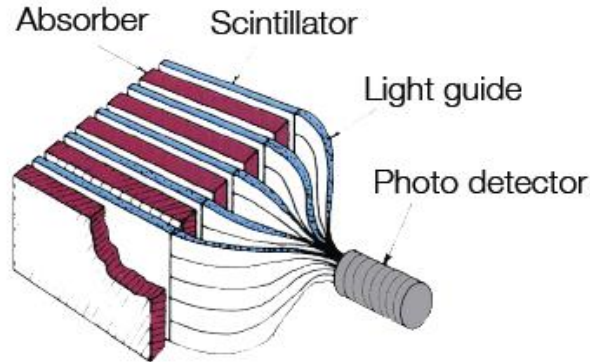


$$\frac{\sigma_{\text{samp}}}{E} = \frac{2.7\%}{\sqrt{E [\text{GeV}]}} \sqrt{\frac{s [\text{mm}]}{f_{\text{samp}}}}$$

$$\frac{\sigma E}{E} = 3.2\% \sqrt{\frac{E_c [\text{MeV}] \cdot t_{\text{abs}}}{F \cdot E [\text{GeV}]}}$$

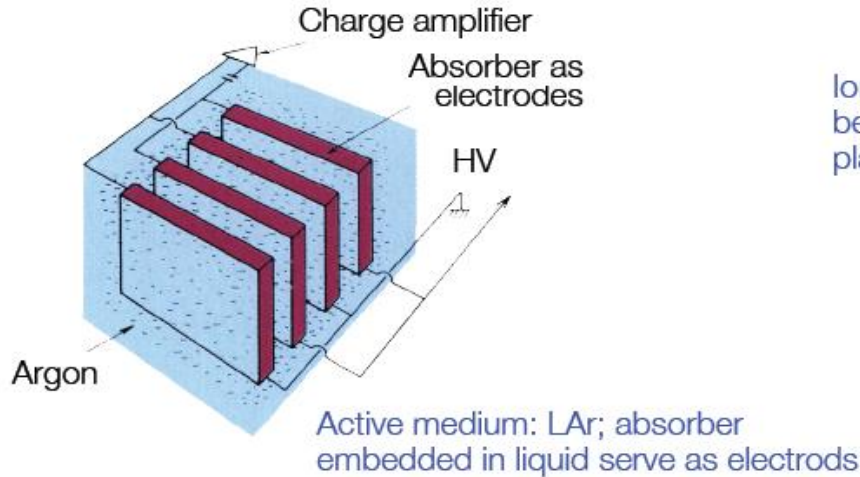
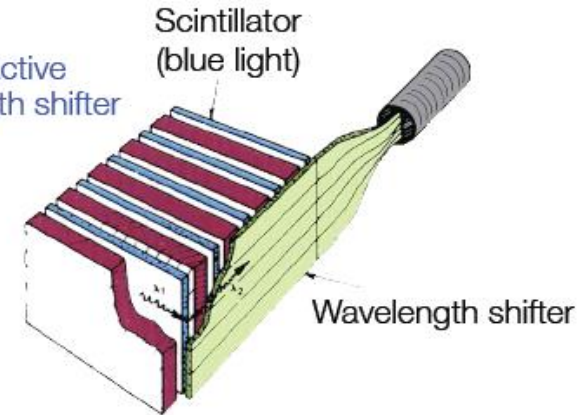
EM sampling calorimeter examples

Scintillators as active layer;
signal readout via photo multipliers

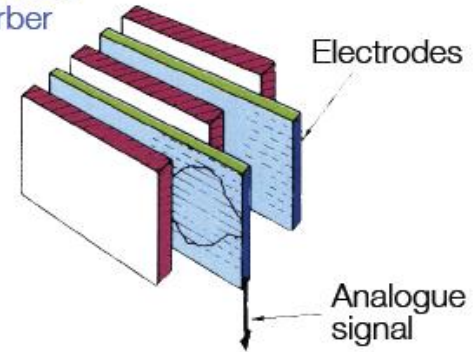


Possible setups

Scintillators as active layer; wave length shifter to convert light



Ionization chambers
between absorber
plates

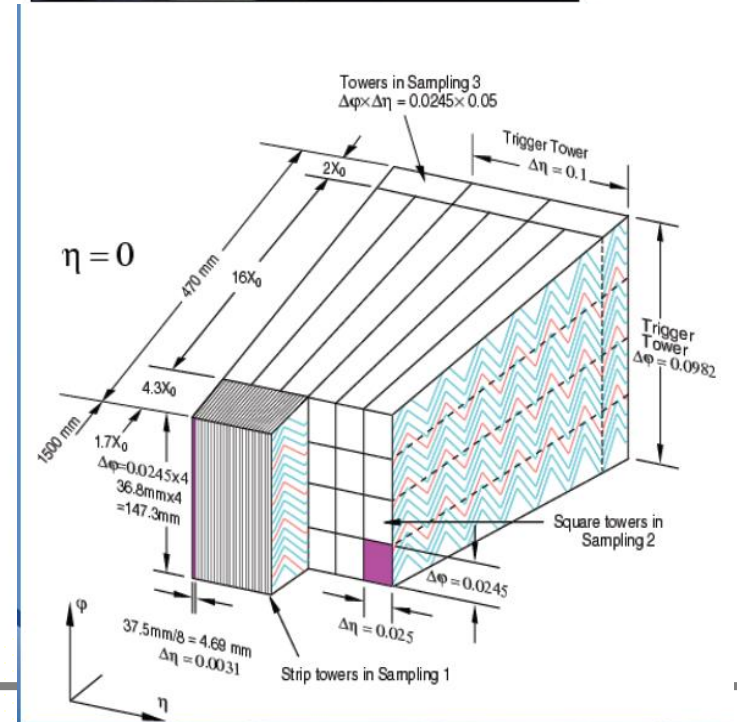
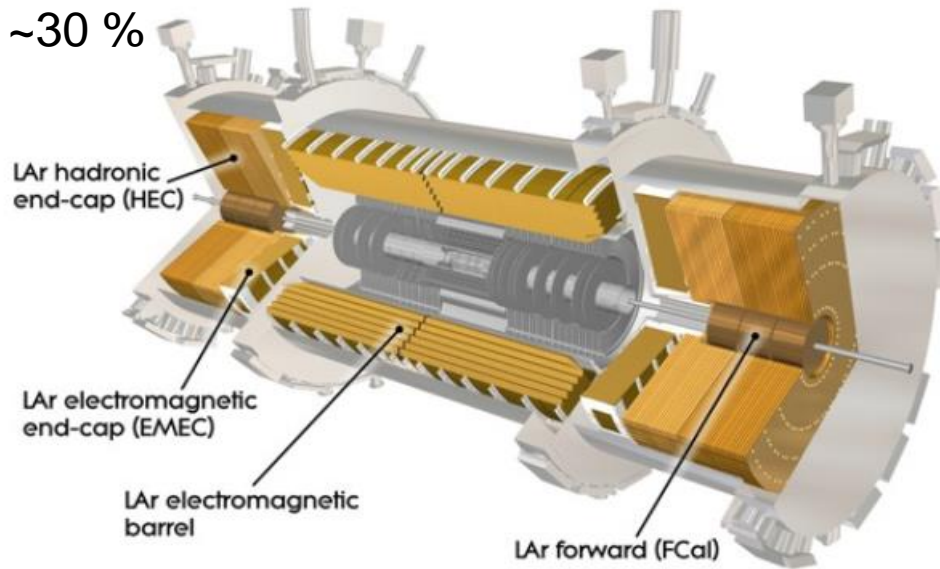


ATLAS Lar EM Calorimeter

Example:
ATLAS Liquid Argon Calorimeter

Main optimisation : constant term and γ/π^0 separation

$f_{\text{samp}} \sim 30\%$



Trigger parenthesis

e/γ

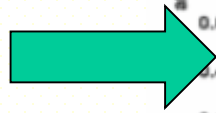
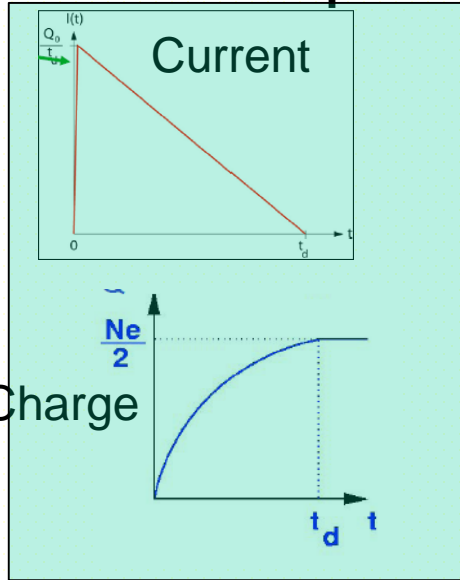
Reconstruction

Calibration

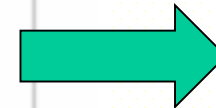
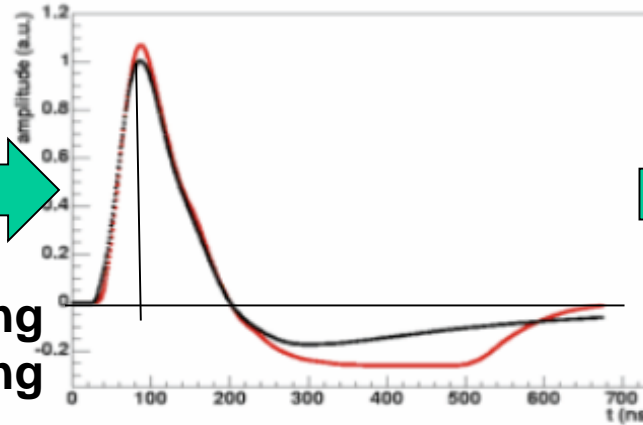
Performance

From signal cell to cell energy (1)

Detector output



**Filtering
Shaping**



Digitisation

Amplitude
digitised on
n bits : adc counts
12 bits : 0-4096
(when no signal,
measure pedestal)

$$E_{\text{cell}} = F(\mu\text{A} \rightarrow \text{MeV}) \times F(\text{adc} \rightarrow \mu\text{A}) \times (\text{adc-ped})$$

$F(\text{adc} \rightarrow \mu\text{A})$: take into account electronics chain gain.

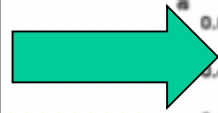
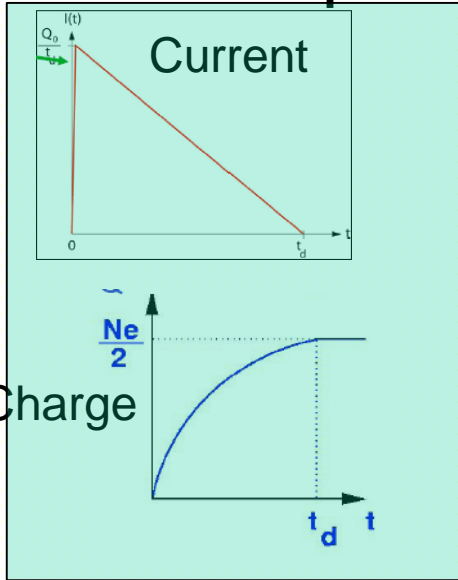
Calibration system can be laser signal in a crystal or inject charge at detector output as similar as possible to signal (but residual bias !)

Measure or correction for linearity. To be done for all channels !

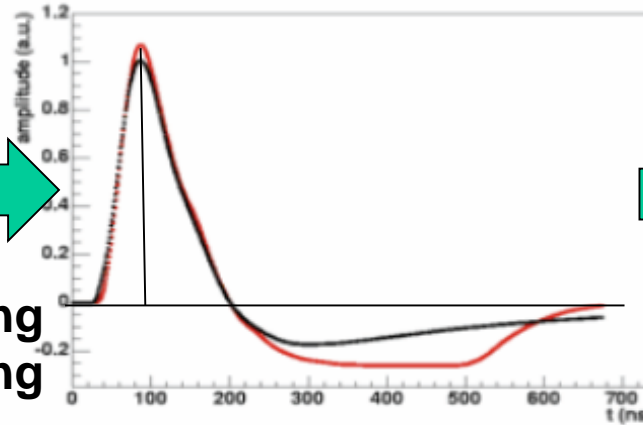
Stability measurement with time / temperature

From signal cell to cell energy (2)

Detector output



**Filtering
Shaping**



Digitisation

Amplitude
Coding on
n bits : adc
(when no signal,
Measure pedestal)

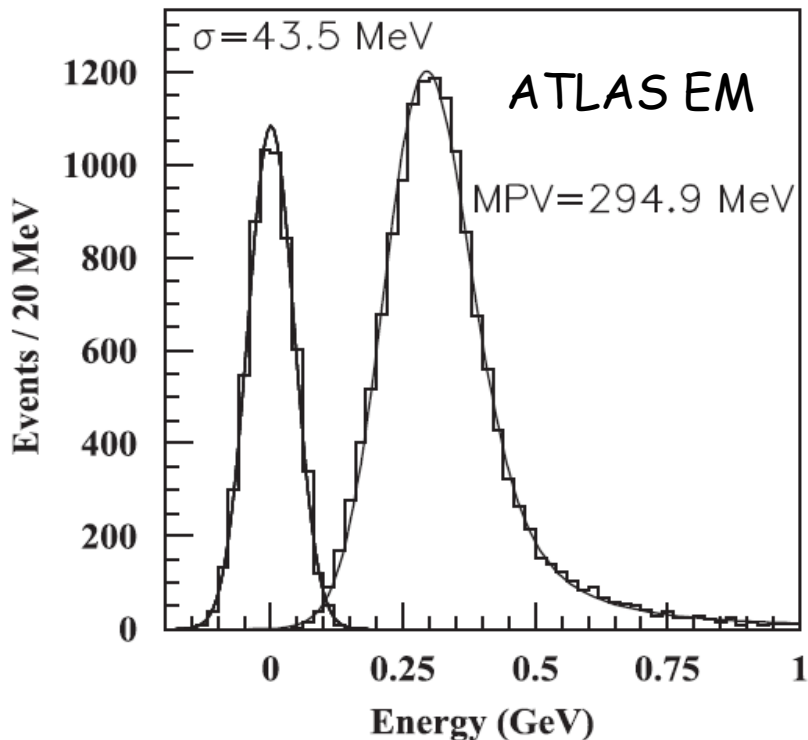
$$E_{\text{cell}} = F(\mu\text{A} \rightarrow \text{MeV}) \times F(\text{adc} \rightarrow \mu\text{A}) \times (\text{adc-ped})$$

$F(\mu\text{A} \rightarrow \text{MeV})$: Can be computed from first principles to 5-10% but not enough accurate (for sampling calorimeters includes sampling fraction)
Usually extracted from beam test with prototype by shooting and reconstructing particles of well know energy
Still not accurate ultimately.....

μ (mip) signal in calorimeter

Muons will not produce showers in calorimeter but deposit Minimum Ionizing Particle energy (dE/dx at minimum)

- Can be used for rough calibration / Inter calibration / time dependence
- Difficult to extract absolute EM energy scale as e/μ for mip $\neq 1$
- Landau spectrum with high energy tail, characterized by Most Probable Value
- Useful quantify is $S/N = MPV/\sigma$ to qualify electronics readout/noise



Shower energy reconstruction

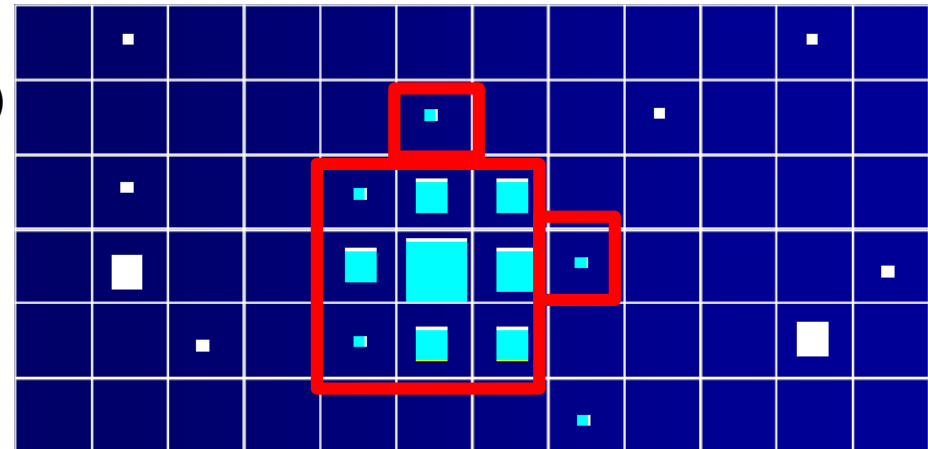
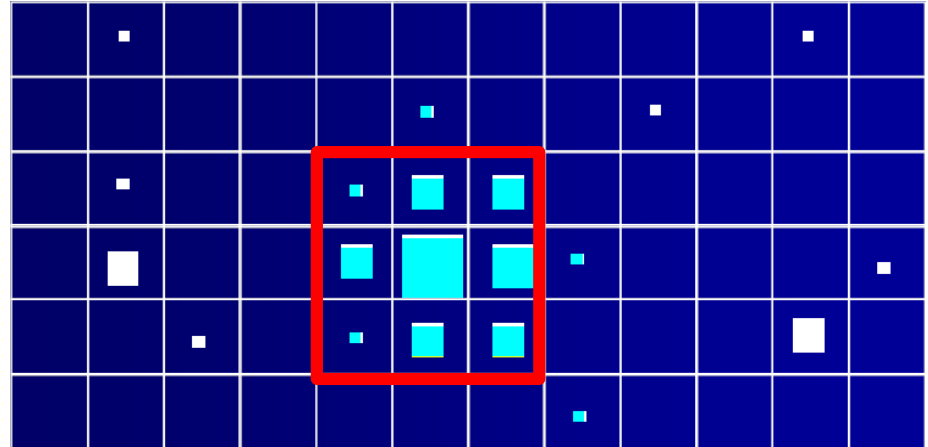
Fixed cluster size :

- Large enough to contains >95 % of EM shower energy
- Small enough to minimize noise and shower separation

$$(\sigma_{\text{noise}} = N_{\text{cells}} \sigma_{\text{inco}} \oplus N_{\text{cells}}^2 \sigma_{\text{coh}})$$

Fast and easy algorithm

Em shower + noise (or other particle)

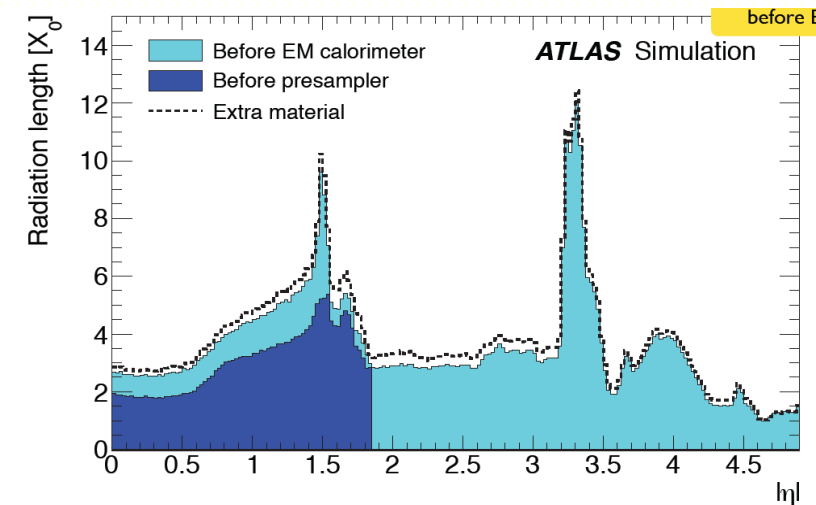
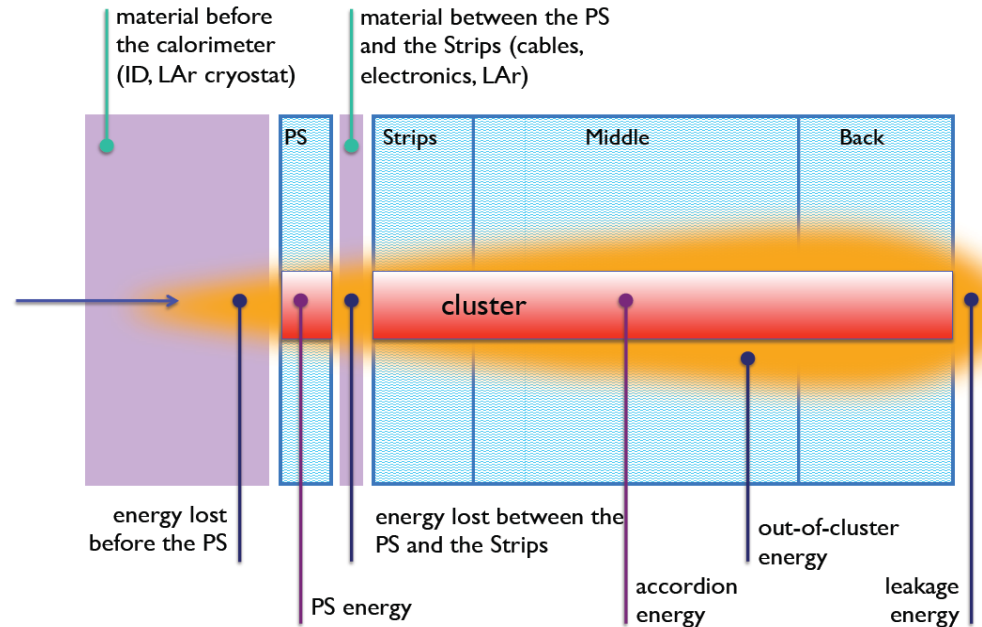
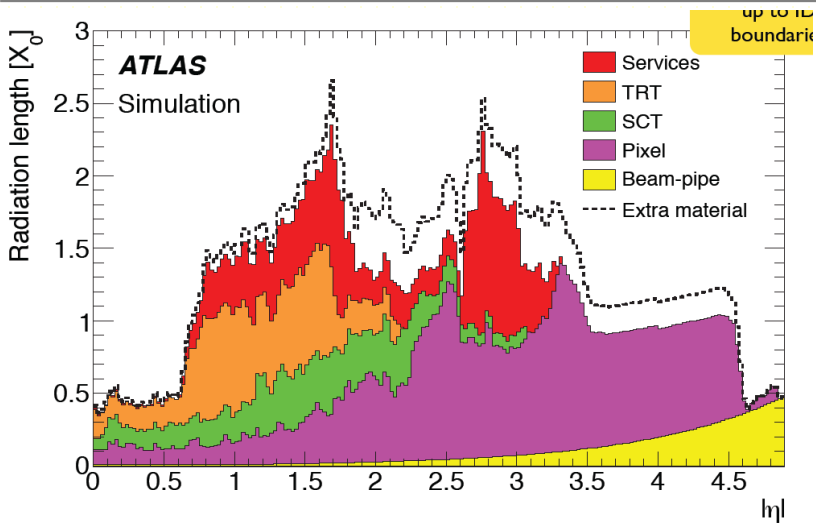


Topological algorithm :

- Consider all cells with $E > E_{\text{cut}}$ (3σ noise)
- Start from a seed (max)
- Add neighbour cell if $E > E_{\text{cut}}$

Iterative process. Can achieve same energy resolution but more difficult for linearity (calibration) and noise contribution (different from one shower to another)

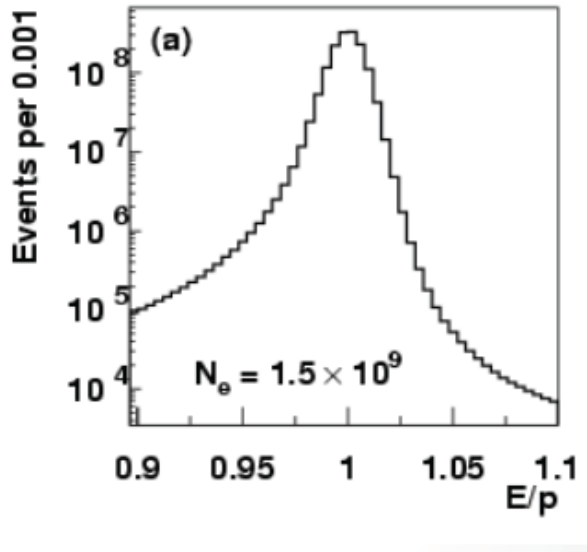
From cluster to particle energy



Energy lost upstream, laterally and longitudinally for any calorimeter
+presampler for ATLAS

In situ particle energy calibration

- Can use $E(\text{cal})/p(\text{tracker})$ if material upstream uniform and not large



Example of KTeV CsI calorimeter :

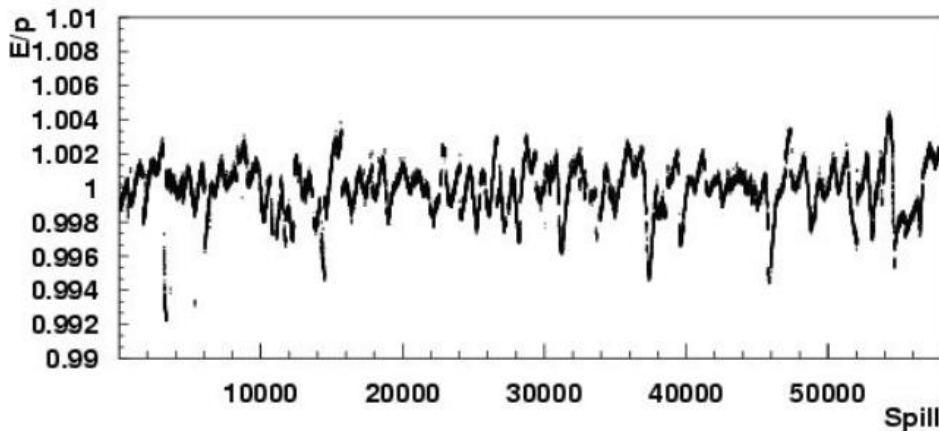
use electrons from $K_L \rightarrow \pi e \nu$

Set absolute energy scale

Crystal to crystal calibration

Time dependence of signals

Quite difficult at LHC with material variation along $\eta \rightarrow E/p$ distribution with too many tails



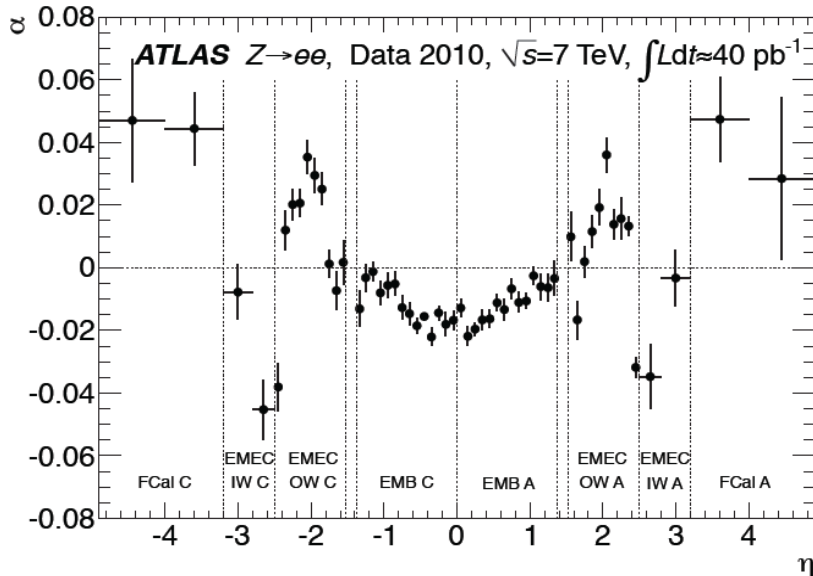
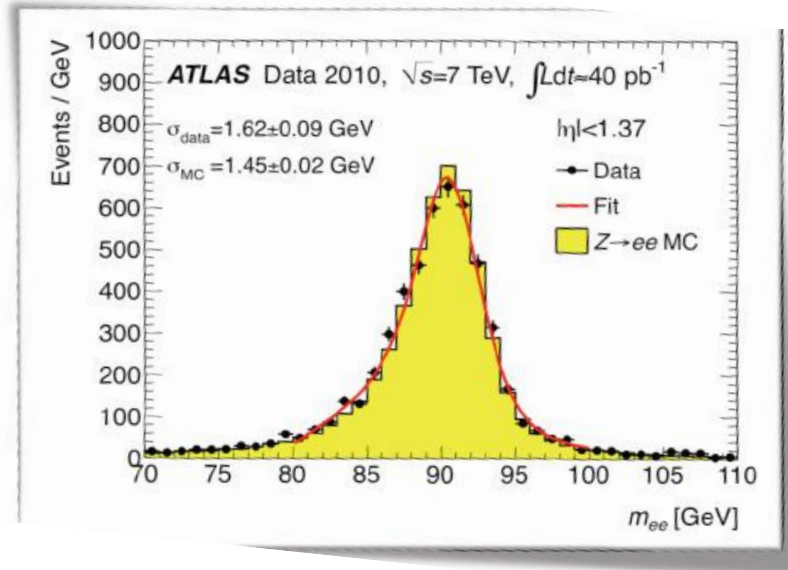
In situ particle energy calibration (3)

- Use mass constraint on well known particle : $Z \rightarrow e+e-$ @ LHC

$$m = \sqrt{2E_1 E_2 (1 - \cos(\theta_{12}))}$$

$$E^{\text{corr}} = E (1 + \alpha_i)$$

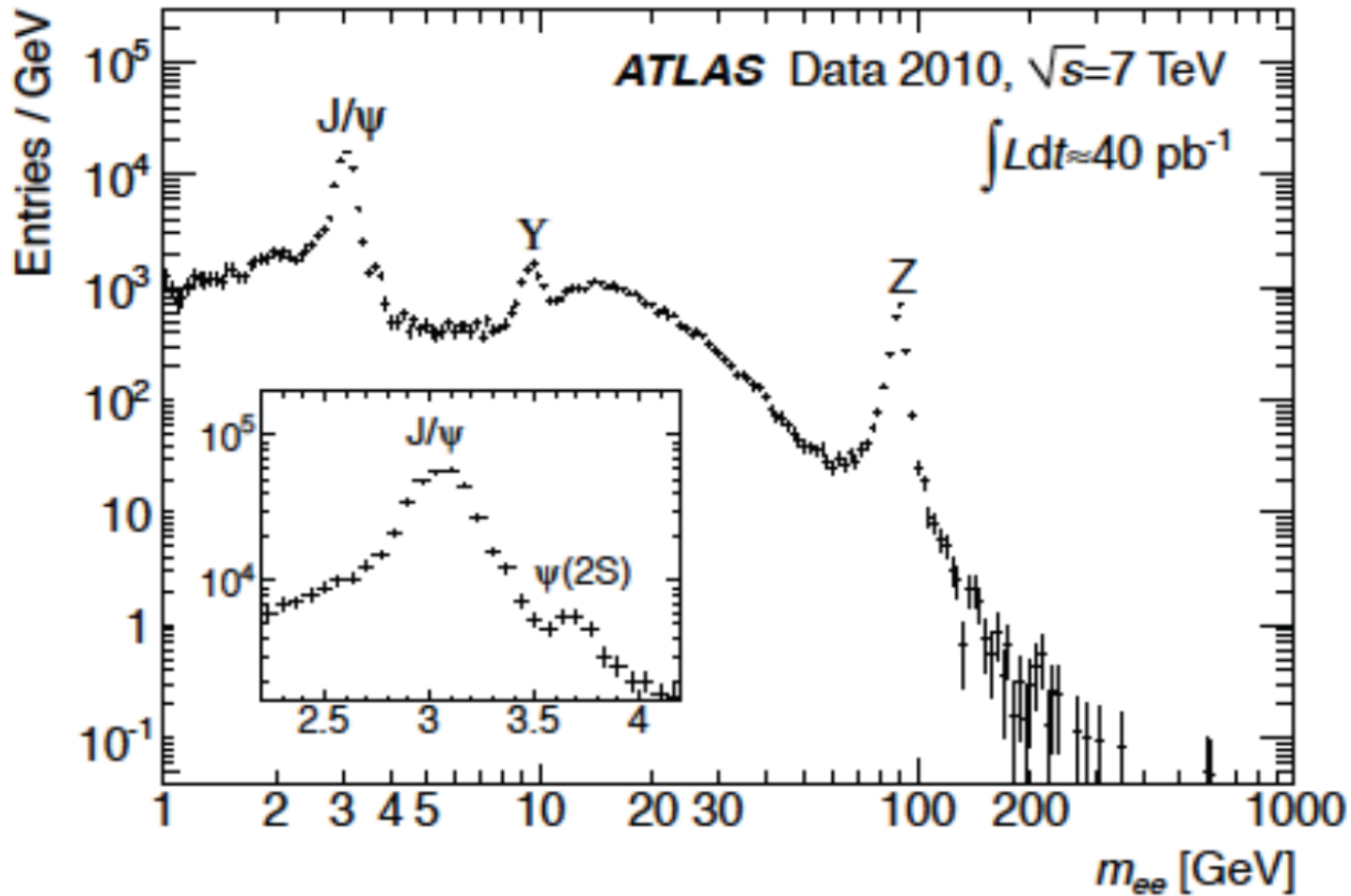
$$m_{ij}^{\text{corr}} \simeq m_{ij} \left(1 + \frac{\alpha_i + \alpha_j}{2} \right)$$



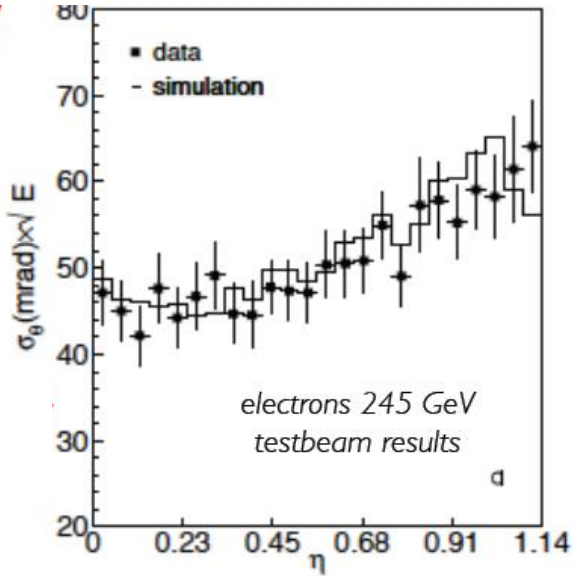
With more stat :

- Reduce region for each α + along φ
- Can use $J/\psi \rightarrow e+e-$ for low energy (linearity)
- Needs to extrapolate γ from simulation or $Z \rightarrow ee\gamma/\mu\mu\gamma$

e^+e^- resonances



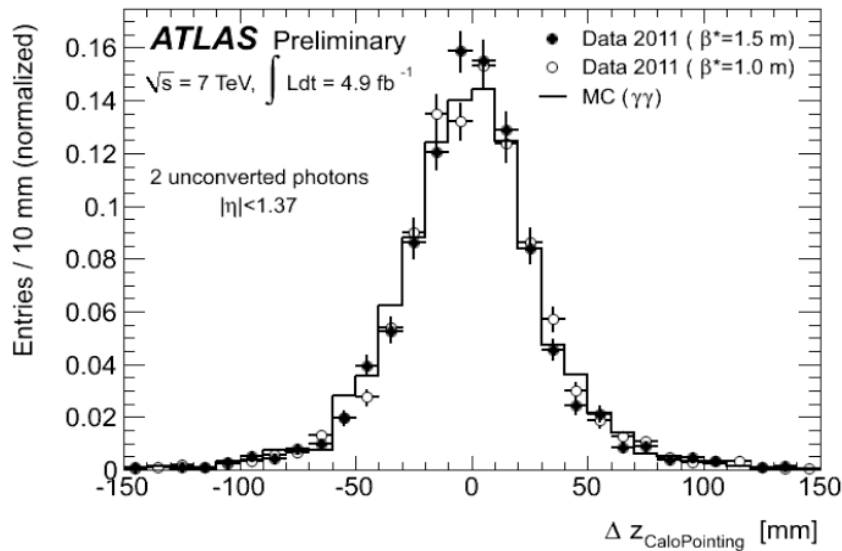
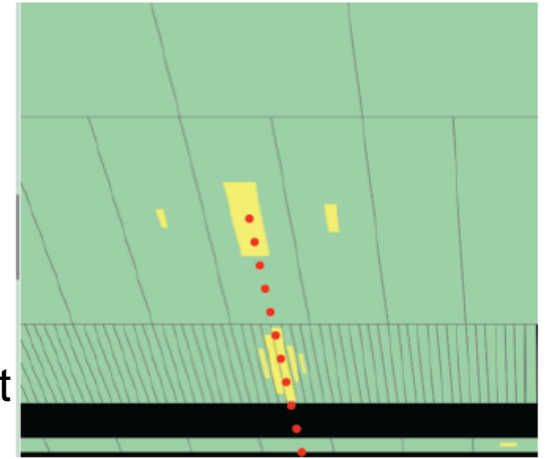
Photon pointing in ATLAS



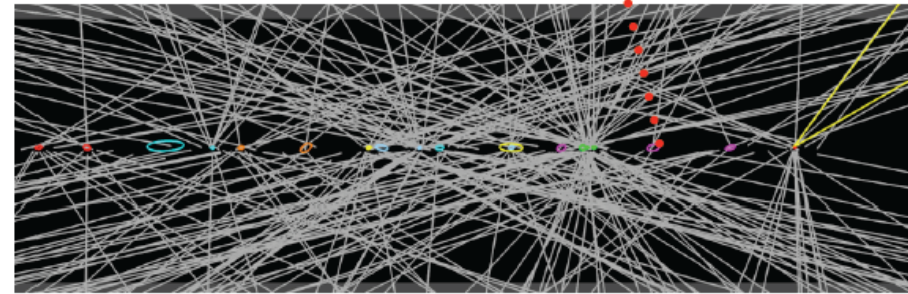
Barycentre in strips and middle section
 → Angular measurement

$$\sigma_\theta = 60 \text{ mrad}/\sqrt{E} [\text{GeV}]$$

Z vertex position measurement



(not to scale)



Zoom on collision interaction

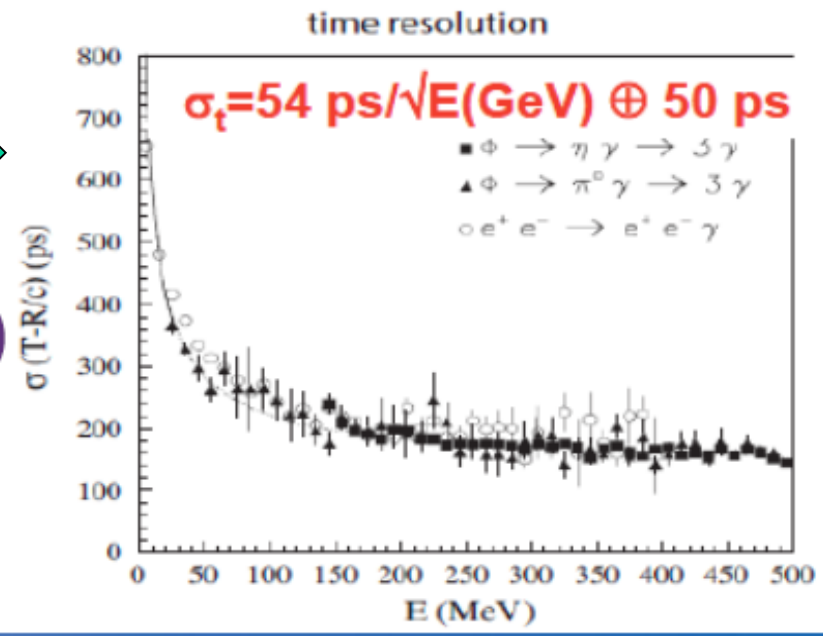
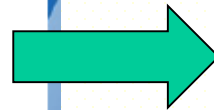
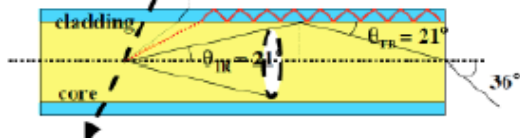
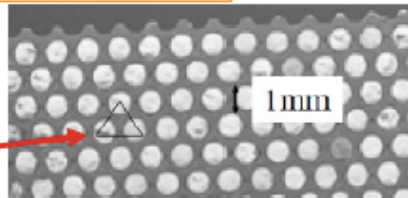
Timing resolution

Shower (electron/photon) time measurement can also be achieved, can be useful to reject out of time events (accidentals) with respect to collision
KLOE calorimeter

Fine sampling lead/scintillating fibers calorimeter

- Volume Ratio Fiber:Lead 50:50
- Energy sampling fraction 13 %
- $X_0 = 1.6 \text{ cm}$ $\rho = 5.3 \text{ g/cm}^3$

Triangular shape:
high sampling
frequency &
flat response in θ



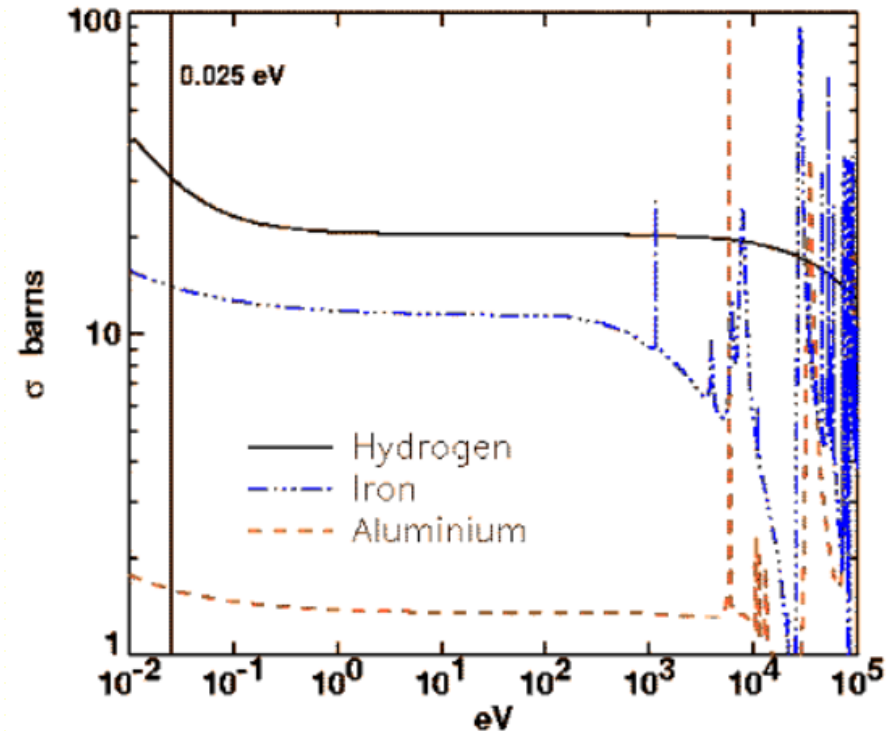
Time measurement in calorimeter, promising way to mitigate "in time" pile-up at LHC

neutrons

Table 12-1. Average number of collisions required to reduce a neutron's energy from 2 MeV to 0.025 eV by elastic scattering

Element	Atomic Weight	Number of Collisions
Hydrogen	1	27
Deuterium	2	31
Helium	4	48
Beryllium	9	92
Carbon	12	119
Uranium	238	2175

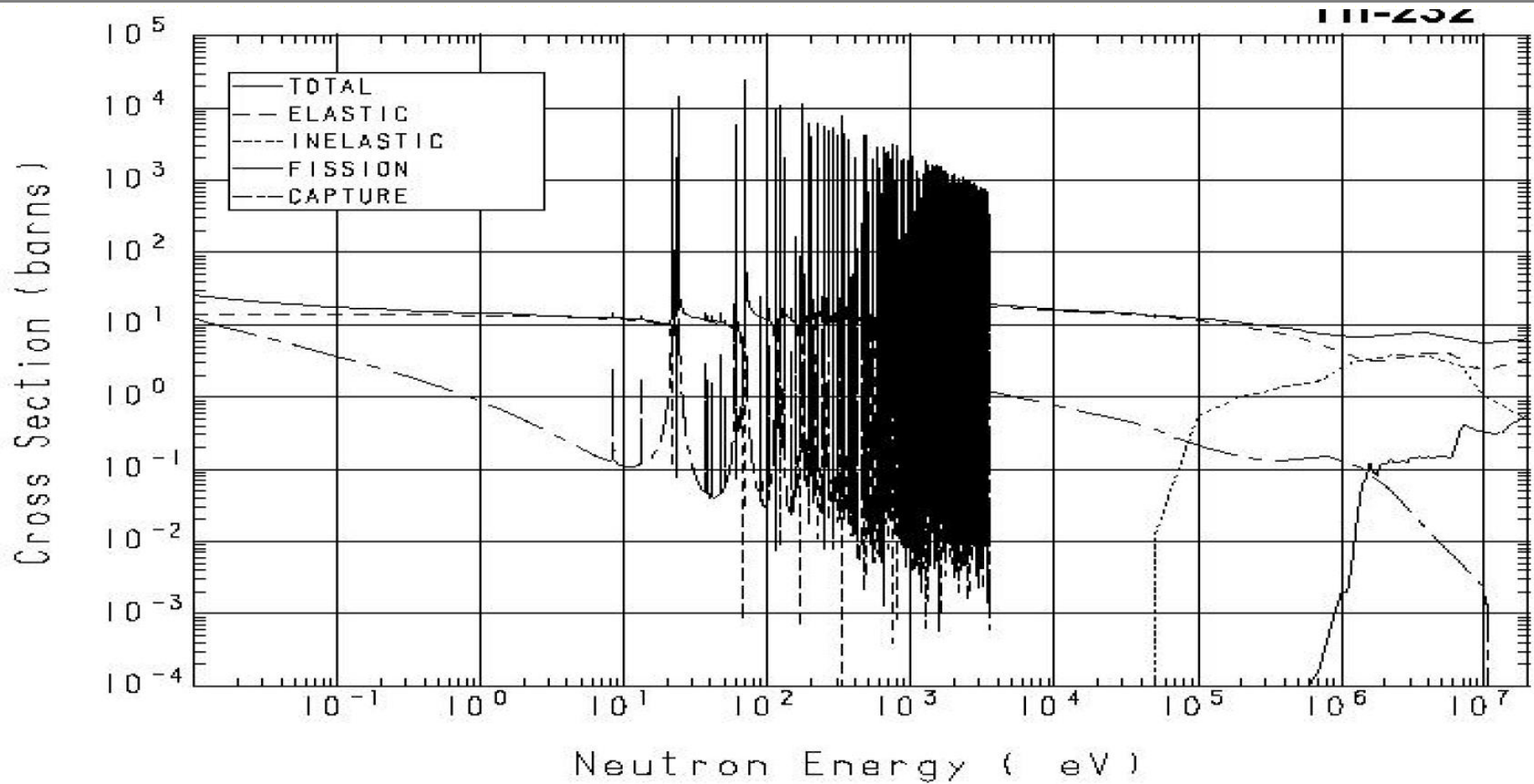
Neutron Cross Sections



Capture may be increased at some energy due to resonance effect in the total cross section...

T (K)	E_0 (eV)	v_0 (m s ⁻¹)	\bar{E}_{th} (eV)
300	0,0253	2200	0,038
400	0,034	2600	0,051
600	0,052	3100	0,075
800	0,069	3600	0,103
1000	0,086	4000	0,129

Cross section on Th-232

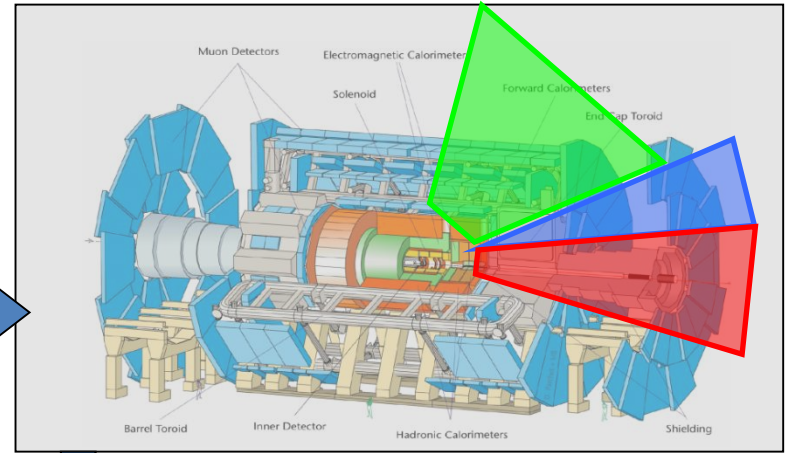


Consequences on LHC experiment hall

Background in Atlas cavern

Background comes from residues of p-p interactions (through spallation process):

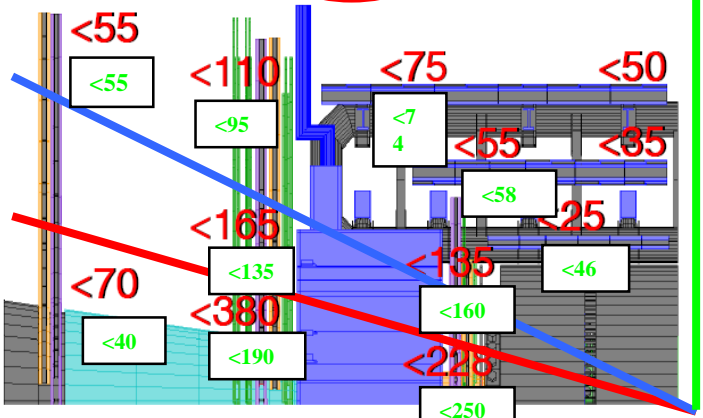
- Huge production of *neutrons*, thus creating γ , thus creating e , etc...
- Also at higher energy, n and γ create ionizing particle (mainly: p , e^+ , e^-)
- Direct background: μ and punchthrough (smaller)



Neutron "gas" in the cavern (-> therm. of neutrons)

$E_{cin}=10$ MeV : $v_n \sim 15\% c$ (23 ns pour 1m)
 10 keV : $\sim 5 \cdot 10^{-3} c$ (0.7 μs pour 1m), out of time

Background count rates (kHz/tube) at $L = 10^{34} \text{ cm}^{-2} \text{ s}^{-1}$



- (Numbers include a safety factor of 5.)
- pp x section for part. prod. (~1.2)
 - rad. propagation in calo. and shielding (~2.9)
 - efficiency in chambers (~1.4)

Atlas needs to measure cavern background using muon spectrometer) in order to reduce uncertainty on background for s-LHC.

10 kHz/cm^2
 $\epsilon_n \text{ hit} \sim 10^{-4} \text{ à } 10^{-3}$
 $\epsilon_\gamma \text{ hit} \sim 4-8 \cdot 10^{-3}$

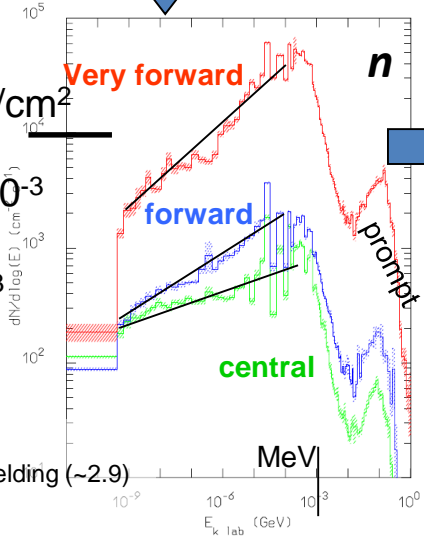


Figure 5-67 The expected neutron flux as a function of neutron energy in different rapidity regions of the muon spectrometer (top curve: $2.3 < \eta < 2.7$, middle curve: $1.4 < \eta < 2.3$ and bottom curve: $\eta < 1.4$).

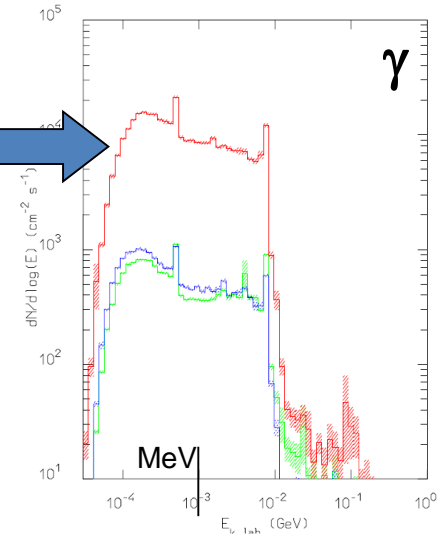
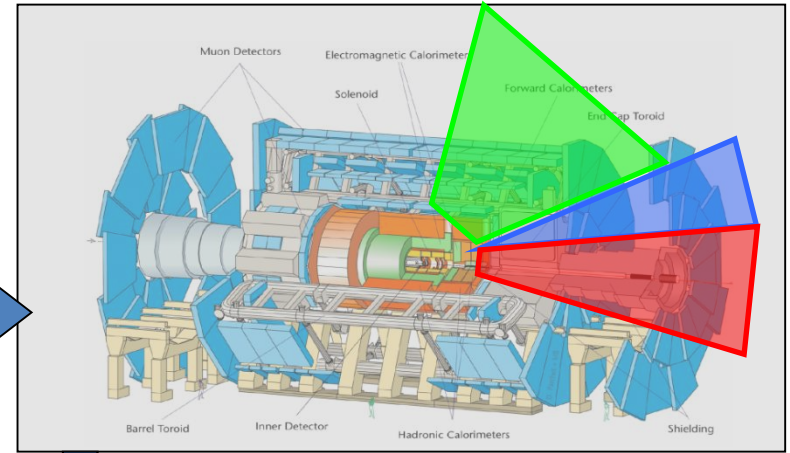


Figure 5-66 The expected photon flux as a function of photon energy in different rapidity regions of the muon spectrometer (top curve: $2.3 < \eta < 2.7$, middle curve: $1.4 < \eta < 2.3$ and bottom curve: $\eta < 1.4$).

Background in Atlas cavern

Background comes from residues of p-p interactions (through spallation process) :

- Huge production of *neutrons*, thus creating γ , thus creating e , etc...
- Also at higher energy, n and γ create ionizing particle (mainly: p , e^+ , e^-)
- Direct background: μ and punchthrough (smaller)



Neutron "gas" in the cavern
(-> therm. of neutrons)

$E_{cin}=10 \text{ MeV} : v_n \sim 15\% c$ (23 ns pour 1m)
10 keV : $\sim 5 \cdot 10^{-3} c$ (0.7 μs pour 1m), out of time

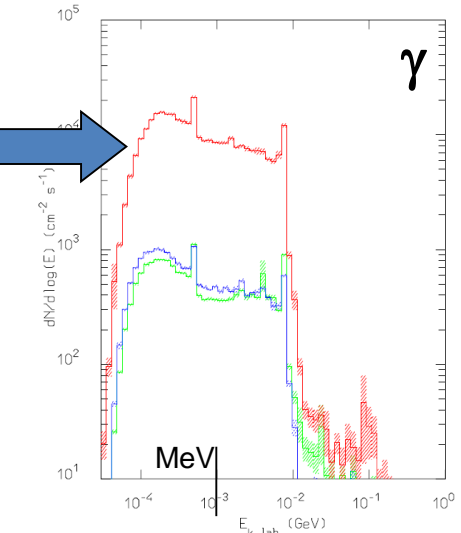
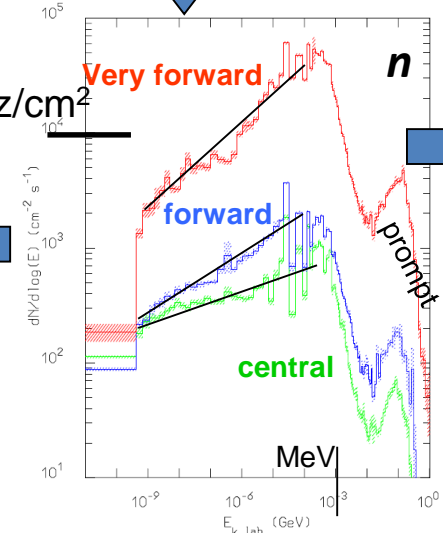
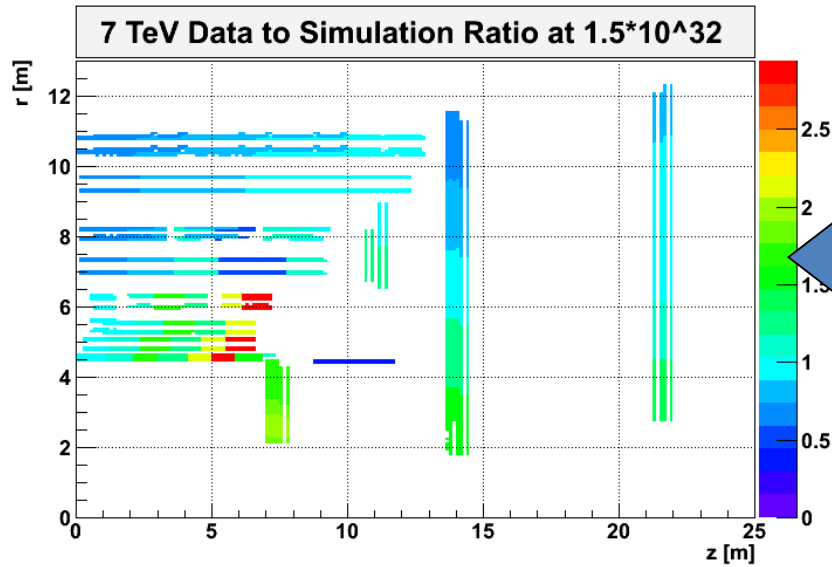


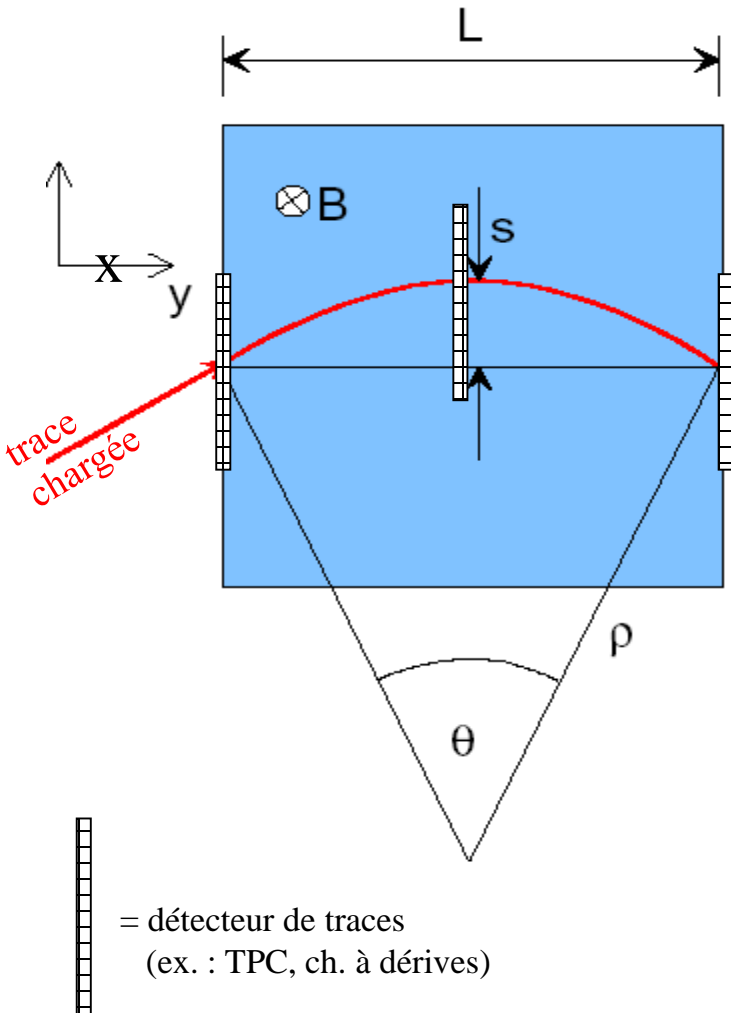
Figure 5-67 The expected neutron flux as a function of neutron energy in different rapidity regions of the muon spectrometer (top curve: $2.3 < \eta < 2.7$, middle curve: $1.4 < \eta < 2.3$ and bottom curve: $\eta < 1.4$).

Figure 5-66 The expected photon flux as a function of photon energy in different rapidity regions of the muon spectrometer (top curve: $2.3 < \eta < 2.7$, middle curve: $1.4 < \eta < 2.3$ and bottom curve: $\eta < 1.4$).

(dernière simulation : facteur de sécurité ~ x2)

Magnets

Charge track momentum measurement in a magnetic field



$$p_T = qB\rho$$

$$p_T \text{ (GeV/c)} = 0.3B\rho \quad (\text{T} \cdot \text{m})$$

$$\frac{L}{2\rho} = \sin \theta/2 \approx \theta/2 \rightarrow \theta \approx \frac{0.3L \cdot B}{p_T}$$

$$\Delta p_T = p_T \sin \theta \approx 0.3L \cdot B$$

$$s = \rho(1 - \cos \theta/2) \approx \rho \frac{\theta^2}{8} \approx \frac{0.3}{8} \frac{L^2 B}{p_T}$$

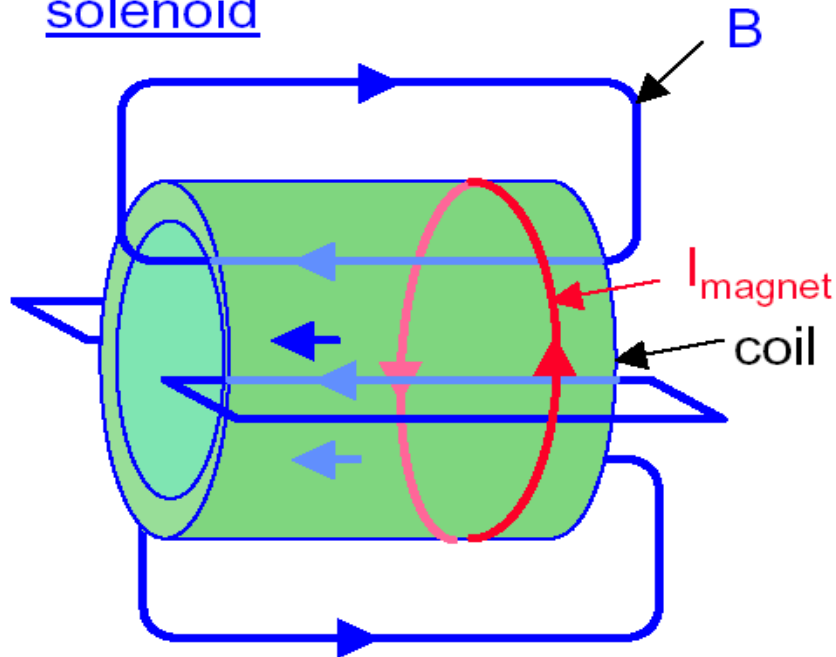
La résolution est dégradée par :

diffusion multiple (matière au milieu)

ET désalignement

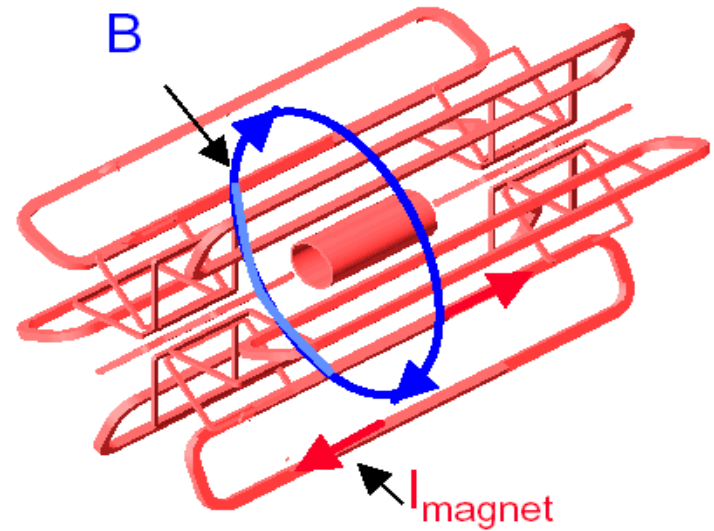
Examples of magnetic field configuration

solenoid



- + Vertex information usefull
- + Large homogenous field inside coil
- weak opposite field in return yoke
- Size limited (cost)
- rel. high material budget

toroid

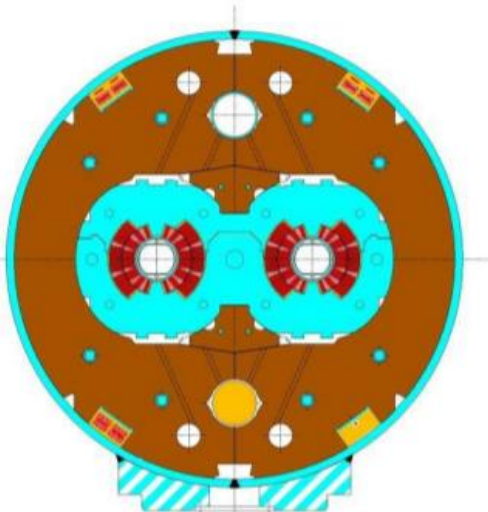


- + independant muon system (redondancy)
- + Rel. large fields over large volume
- + Rel. low material budget
- non-uniform field
- complex structure
- Vertex non-usable

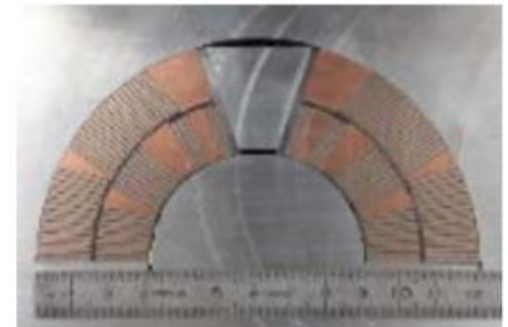
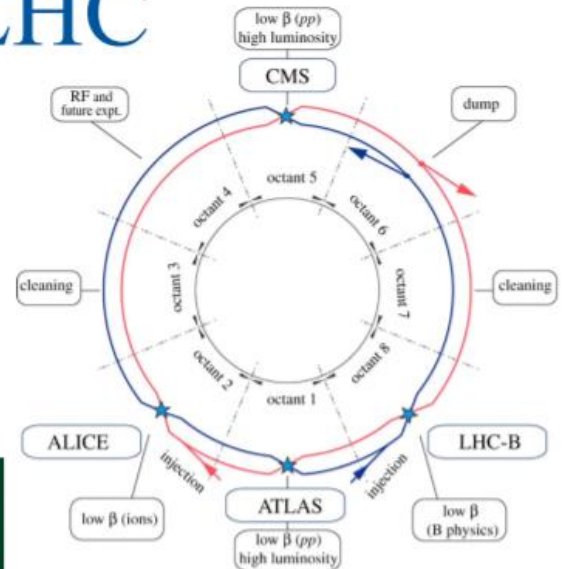
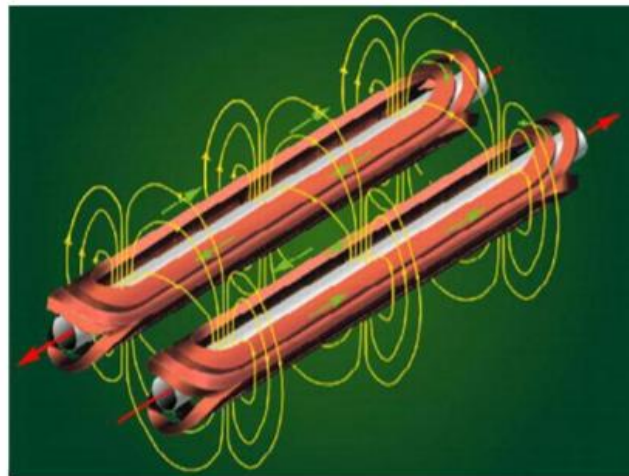
Superconducting devices in LHC

Magnets

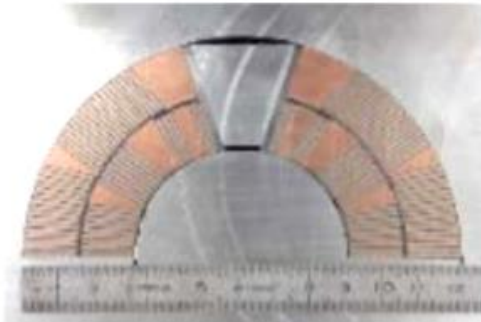
- **LHC ring magnets (Nb-Ti): Rutherford cables**
 - 1232 main dipoles: 8.3 T x 15 m
 - 392 Main quadrupoles 223 T/m (7 T) x 4 m
 - 7600 other SC magnets (cable or wire)



- RF cavities (Nb coating)



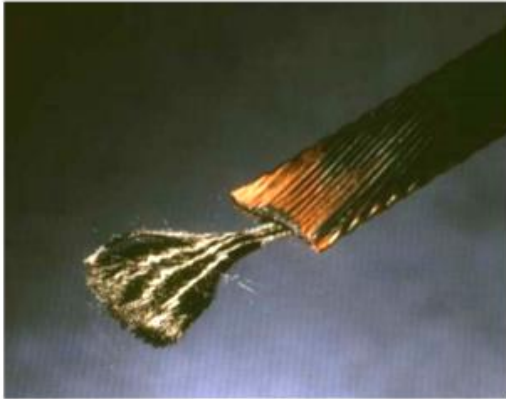
➤ **Rutherford Nb-Ti cable: a key technology for LHC**



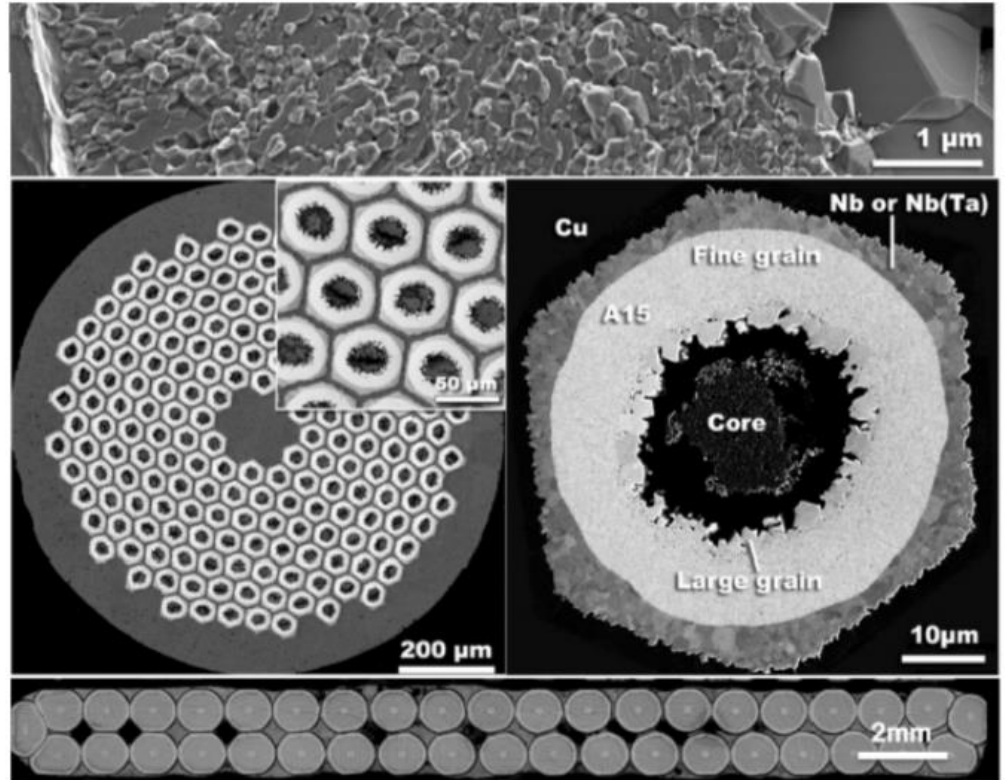
O

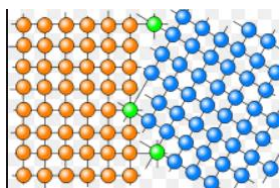
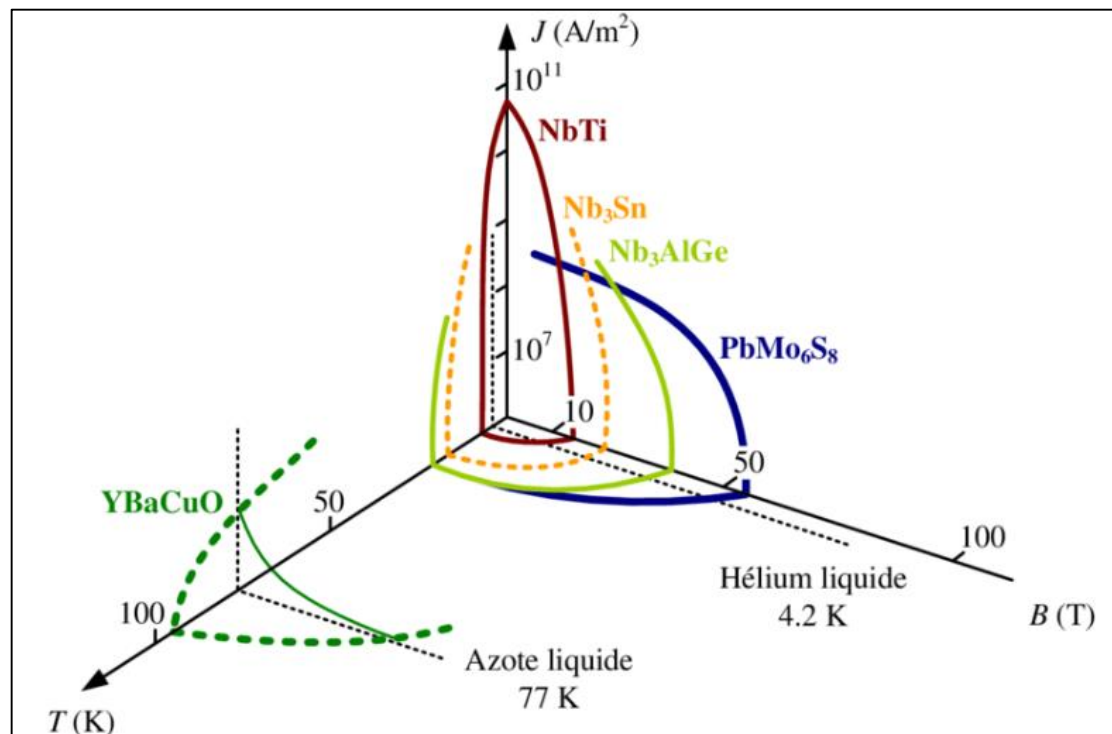
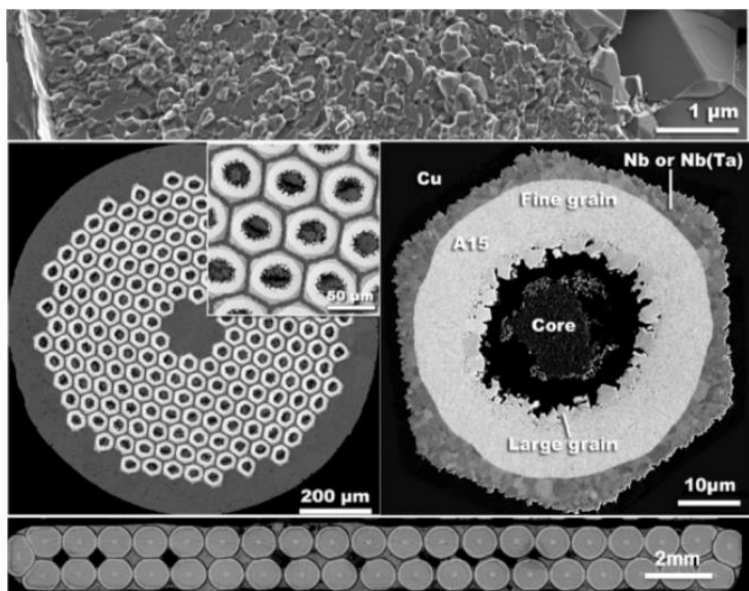
	Tevatron	HERA	RHIC	LHC
Dipole field	4.4 T	5.3 T	3.5 T	8.3 T
Number of strands	23	24	30	28-36
Cable current	4 kA	5.5 kA	5 kA	11.8 kA

cables



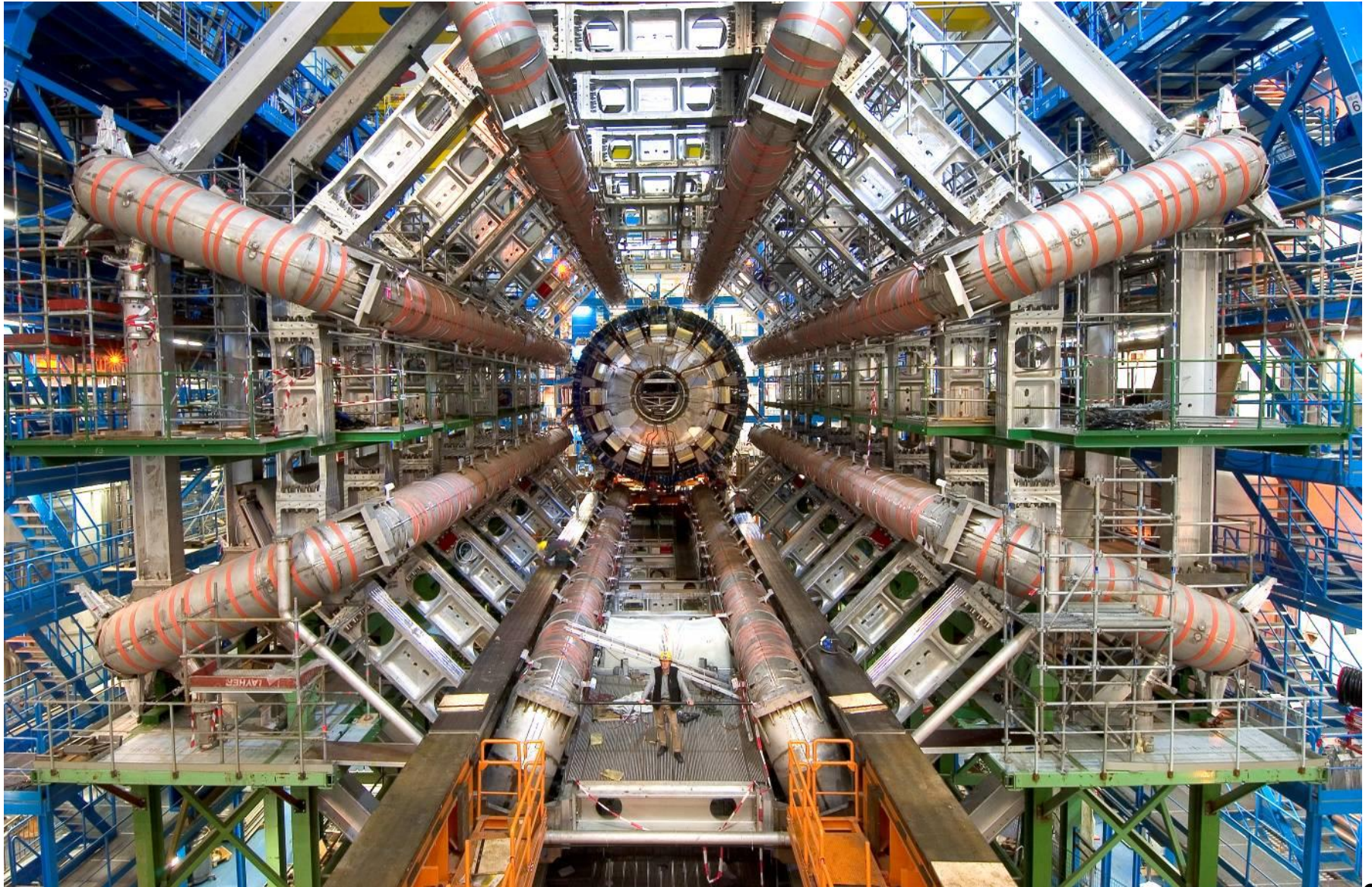
ess)

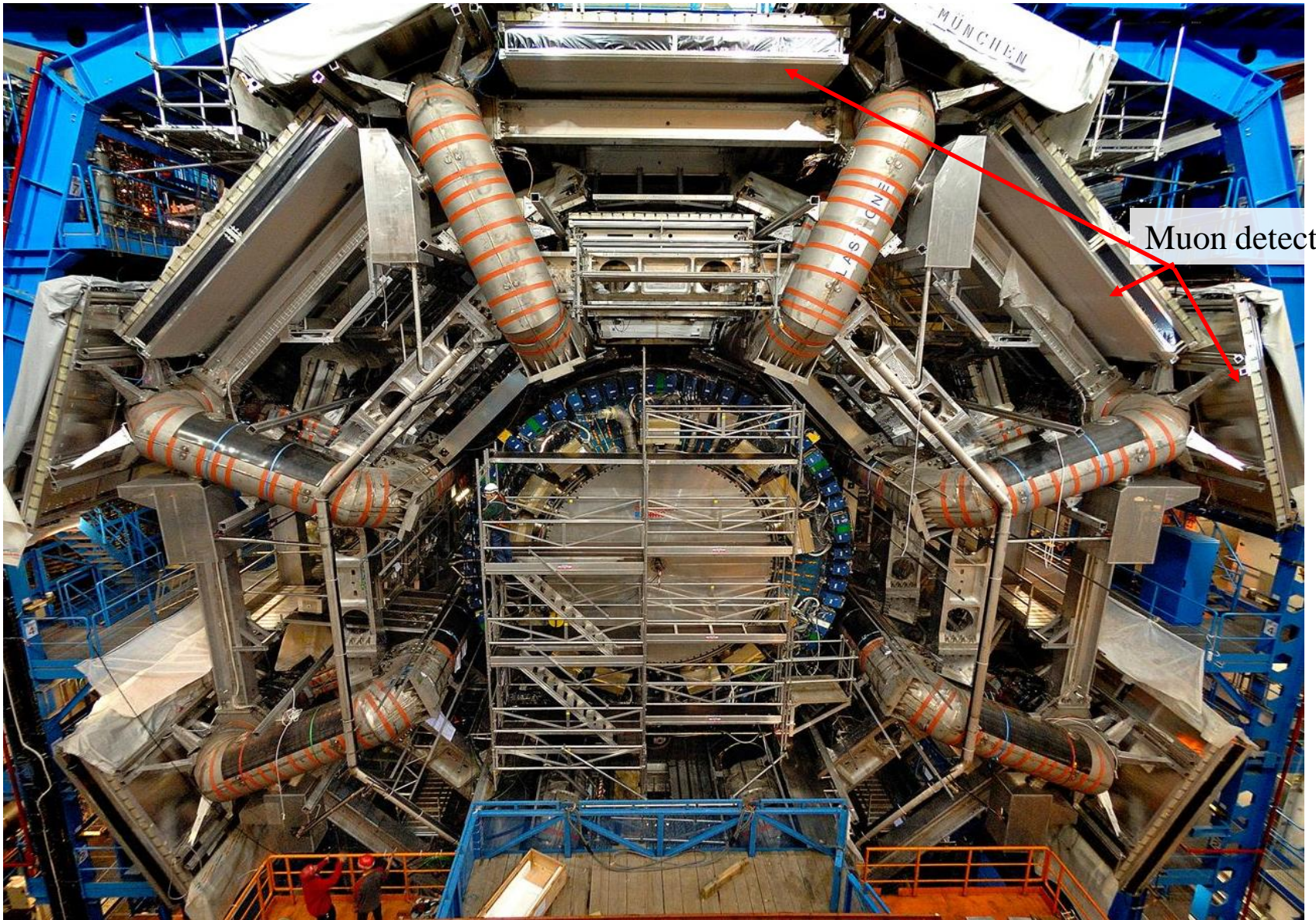




Critical current limited by density of cable defects
(grain boundary / joint de grain)

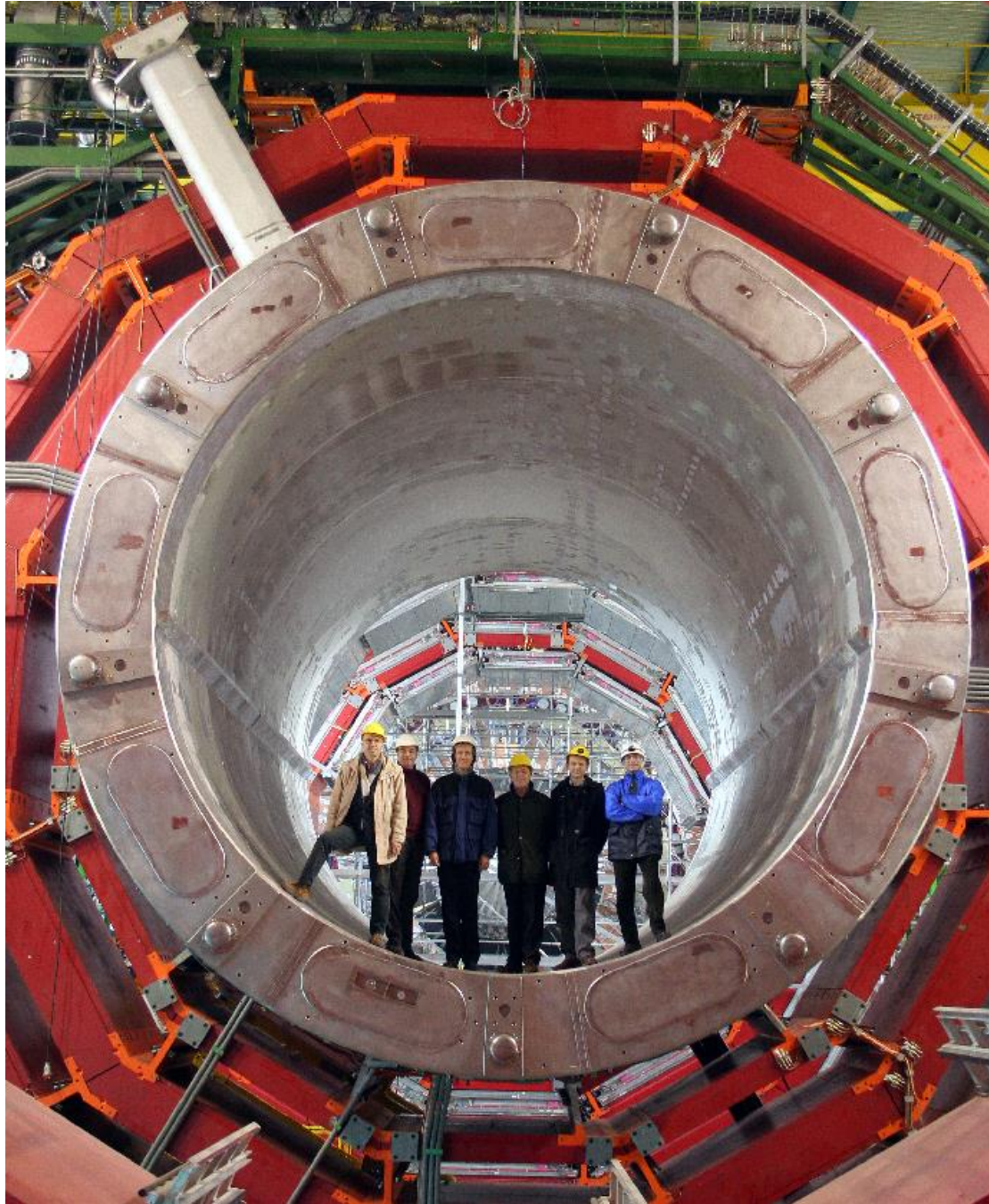
Magnetic fields : supraconducting magnets of ATLAS





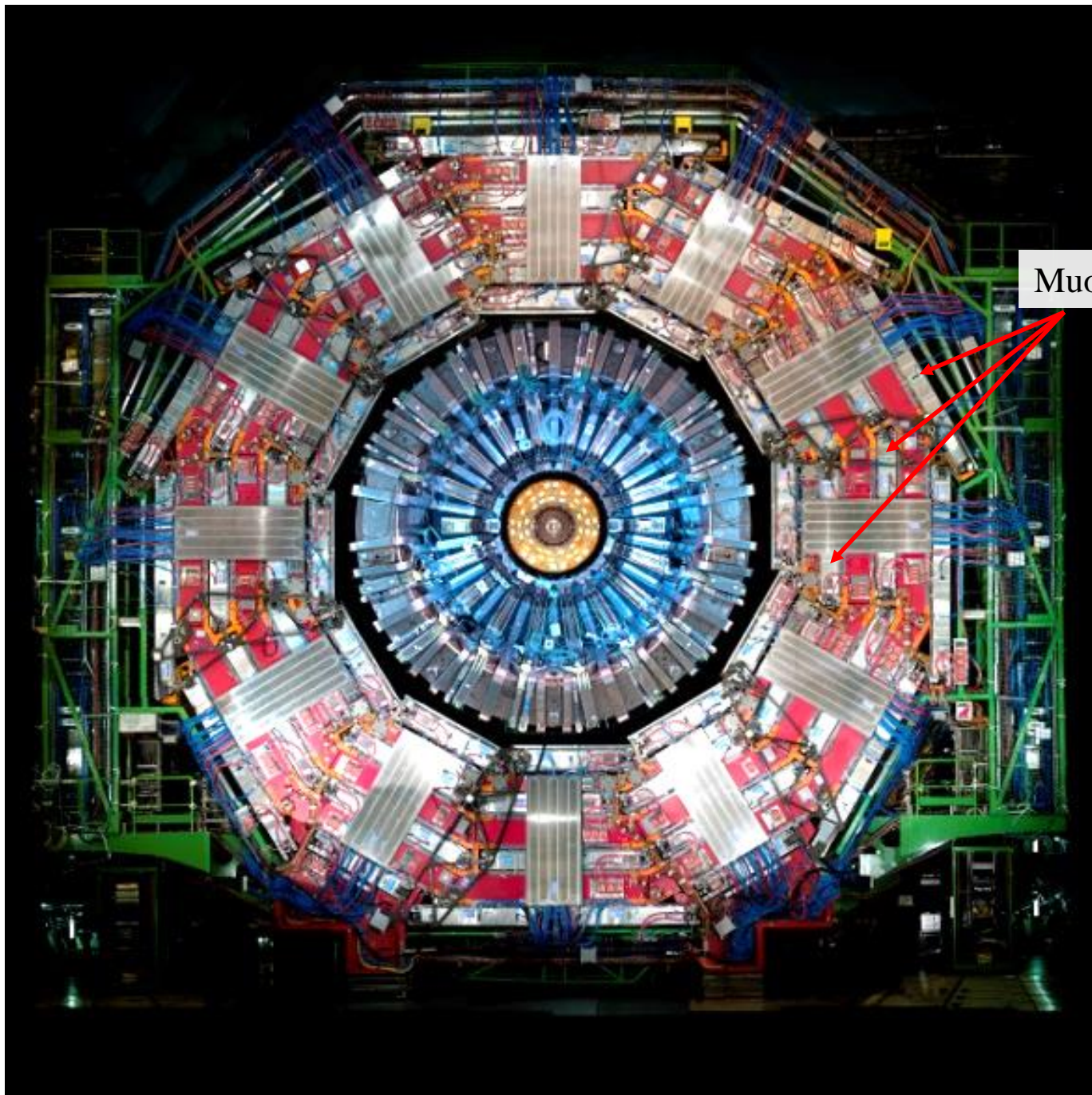
Muon detectors

Champs magnétiques possibles :
aimant solénoïdale de CMS



Muon detectors





Muon detectors



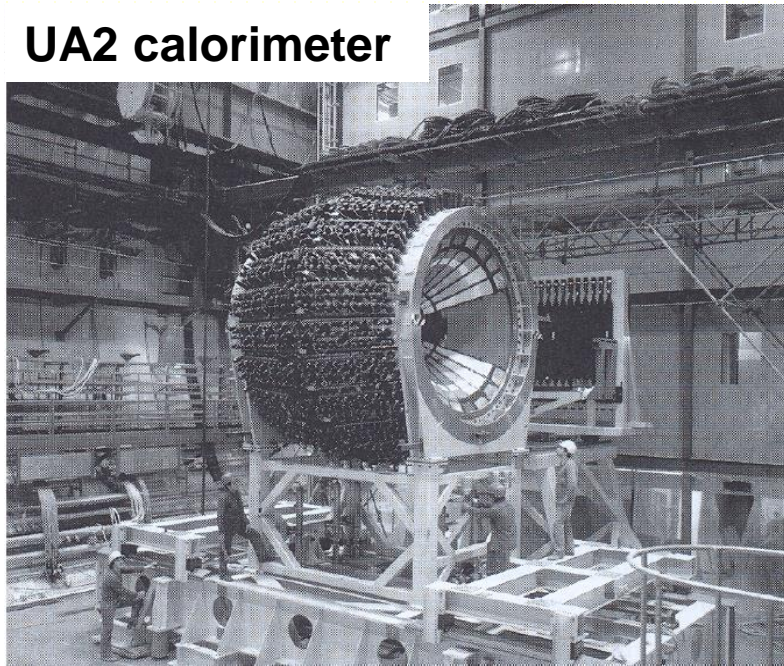
backup

Example of calorimeters

Collider calorimeters : Geometry is usually more complex, need to cover almost 4π solid angle (Missing energy) but also to extract signals. Usually central part with cylindrical geometry (barrel) and small angle part at each end (endcap/forward)

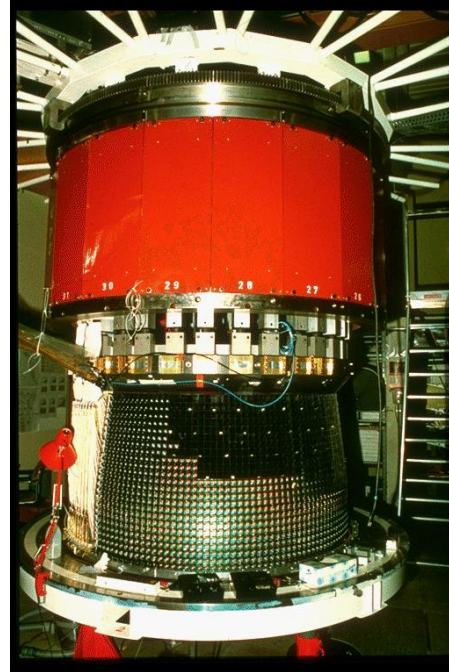
SPS experiments UA1 and UA2

UA2 calorimeter



Calorimeter had a crucial role in W/Z discoveries :next slides

LEP experiments :



L3 had a EM calo with excellent energy resolution (γ) :
11 000 BGO crystals

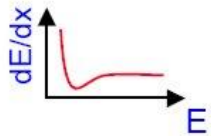
But no real impact on main physics topics at LEP

Other experiments (ALEPH, DELPHI and OPAL) put more emphasis on TPC, and Calorimeter granularity

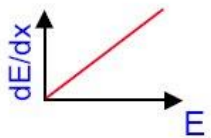
Electromagnetic shower

e^+ / e^-

- Ionisation

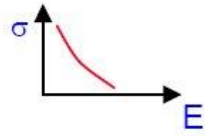


- Bremsstrahlung

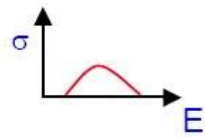


γ

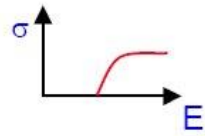
- Photoelectric effect



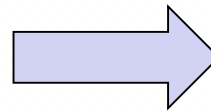
- Compton effect



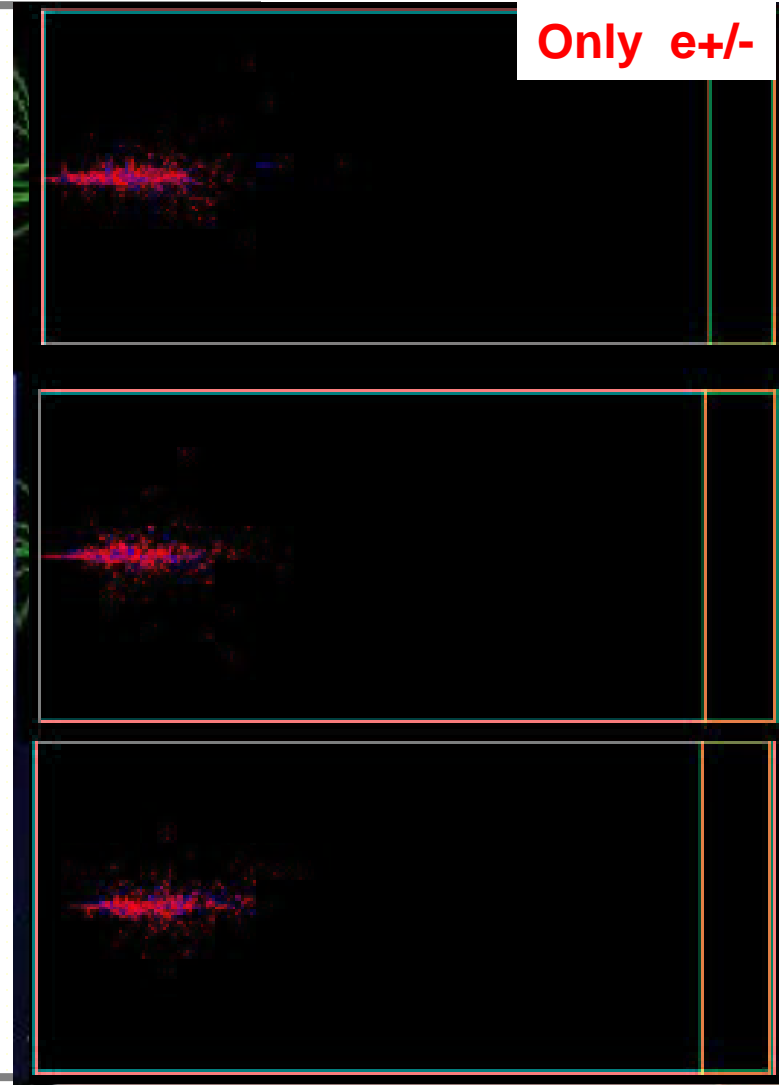
- Pair production



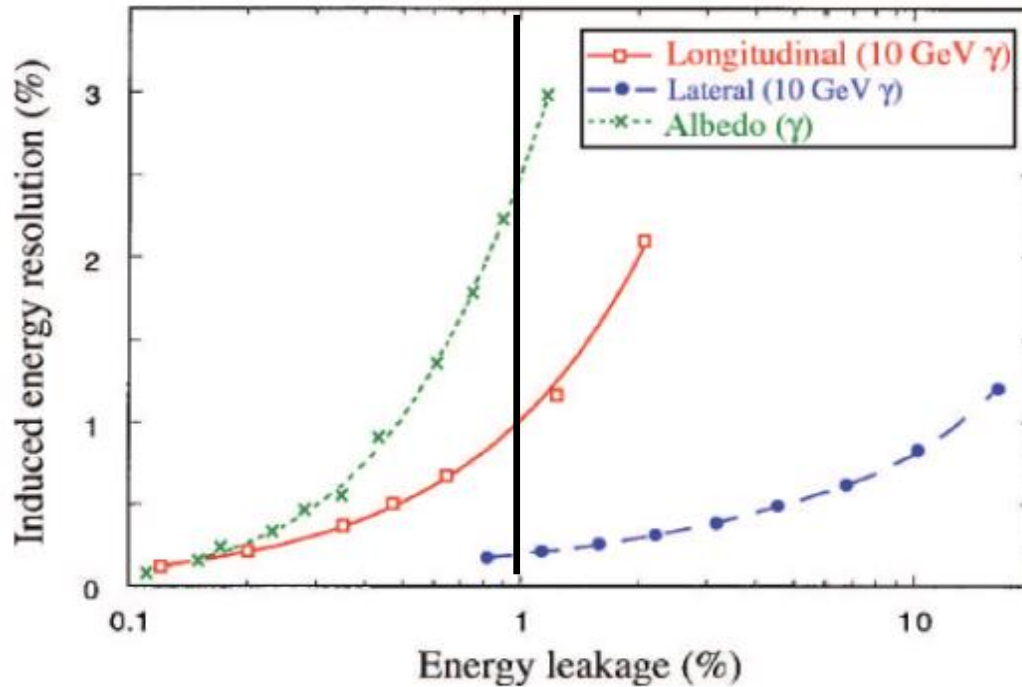
20 GeV e^-



Only $e^+/-$



Impact of leakage



Leakage fluctuation usually not poissonian \rightarrow induces low energy tails
Longitudinal leakage worsens more the resolution than lateral leakage at fixed value.
Albedo (back scattering photon) usually dominated by dead material energy loss
in front of calorimeter

Sampling calorimeter with gas

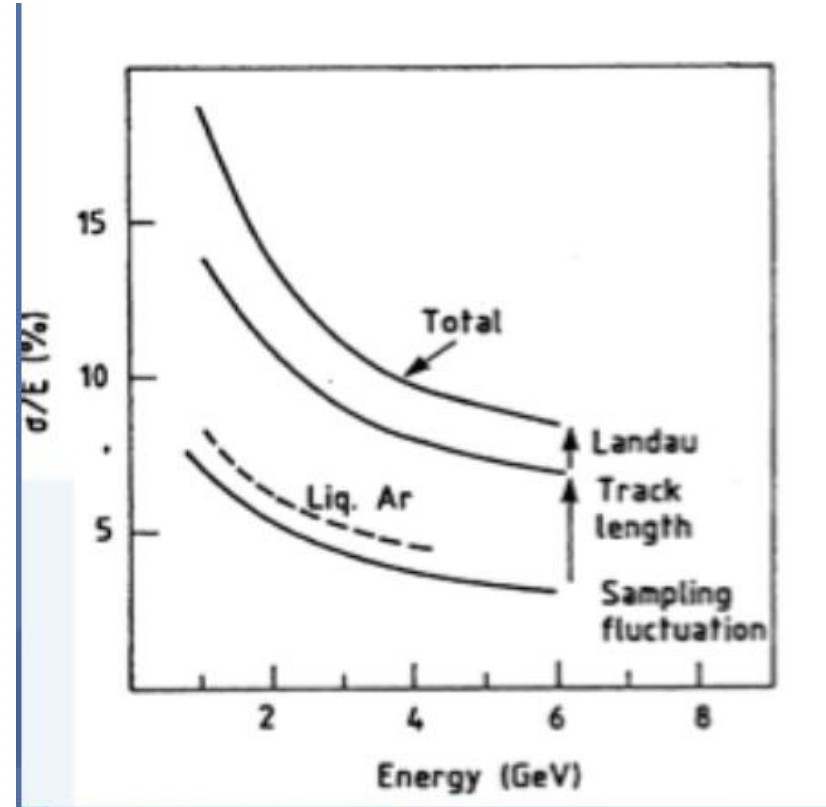
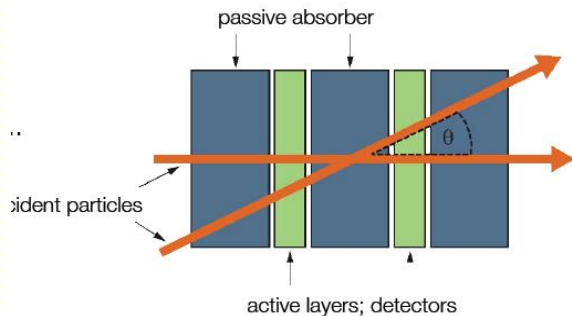
Gas low density medium

Usually poor energy resolution:

- Small sampling fraction (so need larger gap)

- + Track length fluctuation : low electron can travel much in gap

Resolution increases with \sqrt{s}



- + Landau fluctuation

Asymmetric energy deposit in thin active layer (non Gaussian energy measurement)

Calorimeter with gas detector not optimal for good resolution

$$\left[\frac{\sigma(E)}{E} \right]_{\text{Landau fluctuations}} \propto \frac{1}{\sqrt{N} \ln(k \cdot \delta)} \quad \delta \text{ proportional to density}$$

From cluster to particle energy (2)

$$E_{reco}^{cal} = a(E_{reco}^{acc}, |\eta|) + b(E_{reco}^{acc}, |\eta|)E_{ps}^{cl LAr} + c(E_{reco}^{acc}, |\eta|)(E_{ps}^{cl LAr})^2 \quad (\text{upstream})$$

$$+ f_{acc}(X, |\eta|) \times (1 + f_{out}(X, |\eta|)) \times \left(\sum_{i=1}^3 E_i^{cl LAr} \right) \left(1 + f_{leak}(X, |\eta|) \right) \times F(\eta, \varphi)$$

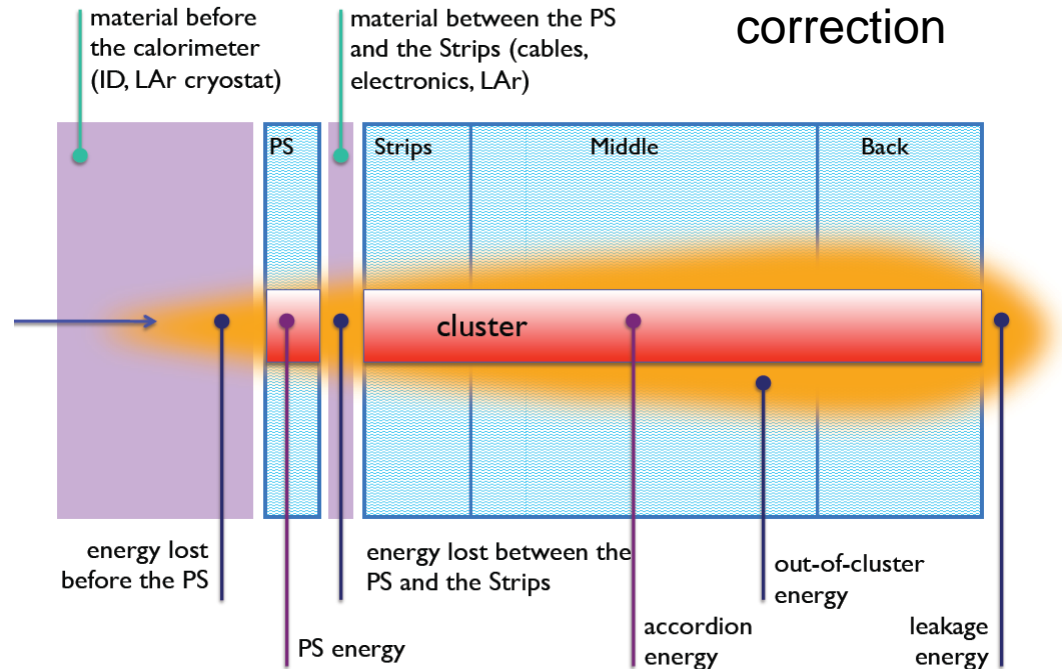
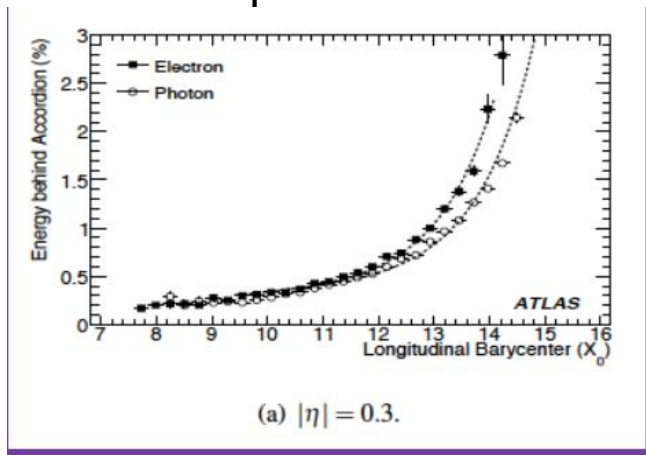
geometry

lateral

longitudinal

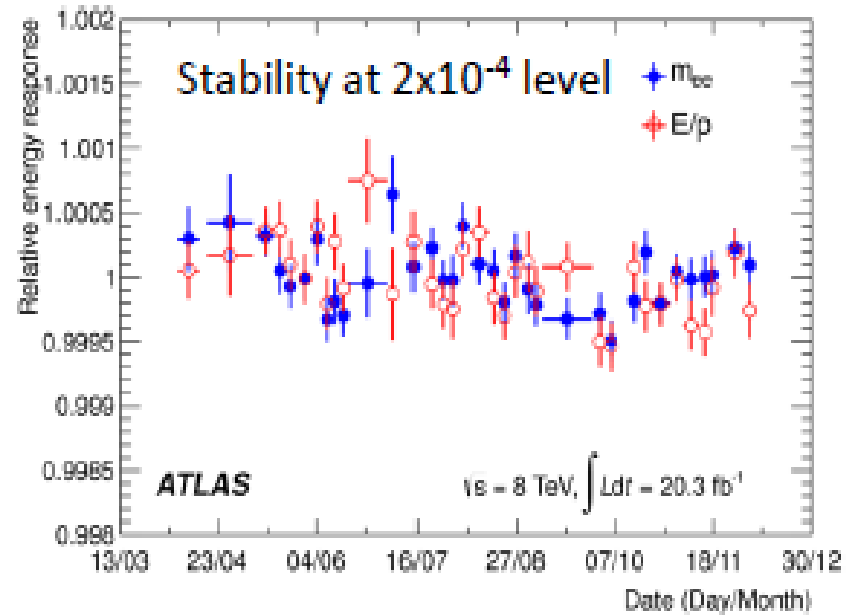
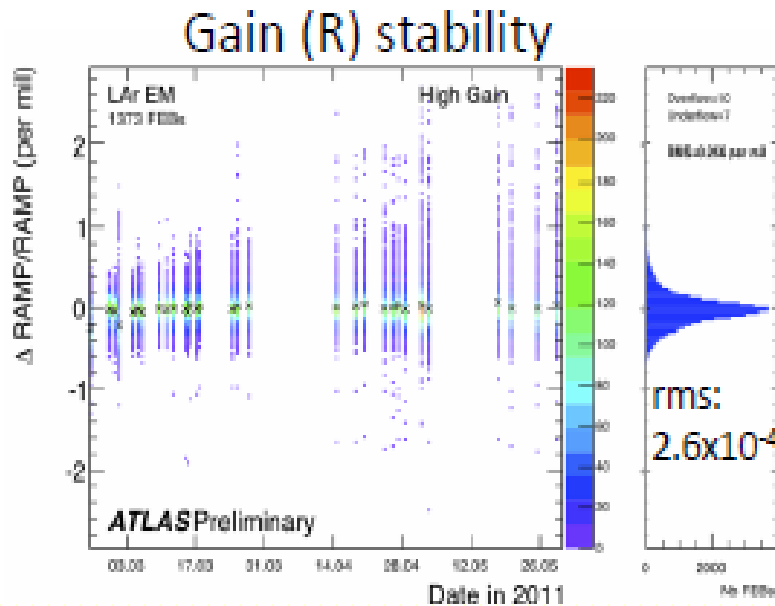
Energy position correction

Parameters/function determined on simulation events, different for electron/photon

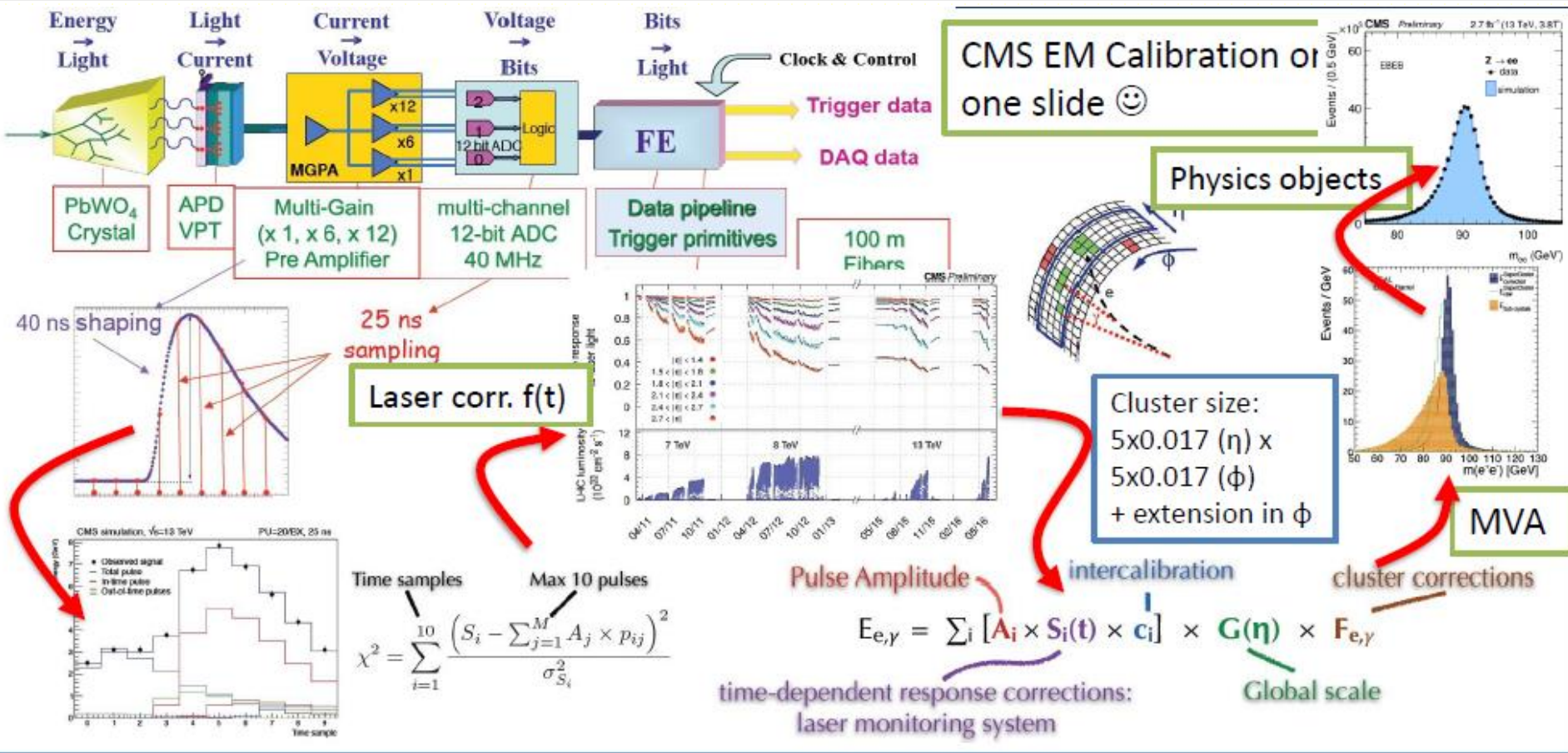


But still not ultimate correlation as detector description/simulation not perfect

Time stability of ATLAS Calo



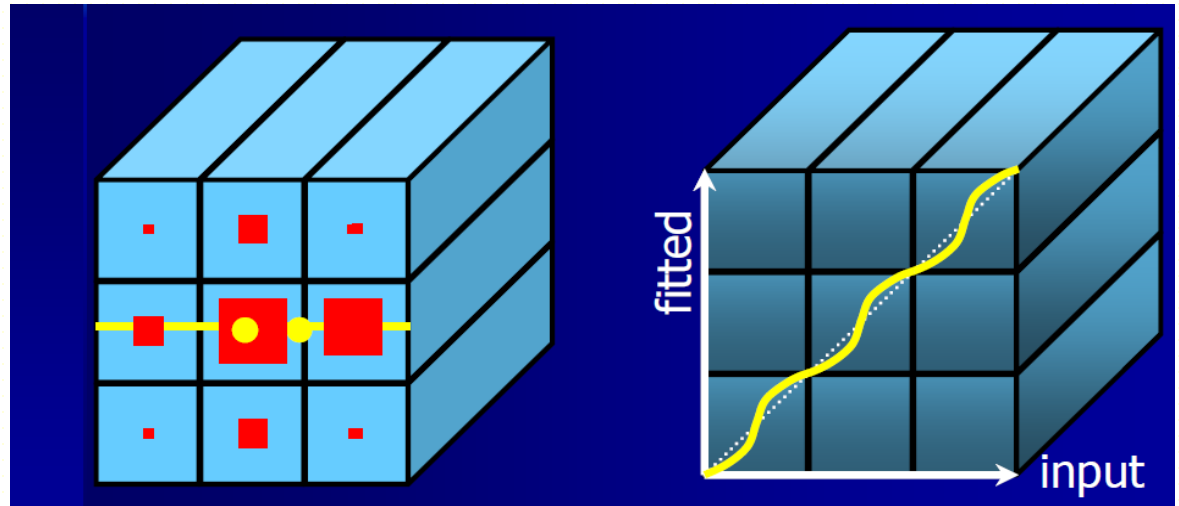
Calibration not easier in CMS !



Shower position reconstruction

Energy weighted barycentre

$$E_{rec} = \sum_{i,j} E_{ij}$$
$$x = \frac{1}{E_{rec}} \sum_i x_i \cdot E_i$$
$$y = \frac{1}{E_{rec}} \sum_j y_j \cdot E_j$$



Bias due to finite cell size : S shape \rightarrow correction to apply
If longitudinal segmentation can also estimate shower depth from

$$X = \sum X_i^0 E_i / E_{rec}$$

From barycentre per layer \rightarrow Shower direction